

INAUGURAL – DISSERTATION

zur
Erlangung der Doktorwürde
der
Naturwissenschaftlich-Mathematischen Gesamtfakultät
der
Ruprecht-Karls-Universität Heidelberg

vorgelegt von
M.Sc. (Soil Science) Ines Mulder
aus Datteln

Tag der mündlichen Prüfung: 04.02.2015

Volatile Organohalogens from Fluid Inclusions of Rocks and Minerals

Gutachter:

Prof. Dr. Heinz Friedrich Schöler

Prof. Dr. Ulrich Anton Glasmacher

Dedicated to my inspiring teacher Prof. Dr. J. B. Dixon,
who has been first to put the idea
of becoming a PhD student into my mind.

Abstract

Volatile organic halocarbons (VOX) play an important role in atmospheric processes. However, biogeochemical release mechanisms from terrestrial environments are complex, not well understood in most parts and a clear view of their relative importance is lacking. Previously, the lithospheric VOX formation potential was subject of only few studies.

In the first part of this thesis the development of a new method for the analysis of VOX from rocks and minerals is reported in order to investigate terrigenic VOX formation potential. The purge and trap GC-MS system was optimized for the analyses of halogenated volatile organic compounds having boiling points as low as -128 °C for carbon tetrafluoride (CF₄).

The design of the U-shaped glass lined steel tube (GLT™) cold trap for sample preconcentration and the rapid desorption via resistant heating transferred the desorbed analytes directly onto the GC column via a deactivated capillary column retention gap made sample re-focussing unnecessary. Furthermore, a special air-tight grinding device was developed in which samples ranging from soft halite (hardness 2, Moh's scale) to hard quartz (hardness 7) are effectively ground to average diameters of 1000 nm or below, thereby releasing gases from fluid inclusions of minerals. The gases are then purged from the grinding chamber with a He carrier gas flow.

In the second part of this work, the newly developed method is applied to a set of various mineral and rock samples including fluorite, quartz and halite. The analytical results from GC-MS prove the presence of a wide spectrum of volatile compounds from FIs trapped in various minerals. SF₆ and CF₄ were released from fluorites. Methyl bromide, dichloroethene and dichloroethane were detected in quartz samples from the Archean Yilgarn craton in Australia. Methyl chloride (MeCl) has been detected from almost all samples, including halites, fluorites, quartz and dolerites. Initial heating experiments with halites using purge-and-trap GC-MS as well as pyrolysis-GC-MS demonstrated the important role of temperature in MeCl and VOX formation.

Finally, in the last part of this dissertation a case study on one possible formation pathway for the volatile compounds MeCl and dimethylsulfide (DMS), via thermolytic degradation of the amino acid derivative methyl methionine is investigated. A fast response of MeCl and dimethylsulfide emission upon heating of freeze-dried samples at 40 °C was observed and made this a plausible abiotic volatile formation mechanism. Besides the mechanistic studies with methyl methionine and structurally related substances, the emission of MeCl and DMS from fluid inclusions, soil samples of terrestrial salt lakes and air sampled immediately above the salt lake surfaces indicated the relevance of this formation pathway for hypersaline environments.

Zusammenfassung

Flüchtige organische Halogenkohlenwasserstoffe (VOX) spielen eine wichtige Rolle in chemischen Prozessen der Atmosphäre. Allerdings sind die biogeochemischen Mechanismen die zu diesen Prozessen beitragen komplex, und oftmals fehlt ein klares Verständnis von Bildungswegen und deren Auswirkungen. Das lithosphärische VOX-Bildungspotential wurde bisher in nur wenigen Studien angedeutet.

Der erste Teil der vorliegenden Arbeit dokumentiert die Entwicklung einer neuen Methode zur Analyse von VOX aus Mineralen und Gesteinen. Das Purge-and-Trap GC-MS-System wurde für die Analyse halogenierter flüchtiger Verbindungen mit Siedepunkten bis zu -128°C (Kohlenstofftetrafluorid) optimiert. Das Design der U-förmigen, innen mit Glas beschichteten, Anreicherungsprobenschleife und der schnelle Desorptionsschritt mittels Widerstandsheizung, der die Analyten über ein ‚Retention-Gap‘ direkt auf die GC-Säule transferiert, ersparte eine Re-Fokussierung auf der Säule. Außerdem wurde ein spezielles Mahlgefäß entworfen, das dazu diente, Proben von weichen Haliten (Moh's Härte 2) bis zu harten Quarzen (Moh's Härte 7) effektiv auf eine Durchschnittskorngröße von 1000 nm oder darunter zu mahlen und dadurch Gase aus den Fluideinschlüssen der Minerale freizusetzen. Die Gase werden dann mit dem He Trägergas aus dem Mahlbecher transportiert.

Im zweiten Teil dieser Arbeit, wurde die entwickelte Methode zur Analyse eines Probensatzes verschiedener Minerale und Gesteine, mit u.a. Fluorit, Quarz und Halit eingesetzt. Die analytischen Ergebnisse der GC-MS zeigten, dass eine große Bandbreiten an flüchtigen organischen Verbindungen in den Fluideinschlüssen der Minerale vorhanden ist. SF_6 und CF_4 wurden aus Fluoriten freigesetzt. Methylbromid, Dichlorethen und Dichlorethan wurden aus Quarzen des archaischen Yilgarn Kratons in Australien detektiert. Methylchlorid (MeCl) wurden in fast allen Proben nachgewiesen, inklusive den Haliten, Fluoriten, Quarzen und Doleriten. Erste Heizversuche mit GC-MS und Pyrolyse-GC-MS zeigten, dass die Temperatur eine wichtige Rolle in der MeCl und VOX-Bildung spielt.

Schließlich wird im letzten Teil der Arbeit eine Fallstudie zu einem möglichen VOX-Bildungsmechanismus, dem thermolytischen Abbau des Aminosäurederivats Methylmethionin zu MeCl und Dimethylsulfid (DMS), vorgestellt. Ein schneller Anstieg von MeCl und DMS Emission war zuvor beim Heizen auf 40°C von gefriergetrockneten Bodenproben beobachtet worden und ließ dieses daher einen plausiblen Bildungsweg erscheinen. Neben den mechanistischen Studien mit Methylmethionin und strukturell verwandten Substanzen, deuteten Emissionen von MeCl und DMS auch aus Fluideinschlüssen und Boden- sowie Luftproben von terrestrischen Salzseen die Relevanz dieses thermolytischen Bildungswegen für hypersaline Milieus an.

Table of Contents

Table of contents	i
List of Abbreviations	v
<u>CHAPTER 1: Introduction and Literature Review</u>	<u>1</u>
1.1. Introduction and Objectives	2
1.1.1. General remarks	2
1.1.2. Thesis objectives	3
1.1.3. Structure of thesis	4
1.2. Investigation of fluid inclusions	5
1.3. Organic matter in the lithosphere	8
1.4. Organic matter in fluid inclusions	16
1.5. VOC, VOX and naturally produced organohalogens	19
1.6. Geogenic organohalogens	21
1.7. Behaviour of halogens in rocks and magmas	25
1.8. Halogenation reactions in geologic matrices	29
1.8.1. Relevant halogenation reactions	31
1.8.2. VOX forming halogenation reactions in soils	34
1.8.3. Volcanic VOX formation	36
1.8.4. Hydrothermal VOX formation	37
1.8.5. Radiochemical halogenation/ reactions with molecular fluorine	38
<u>CHAPTER 2: Method development</u>	<u>40</u>
2.1 Introduction	41
2.2. Experimental	44
2.2.1. Grinding device	44
2.2.2. Analytical system	45
2.2.2.1. Purge and trap unit	46
2.2.2.2. GC-MS	48

2.2.2.3. Measurement of samples	50
2.3. Results and discussion	50
2.3.1. Grinding procedure	50
2.3.2. Chromatographic optimization	53
2.4. Conclusions	58
CHAPTER 3: Sample Screening	59
<hr/>	
3.1 Introduction	60
3.2. Materials and Methods	62
3.2.1. Samples and their treatment	62
3.2.2. GC-MS	65
3.2.3. Ion chromatography	68
3.2.4. Carbon content	69
3.2.5. Major and trace elements (XRF)	69
3.2.6. X-ray diffraction	70
3.2.7. Py-GC-MS	71
3.3. Results and Discussion	72
3.3.1. Sample treatment and technical problems	72
3.3.2. GC-MS	73
3.3.3. Ion chromatography	83
3.3.4. Carbon content	87
3.3.5. Major and trace elements (XRF)	88
3.3.6. Results XRD	89
3.3.7. Py-GC-MS	92
3.4. Conclusions	93
CHAPTER 4: Case Study: Thermolysis of MeMET yielding MeCl and DMS	95
<hr/>	
4.1 Introduction	96
4.2. Materials and Methods	98

4.2.1. Chemicals	98
4.2.2. Soil and salt samples	98
4.2.3. Air samples	100
4.2.4. Studies with MeMET and model substances	101
4.2.5. Amino acids from soils	101
4.3. Results and Discussion	102
4.3.1. Volatile compounds from salts, soil and air samples	102
4.3.2. Temperature dependence of MeCl and DMS release from MeMET	108
4.3.3. Postulated reaction pathways for thermolytic MeCl and DMS formation	111
4.3.4. VOX and VOSC released from soils under experimental conditions	114
4.4. Conclusions	116
<u>CHAPTER 5: Summary and Conclusions</u>	<u>117</u>
Acknowledgements	121
Bibliography	123
<u>6: Appendix</u>	<u>136</u>
Table 6.1: List of available samples	137
Table 6.2: Volatile compounds from minerals and rocks 12/2009-08/2010	140
Table 6.3: Volatile compounds from ground and heated halites and gypsum 04/2010	141
Table 6.4a: Volatile compounds from granites, fluoites and quartz 08/2011	142
Table 6.4b: Volatile compounds from fluorite and halite 11/2011	142
Table 6.5: Results from halites 01/2012	143
Table 6.6: Results from mixed samples 05-08/2012	144
Table 6.7: Results from quartz 05-08/2012	145
Table 6.8: Anion concentrations of halite samples	146
Table 6.9: Organic carbon concentrations of halite samples	147

Table 6.10: Examples of aliphatic and aromatic hydrocarbons from FI	148
Table 6.11: VOSC from minerals	149
Method: Synthesis of MORB glass	149
Figure 6.1: Stainless steel cylinder for sample evacuation	150
Figure 6.2: Construction drawing of moveable rack for gas mixing station	151
Figure 6.3: Construction scheme of sample evacuation/gas mixing station	152
Figure 6.4: Construction drawing of aluminum heating block for water trap	153
Declarations	154

List of Abbreviations

BTEX	Benzene, toluene, ethylbenzene and xylenes
CFC	Chlorofluorocarbons
CRM	Certified reference material
df	thickness film
DFG	Deutsche Forschungsgemeinschaft
DMDS	Dimethylsulfide
DMS	Dimethylsulfide
DMSO	Dimethylsulfoxide
DMSO ₂	dimethylsulfone
ECD	Electron capture detector
EPA	Environmental Protection Agency
FID	Flame ionization detector
GC	gas chromatography
GC-MS	Gas chromatography-mass spectrometry
GLT	Glass lined tubing
IC	Ion chromatography
ID	inner diameter
m/z	mass-to-charge ratio
MeBr	methyl bromide, bromomethane
MeCl	methyl chloride, chloromethane
MeMET	methyl methionine
MET	methionine
MSD	Mass selective detector
NIST	National Institute of Technology
NOM	Natural organic matter
OM	Organic matter
PLOT	Porous Layer Open Tubular
Py-GC-MS	Pyrolysis-gas-chromatography
RHS	Reactive halogen species
RIC	reconstructed ion chromatogram
TGMS	Thermogravimetry-Gas-chromatography-Mass Spectrometry
THM	Trihalomethane
TIC	total ion chromatogram
VOC	Volatile organic compound
VOSC	Volatile organic sulfur compound
VOX	Volatile organohalogen
XRD	X-ray diffraction
XRF	X-ray fluorescence

1

Introduction and Literature Review

1.1. Introduction and Objectives

1.1.1. General remarks

In the 1823 German Yearbook of Chemistry and Physics, author J.L.G. Meinecke formulated the following:

„Die oberflächliche Atmosphäre wird erst thätig durch die Erde, wozu sie gehört und der sie als geringer Körper anhängt.“ (The superficial atmosphere comes to act through the earth, to which it belongs and to which it is attached as a minor body.)

In his article the professor, in the language of his time, flamboyantly speculates over emissions from the earth interior influencing meteorological phenomena (lightning), causing periodically occurring unhealthy steams (malaria) and considering the presence of ‘atmospheric air’ in geologic matrices as an explanation for the formation of organic life (fossils). Nevertheless, his approach of focusing on the lithosphere and lithospheric processes and his strive to fathom their impact on atmospheric processes is probably more up to date now than ever.

Although the atmosphere ($5.13 \cdot 10^{18}$ kg) on a weight basis is small compared to the rest of the earth (total $5.97 \cdot 10^{24}$ kg; continental crust $22.5 \cdot 10^{21}$ kg, oceanic crust $4.6 \cdot 10^{21}$ kg), its composition and reactions are of pivotal importance to life on earth, such as the protection of organisms from ultraviolet light or a balanced heat budget at favourable temperatures (Warneck and Williams, 2012). However, the atmosphere derived primarily from thermal outgassing at the beginning of earth history. Earth’s influence on atmosphere and climate is most apparent in volcanic eruptions, ejecting large aerosol particles and SO_2 , forming secondary aerosols.

Since the discovery of the ozone hole over Antarctica in the 70ies, intensive atmospheric research has shown that mainly man-made volatile aliphatic hydrocarbons (chlorofluorocarbons and halons) take a significant part in atmospheric ozone destruction. Naturally produced methyl chloride and methyl bromide were recognized also as important precursors for the ozone depleting chloro- and bromo-species (Molina and Rowland, 1974). Halogenated species can also be powerful greenhouse gases, especially the fluorinated ones with CF_4 having by far the longest lifetime of 50,000 years (IPCC, 2013). In the past large amounts of fluorinated gases were emitted by industrial processes. The amounts of chlorofluorocarbons (CFCs) released were reduced since a phase-out management

plan of these substances was universally ratified in the Montreal protocol in 1987. An understanding of the natural formation of volatile organic halocarbons (VOX) was developed in recent years and is still subject of ongoing studies. Schöler and Keppler (2003) subdivide their abiotic formation within terrestrial environments into three groups: biomass burning (methylhalides), early diagenetic processes in soils and sediments (VOX, haloacetic acids) and volcanic activity (VOX). Halogenated volatile organohalogens formed in the lithosphere received little attention and accordingly the number of studies concerned with naturally halogenated organics from rocks and minerals is limited. Naturally produced halogen compounds were the central subject of the DFG research unit 763, Natural Halogenation Processes in the Environment - Atmosphere and Soil. The lithosphere is part of the environmental compartment of the pedosphere, the soil, where it interacts with the atmosphere, hydrosphere and biosphere. This Ph.D. thesis has been supported in parts by the research unit.

Today, a geogenic formation of VOX has been evident from hydrologic studies and measurements of volcanic emissions, including a handful of studies from rocks and minerals. However, we are far from an in-depth understanding of their geogenic occurrence, processes of their formation and contributions to atmospheric processes.

Therefore, the viewpoint of this thesis focusses on the occurrence and formation of VOX in the lithosphere.

1.1.2. Thesis objectives

Aim of this dissertation was to investigate additional groups of rocks and minerals for their VOX-formation potential. Minerals are known to host fluid inclusions (FI) that trap liquids, gases and solids. Additionally, rocks and minerals offer an extremely wide spectrum of diagenetic conditions such as temperature, pressure and salinity of the mineral forming fluid. In view of this multitude of possible formation conditions during diagenesis and metamorphosis, this work intends to contribute to an improved estimation on the atmospheric input from this compartment. Furthermore, we strive to provide a stronger scientific basis for halogenation reactions in the lithosphere with respect to volatile organohalogen generation.

In order to conduct a sample screening of the VOX content of FIs in a divers set of minerals and rocks, a method suitable for the detection of low boiling point compounds had to be developed. Observations on halites during the subsequent sample screening brought forward the in-depth

investigation of one possible formation pathway of methyl chloride (MeCl) and dimethylsulfide (DMS) via an amino acid derivative as precursor.

1.1.3. Structure of thesis

According to the study objectives, this thesis is subdivided into three chapters. **Chapter 2** describes the method development to investigate VOX from FIs of rocks and minerals. **Chapter 3** summarizes results of the screening of rocks and minerals for their VOX content and **Chapter 4** contains a case study on MeCl and DMS and documents the investigation of one potential formation pathway. Each chapter has a preceding introductory section summarizing relevant literature data allowing the reader to understand and comprehend the respective context without the need of the other chapters. **Chapter 5** comprises an overall summary and conclusions.

This introductory **Chapter 1** will now discuss briefly aspects of general importance to the subject of the study. Terms of fluid inclusion research and VOX will be defined. A literature review on organic matter in the geosphere in general as well as in fluid inclusions in particular follows. Known geogenic VOX occurrence will be summarized and the behavior of halogens in rocks and magma is outlined. Finally, possible geogenic halogenation reaction pathways will be discussed.

1.2. Investigation of fluid inclusions

Fluid inclusion analyses are a widely used geochemical tool to determine thermobaric and chemical evolution of geologic systems.

Most naturally grown crystals contain inclusions of other minerals, melts, fluids and gases, which were originally present at the mineral surfaces during crystal growth and then included. The term “fluid” or “fluid inclusion” (FI) does not imply that their contents are liquid but rather refers to the fluid captured, from which the mineral formed.

Thus, FIs are important archives and their investigation allows to gather information on original fluid composition. Several generations of FIs can be present and for probably most FI analysis performed by geologists, it is crucial to differentiate between primary, secondary and pseudosecondary FIs.

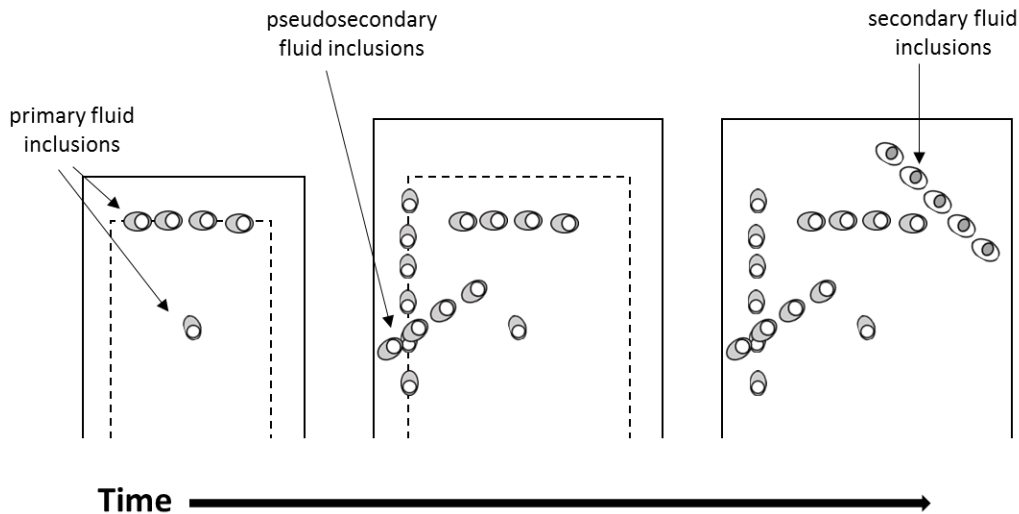


Figure 1.1: Schematic representation of the formation of primary, secondary and pseudosecondary fluid inclusions during crystal growth (adapted from Bodnar, 2003).

Primary FIs that are encapsulated droplets of the solutions from which the mineral crystallized, e.g. in hydrothermally formed minerals like quartz and fluorites. They commonly occur isolated, in small clusters or parallel to crystal faces and are often characterized by ‘negative crystal shapes’, result of re-crystallizations to reducing the surface energy. Observations on their density and

compositions allow to conclude on the trapping conditions. Secondary FIs do not reflect the conditions of mineral formation. If the crystal fractures upon tectonic stress, a new fluid can cause the crack to anneal, while including another generation of FIs. Those secondary FIs commonly occur along paths tracing the annealed crack and often cutting across growth zones of the mineral. Some cracks however are already formed during crystal growth and thus their time of formation is equivalent to primary inclusions but their appearance resembles more those of secondary FIs, thus they are termed pseudo-secondary FIs (Figure 1.1).

In prepared thick sections (100 to 300 μm thickness) of minerals or rocks FIs can be observed with a regular polarization microscope as their size typically ranges from 5 to 100 μm (Markl, 2004). Figure 2 shows an example of a multi-phase inclusion in quartz. The exsolution into liquid and gas and in some cases precipitation of multiple daughter crystals, such as halite, sylvite or barite, upon cooling of an originally homogeneous fluid trapped at high temperatures is a common phenomenon.

FI microthermometry is performed on selected chips of thick sections and is based on the phase changes occurring within the FIs during heating and cooling. Employing a heating/freezing stage the reverse process can be observed. When heating the FI the solids melt and the vapor bubble shrinks until it finally disappears at the temperature of homogenization. This temperature represents the minimum trapping temperature and gives an indication of the bulk density of FI. The temperature of melting is defined as the temperature at which the last (usually ice-) crystal melts under reversed equilibrium conditions. It provides information on the chemical composition and the salinities of the mostly aqueous solutions can be calculated as NaCl-equivalents (Roedder, 1962). When the approximate compositions are known, e.g. if it is a $\text{CH}_4\text{-H}_2\text{O}$ or $\text{NaCl-H}_2\text{O}$ mixture, and the temperature of homogenization known, diagrams of the corresponding isochores can be used to determine density and trapping temperature.

Also observed via microthermometry is the thermal decrepitation upon heating. This process is irreversible as the FIs are destroyed once the internal pressure surpasses the confining pressure/lithostatic pressure of the host mineral. Besides the internal pressure of the FIs, parameters controlling their decrepitation are the size of FIs and mineral hardness and cleavage. Quartz is more likely to preserve unaltered FIs than softer minerals.

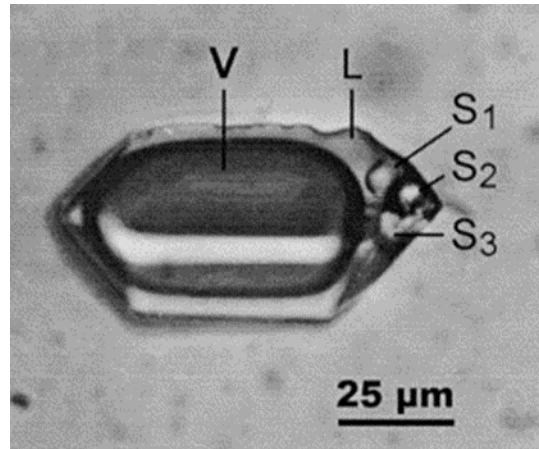


Figure 1.2: Photomicrograph (reprinted from van den Kerkhof and Hein, 2001; with permission from Elsevier) of a multi-phase FI in a smoky quartz containing a large CO₂ vapor bubble (V), surrounded by a saturated liquid phase (L) and three daughter minerals (S₁, S₂, S₃).

Even for halites, experimental studies have shown that leakage and deformation of FIs is not a common phenomenon in halites and that predominantly larger FIs were affected under influence of high geothermal gradients (Wilcox, 1968).

Conclusions on thermobaric history, however, always have to be made with care.

Gas-rich FIs are preserved better than inclusion with a large volume fraction of H₂O as their pressure rises less steep upon increasing temperature.

Raman spectroscopy is another helpful tool in order to observe phase changes of solid, liquid or gaseous components but also to identify polyatomic ions in solutions.

Cathodoluminescence is used in FI research to observe micro textures such as dislocations, microcracks and secondary crystallizations which allow to make conclusions on interactions between FI and host mineral (van den Kerkhof and Hein, 2001).

Vitrinite reflectance is a common tool conjointly used with fluid inclusion study to obtain geobarimetric data (Barker et al., 1998; Barker and Pawlewicz, 1986). Fluorescence of natural hydrocarbon FIs is used in micro-spectrometry to retrieve information on crude oil chemistry (Stasiuk and Snowdon, 1997).

Standard textbooks on fluid inclusion research include the volumes by Roedder (1984), Goldstein and Reynolds (1994) and Samson et al. (2003).

More detail on the chemical composition of FIs and their study is provided in Chapter 2.1.

1.3. Organic matter in the lithosphere

Gas-liquid inclusions can be found in all types of rock. Aside permanent inorganic gases (e.g. N₂, Ar, CO₂, O₂) they often contain methane and its homologues (Roedder, 1984; R. H. Goldstein, 2001). Their precursors are usually considered to be of biotic marine or terrestrial origin and incorporated and altered during diagenesis and catagenesis. A few concepts of the abiotic origin of methane and higher-order hydrocarbons also exist and will be outlined following a short summary on basic terms of organic matter precursor and transformations in sedimentary environments.

Diagenesis is the term for rock forming processes following the deposition of sediments. Usually, sediments are overlain or buried and subsequently exposed to increased pressures and temperatures, which entail organic transformations including soil formation, bioturbation and bacterial action, mechanical reworking, reduction of pore spaces, loss of water, dissolution-precipitation reactions, cementation and recrystallization. The threshold to metamorphism is surpassed with the formation of new minerals starting at around 150-200°C (Markl, 2004). Depending on depositional environment, be it fluvial, lacustrine or marine, associated organic matter (OM) of the sediment is exposed to diagenesis and catagenesis. Catagenesis follows diagenesis and this term is used specifically with reference to OM decomposition. Catagenesis is characterized by thermal bond-breaking and alteration of OM sometimes starting at temperatures as low as 60°C, but generally this stage is reached at 100°C (Killops and Killops, 2009). In early diagenesis, all OM is subject to microbial degradation to form humic substances. Initially, low molecular weight peptides, carbohydrates and amino acids, which are water soluble, can be assimilated by the decomposer communities. Heterotrophic, thermophilic microbes prevail also at elevated temperatures. Extracellular enzymes of fungi and bacteria can hydrolyze insoluble proteins and polysaccharides, making higher molecular weight compounds available. The resistance towards microbial degradation increases from proteins to carbohydrates (forming hexoses and pentoses) to lipids to lignin. The chemical residues from microbial degradation undergo condensation reactions, often between sugars and amino acids. The series of to date still incompletely understood reactions are also known as Maillard reactions (Killops and Killops, 2009; Sposito, 1989) results in highly complex organic residue, also called geopolymers (Killops and Killops, 2009). These dark colored organic residues are called humin in soils, brown coal in coal

mires and kerogen in marine and lacustrine sediments. The precursors to the geopolymers are also called humic substances. As opposed to the generally accepted polymeric concept, they are currently also looked at as supramolecules: an assembly of diverse, relatively low molecular weight components. Instead of covalent bonds, these dynamic associations are thought to be stabilized by hydrophobic and hydrogen bonds, which are also responsible for the apparent large size (Sutton and Sposito, 2005; Piccolo, 2002). Thus, the exact structure of humic substance is still unknown and as the starting materials from which they are forming can differ considerably, the structure of humic substance also depends on location.

To understand involved reaction mechanisms, model compounds have to be employed. The quinones, and especially dihydroxbenzene catechol, are examples for common models of the aromatic fractions of humic substances (see Figure 1.3).

To visualize possible reactions during catagenesis, Figure 1.3 presents the degradation processes for a model vanilloid unit of lignin during coalification. Originally, lignin is produced in the cell walls of plant and some algae via the oxidative coupling of substituted hydroxypropenyl-phenols (*p*-coumaryl), where they are bound covalently to hemicelluloses and provide structural strength for plant growth (Leary, 1980; Vanholme et al. 2010).

With a share of 30% of organic carbon in the biosphere lignin represents the second-most common organic polymer after cellulose (Boerjan et al., 2003) and contributes significantly to humin and brown coal formation but contribute only trace amounts to marine kerogen formation.

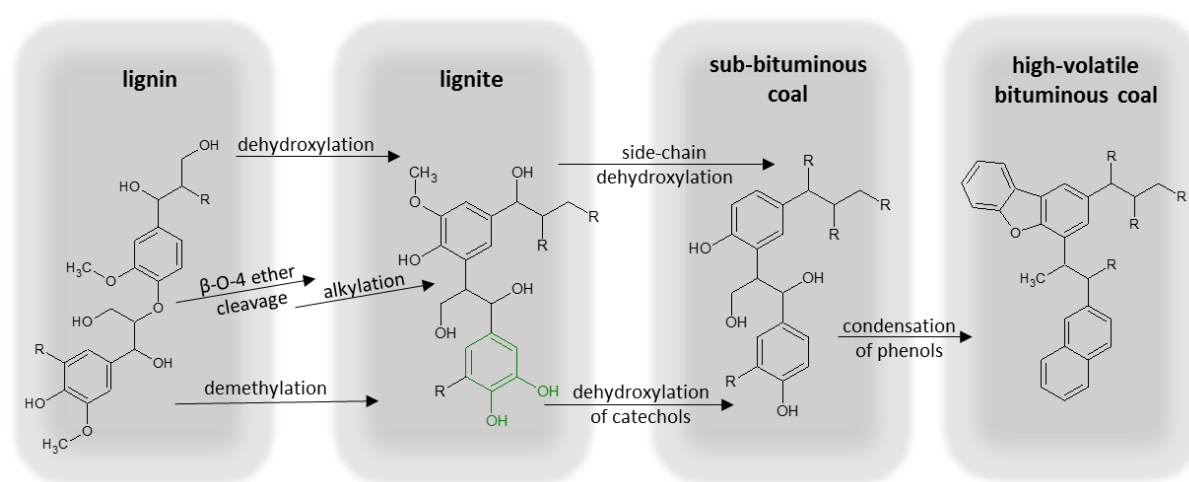


Figure 1.3: Coalification reactions at the example of the vanilloid unit of lignin. Catechol unit in green (after Killops et al. 2004; Hatcher and Clifford, 1997).

The first steps from lignin to lignite are partly mediated by microbial enzymatic attack. Where the β -O-4 ether group is cleaved and phenolic OH groups form, contributing to an increased catechol content, which reaches highest concentrations in lignite. Demethylation and subsequent reductions of hydroxyl groups are increasingly pyrolytically mediated. In the rank stage of bituminous coal, condensation has led to an increase in aromaticity through cyclization and aromatization of side chains. This step also disrupts the morphological structure of wood or plant previously still retained. During the bituminous coal stage, methane, carbon dioxide and water are regarded the main volatile products. Methane and carbon dioxide production increase further towards anthracite formation. Finally, carbohydrates are eliminated and oxygen content decreases, while inherited metal ions seem to be largely retained during peatification and coalification. (Killops and Killops, 2009).

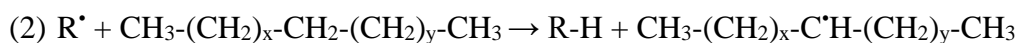
Overall, the observed geochemical changes upon burial are defunctionalization of the carboxyl-, carbonyl- and methoxy- functional groups coupling with an increase of cross linking in the residual mature kerogen. By cleavage of lignin side chains, gaseous and liquids hydrocarbons are produced in low amounts, mostly CH_4 , C_4H_8 and C_{14} liquid hydrocarbons (Salmon et al., 2009).

In order to establish a basis for potential halogenation reactions as will be discussed in section 1.5, it is useful to have a closer look at the reactions generating hydrocarbons. During catagenesis hydrocarbon generation is attributed to two types of reactions: Firstly, n-alkane distribution patterns are best explained by free-radical chain reactions and secondly, randomly positioned single methyl branches on alkenes in oils suggests rearrangement of carbocations formed from alkenes (Kissin, 1987; Kissin, 1998).

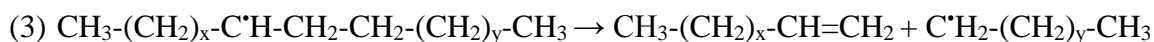
As starting reaction a free radical is formed according to



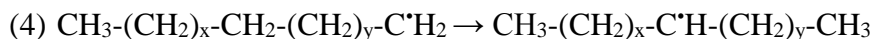
where R^\bullet is an alkyl radical of the formula $\text{C}_n\text{H}_{2n+1}^\bullet$ formed during hydrocarbon generation. Once the radicals with its extremely reactive unpaired electrons are formed the chain-reaction is initiated. The propagation of the chain-reaction can proceed via various reaction schemes such as chain reaction propagation:



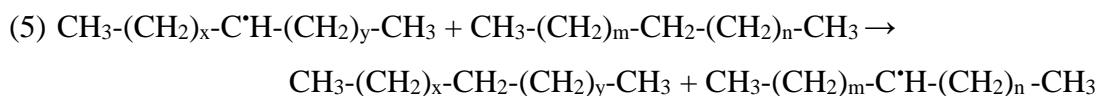
β -scission:



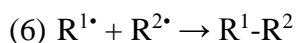
Radical isomerization:



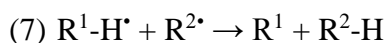
Radical transfer:



The chain-reaction is terminated when the chain reaction is quenched by interaction with another radical via recombination



or disproportionation

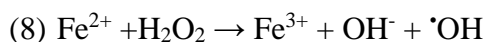


resulting in pairing of the electrons (Killops and Killops 2009).

Thermal cracking in industrial processes also proceeds via radical chain reactions (Gray and McCaffrey, 2002) and the catalyzing characteristics for radical formation of the elements such as iron or nickel (e.g. Greensfelder et al., 1949), or solid acid catalysts such as montmorillonite in industrial applications has long been recognized and employed (Kissin, 1998).

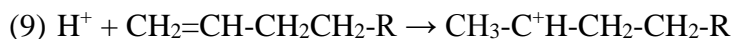
Radical reactions facilitated by e.g. iron, manganese, copper, other transition metal or mineral clay catalysts are also important in early diagenetic stages of organic matter decomposition and new

compound formation (Schöler and Keppler, 2003; Huber et al., 2009; Keppler, 2000). Of special importance in soils is the formation of hydroxyl radicals ($\cdot\text{OH}$) via the Haber-Weiss-reaction,



with the net reaction resulting in a hydroxyl radical (Haber and Weiss, 1932) that can further react with (adsorbed) organic compounds and also trigger chain reactions (Neyens and Baeyens 2003). When Fe^{3+} is reduced by H_2O_2 to Fe^{2+} an iron catalytic Fenton-like reaction cycle has evolved. Under suitable conditions auto-oxidation of Fe^{2+} reducing O_2 to the superoxide $\text{O}_2^{\cdot-}$ radical can follow suite (Barb et al., 1951). See also section 1.8.2 on Fenton chemistry.

The second type of reaction of hydrocarbon generation is the formation of carbocations formed from alkenes, a process that accounts for the occurrence of single methyl branches in oil. An alkane and an α -alkene are the result of hydrogen transfer after cleaving off an alkyl chain. Subsequently, the α -alkene can produce a range of methyl-substituted alkanes by acid catalysis,



yielding the carbocation that in the following can be involved in various rearrangement reactions as summarized in Figure 1.4 (Killops and Killops, 2009).

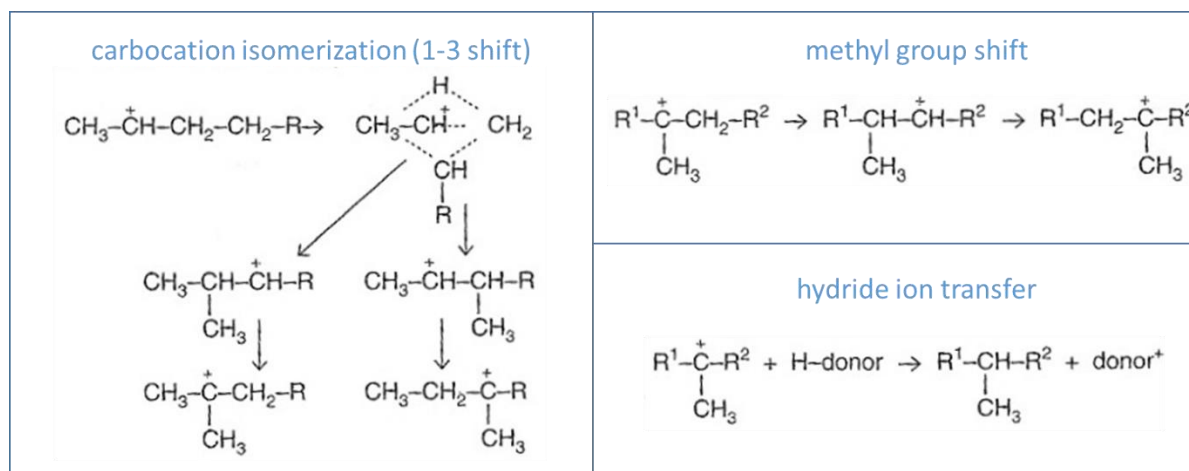


Figure 1.4: Hydrocarbon-generation reactions for methyl-branched alkane formation after carbocation is formed (see equation 9) (after Killops and Killops, 2009).

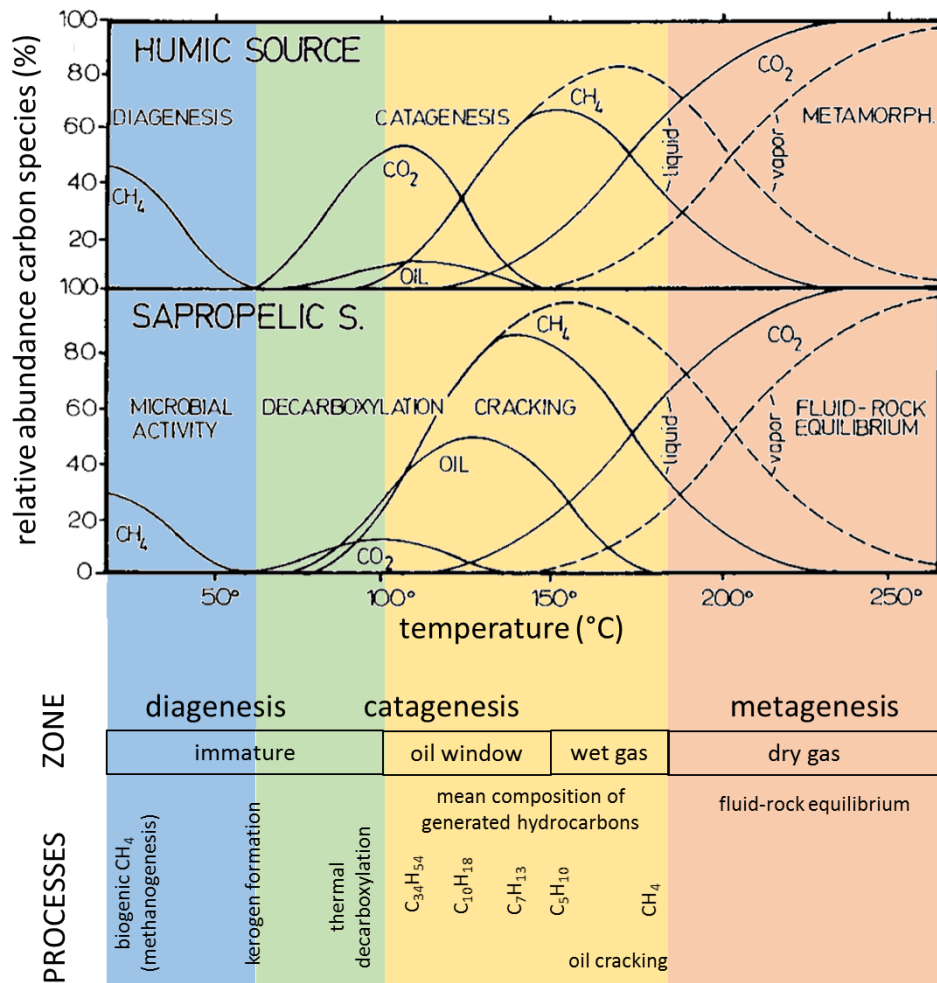


Figure 1.5: The composition of C-containing fluid evolved from a humic (top) and sapropelic (bottom) source as a function of temperature (adapted from Giggenbach (1997) and Killops and Killops, 2009). For temperatures >150 °C compositions are shown as free vapour phase (dashed lines) as well as dissolved in aqueous liquid (solid lines) in equilibrium with crustal rock. The diagenesis-catagenesis boundary is variable and can be placed between 50 and 100 °C.

With regard to the role of light hydrocarbons, especially that of methane, as precursor in VOX formation, an overview of favorable hydrocarbon formation is given in Figure 1.5.

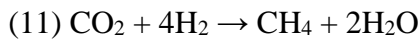
While initial methane production is high due to microbial activity, increased burial and temperatures lead to large amounts of CO₂ being formed as a result of decarboxylation of (humic) kerogens with a maximum at 100 °C. Subsequent temperature increase promotes cracking of kerogen or secondary cracking of higher hydrocarbons, peaking at 150 °C (Giggenbach, 1997). At even higher temperatures the CH₄ and CO₂ content is increasingly controlled by an approaching

equilibrium with the host rock, e.g. the fayalite-magnetite-quartz buffer. Conversely, redox potentials as reflected by CH₄ and CO₂ contents are closely controlled by interaction with Fe(II) and Fe(III) (Giggenbach, 1997).

Methane is predominantly produced by microbial fermentation during diagenesis and upon rising temperature as a result of oil cracking (wet gas stage of catagenesis). Early diagenetic sulfate rich (marine) settings are dominated by methyl type fermentation, e.g. acetate fermentation.

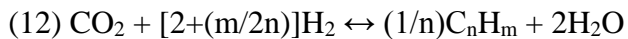


Once sulfate reducing bacteria have exhausted available labile carbon, a sulfate reducing environment has formed and methanogenesis proceeds via carbonate reduction



This second methanogenic pathway is favored as methanogenic substrates such as acetate are depleted, and bicarbonate is available (Abrams, 2005). Both pathways (10) and (11) result in different isotopic signatures. Together with the ratio of ethane (thermogenic) to ethene (bacterial) the methane isotopic ratio is used to estimate the thermogenic influence on hydrocarbon origin (Abrams, 2005).

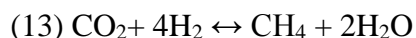
A divergence from the typical thermogenic methane to ethane and propane ratio smaller than 100 when derived from organic matter indicates also an abiotic origin of methane (Fiebig et al., 2009). One possible abiotic formation pathway for methane is of the Fischer-Tropsch type



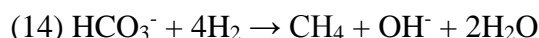
for example at hydrothermal vent as discovered at the East Pacific Rise (Welhan, 1988) and in other crustal fluids in which methane has been discovered. Enrichment of ¹³C in methane is typical for isotopic equilibrium at temperatures > 500°C within the host rock and corresponding isotopic signatures are consistent with the concept of methane formation within the rock prior to hydrothermal extraction (Welhan, 1988). These reduction reactions of the type in equation (12) are thought to occur during magma cooling and in hydrothermal systems during water-rock

interactions (Sherwood Lollar et al., 2002). Sherwood Lollars (2002) isotopic studies on light hydrocarbons C1-C4 in field samples were in favor of a polymerization starting methane precursor to form higher hydrocarbons.

A second possible reaction is the selective abiotic reduction of CO₂,



known as Sabatier's reaction, originally involving nickel as catalyst (Fiebig et al., 2009). This type of reaction was also reported from the Lost City hydrothermal field,



where serpentinization of ultramafic rock provides the hydrogen required for the reaction (Russell et al., 2010). Thus, a third abiotic methane production pathway, also a first step in abiogenesis, independent from a sedimentary organic matter source can be considered next to the classical division of hydrocarbon/methane formation into bacteriogenesis and thermogenesis (Figure 1.6).

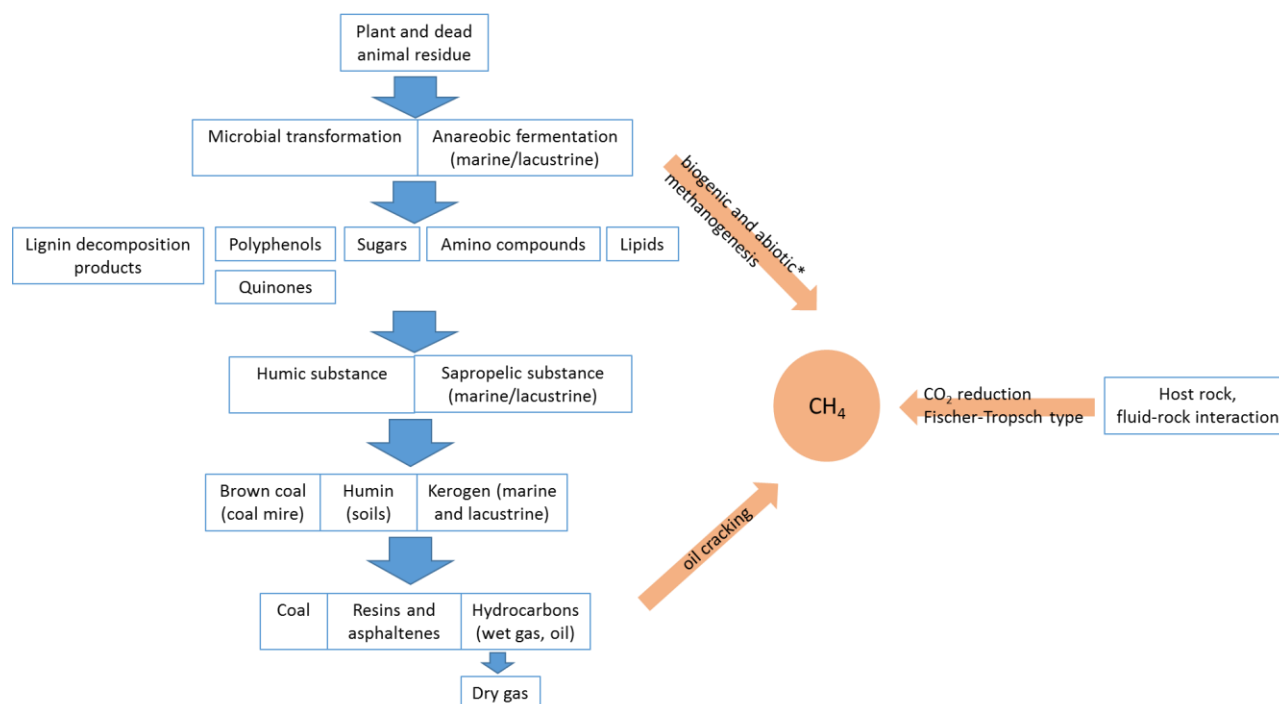


Figure 1.6: Schematic summary of diagenetic, catagenetic and metagenetic (dry gas) stages of decomposition and accordingly hydrocarbon generation. Processes leading to CH₄ evolution are emphasized in light orange. Asterisk indicates reference to Althoff et al. (2014).

Most recently, an abiotic methanogenetic pathway under ambient temperature and pressure as well as oxidizing conditions has been described by Althoff et al. (2014) where iron (II/III), hydrogen peroxide and ascorbic acid are employed as reagents, to convert S-methyl groups of organosulfur compounds into methane. The precursor for this reaction is supplied by biota. Due to low concentrations of total organic matter in ancient rocks, the breakdown of hydrocarbons during metamorphism and loss over time, extractable oil or organic matter from these source rocks, e.g. from early Precambrian, are uncommon. However, in some cases the OM was preserved within FIs for billions of years providing biomarkers and insights into timing and conditions of entrapment or addressing questions of abiotic organic matter formation (see next section 1.4).

1.4. Organic matter in fluid inclusions

The previous section has presented the various sources for hydrocarbons in the geosphere and discussed some of their formation mechanisms. In section 1.2, it was stated that FIs occur in most naturally grown crystals and that they contain entrapments of other minerals, melts, fluids and gasses present at the mineral surfaces during crystal growth. Consequentially, FIs can also represent archives for organic matter e.g. in the form of hydrocarbons, biomarkers (organic compounds, also hydrocarbons, from which biological origin can be inferred) and other organic matter compounds present in the initial fluid.

FI analysis of oil and natural gas bearing FIs has become an important tool in petroleum exploration to investigate porosity evolution, thermal history, source regimes and migration pathway and mechanisms, product type and quality. C₁-C₁₃, BTEX (benzene, toluene, ethylbenzene and xylenes) and organic acids are determined from FIs in relation to oil and gas exploration. Ore geologists evaluate the role of organic matter in terms of transport and deposition of metals in sedimentary basins (Etminan and Hoffmann, 1989). In order to illustrate the diversity of hydrocarbons in FIs, Table 1.1 contains a list of low molecular weight hydrocarbon functional group fragments, as used for identification of their MS spectra. Complementary, Figure 1.7 shows a chromatogram of higher molecular weight *n*-alkanes and *n*-alkan-ols present in oils. A list of aliphatic and aromatic hydrocarbons observed in FIs determined with our GC-MS system (Chapter 2) is provided in the attachment (Table 6.10).

Table 1.1: Major chemical constituents of low molecular weight (C_1 - C_{12}) volatile compounds present in oil fluid inclusions and extracted by online crushing from cuttings samples (from Jorge et al., 2011; based on Barclay et al., 2000).

m/z	Identification	Structure	Description
15	$^+CH_3$ (Methyl)	$^+CH_3$	C_1 fragment ($^+CH_3$); largely methane
57	$^+C_4H_9$ (Butyl)		Contribution of C_4 fragments of higher Paraffin
60	CH_3COOH (Monocarboxylic acid)		Acetic acid
71	$^+C_5H_{11}$ (Pentyl)		Contribution of C_5 fragments of higher paraffin
77	$^+C_6H_5$ (Phenyl)		Contribution of benzenoid species
78	$^+C_6H_6$		Benzene
91	$^+C_7H_7$ (Benzyl)		Toluene; xylene; alkyl-benzenes
97	$^+C_7H_{13}$ (Alkyl cyclic)		C_7 alkylated cyclic alkanes fragments

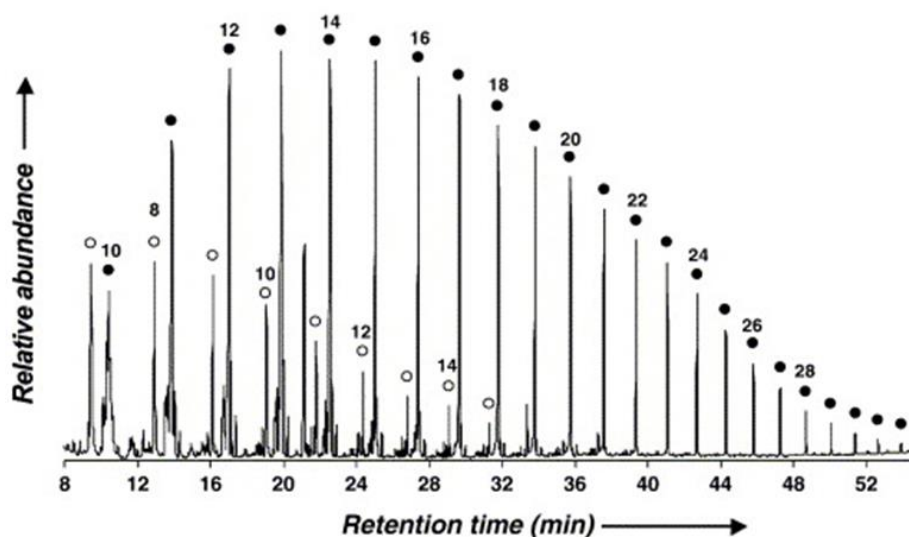


Figure 1.7: Example total ion chromatogram from GC-MS analysis of non-volatile compounds after dichloromethane extraction from crushed FIs (from McCollum et al., 2006; with permission of American Chemical Society). Closed circles are n-alkanes, open circles are n-alkanols. Numbers indicate the carbon chain length. Low molecular weight hydrocarbons have partially been lost during evaporation in sample preconcentration. Isotopic signature data in that study suggested a possible abiotic formation.

OM in FIs could potentially reflect ambient life. When rocks are heated to 200°C to 300°C most large biomolecules are destroyed, while alkanes and aromatic compounds prevail. As pointed out with reference to impact events by Parnell et al. (2006) biomolecules have a higher chance of survival when trapped in a FI.

Stability of complex aromatic hydrocarbons within fluid inclusions at temperatures up to 300 °C is evident (Dutkiewicz et.al., 2003). Therefore, preservation of hydrocarbons in fluid inclusions in crystalline rocks should be possible.

Parallel to the discussion on the origin of methane in section 1.3, hydrocarbons in FIs of igneous rock can be attributed to thermal decomposition from organic matter of overlying sedimentary source rocks. Examples are the a widespread occurrence of bitumen in basement rocks in Scandinavia (Munz, 2001), gas-condensate inclusions with alkane homologues up to C₁₅ in the crystalline basement in South Norway (Munz, 2001) and numerous complex hydrocarbons in granite plutons in the British Isles (Parnell et al., 2006). More extensive lists of hydrocarbon occurrences associated with igneous rocks can be found in Schutter (2003) and Potter and Konnerup-Madsen (2003). Ketone isomer formation was attributed to flash pyrolysis of kerogen during the intrusion of dolerite into overlying strata, which was recognized as the first and oldest phase of hydrocarbon migration in 1280 Ma sill within the Mesoproterozoic Roper Group in the Roper Superbasin, Australia (Dutkiewicz et al., 2004). In the same formation, the occurrence of the biomarkers monomethylalkanes, pentacyclic terpanes chiefly comprising hopanes and diahopanes, and minor amounts of steranes and diasteranes was attributed to input from cyanobacterial organic matter and a minor contributions from eukaryotes derived from overlying Proterozoic source rock (Dutkiewicz et al., 2004).

In contrast, there are several examples for hydrocarbons from FIs in crystalline rocks where an abiotic formation mechanism was indicated.

Sherwood Lollar et al. (1993 and 2006), showed that deep subsurface fluids in Canadian and Fennoscandian (Precambrian) shield rocks are dominated by reduced gases such as CH₄ and up to 30 vol%. ¹³C-enriched CH₄ supports an abiotic gas formation. Other studies explained the hydrocarbons within FIs by an abiotic origin, including hydrocarbon gas inclusions in Ilimaussaq igneous complex in southern Greenland (Konnerup-Madsen et al., 1979; Potter and Konnerup-Madsen, 2003), methane-bearing fluid inclusions in alkaline igneous intrusions of the Kola igneous province (Potter et al., 1998) methane and higher hydrocarbons in granite and dolerite intrusions

at Siljan, Sweden (Jeffrey and Kaplan, 1988), hydrocarbon inclusions containing saturated and unsaturated aliphatics in pegmatite quartz in granite at Strange Lake, Canada (Salvi and Williams-Jones, 1997) methane and higher hydrocarbons in fractures in crystalline rocks of the Canadian shield (Sherwood Lollar et al., 2002).

In summary, FIs archive organic matter of the initial fluid, be it of biotic or abiotic origin. The amount of fluid inclusion studies on a wide range of different organic matter compound is huge. The occurrence of hydrocarbons within FIs of rocks of sedimentary and diagenetic systems is obvious. Little is known about halogenated organic species (see also section 1.5).

Hydrocarbons observed are suitable to serve as precursors for potential halogenation reactions. Investigations on halogenated organic compounds from FIs are not part of standard (petrological, industrial) FI analysis and will be included in the preceding section 1.5 and are also part of the introduction to Chapter 2.

1.5. VOC, VOX and naturally produced organohalogens

For the term volatile organic compounds, abbreviated VOC, numerous definitions are in use. In this work, VOC is used as the general term for the group of organic chemicals with low boiling points, i.e. compounds that are gaseous at standard temperature and pressure. Numerous compounds fall in this category and they can be naturally produced or man-made. They are likewise as ubiquitous as they are varied and can be sulfurated, nitrated or halogenated.

VOSC, abbreviated for volatile organic sulfur compounds, contains at least one sulfur atom and this group is an important agent in aerosol formation via oxidation to acidic H_2SO_4 , impacting cloud condensation, local climate and the radiation budget (Charlson et al., 1992). VOSC are partly subject of Chapter 4 and Table 1.3 provides an overview of these compounds observed in rocks and minerals.

VOX, volatile organic halocarbons, is used as a more specific term for the sub-group of the VOCs bearing at least one halogen, which can be fluorine, chlorine, bromine or iodine. Halons, a group of low boiling-point hydrocarbons with at least one hydrogen substituted by a halogen, belong to this group. Also included in the term VOX are the renowned CFCs (chlorofluorocarbons) and HCFS (hydrofluorocarbons). Popular for their stability and low boiling points CFCs were used

amongst others as refrigerants, propellants and fire extinguishing agents. Their extraordinary longevity in the atmosphere, where they are enriched over time and act as greenhouse gases and participate in catalytic ozone depletion lead to their banning for industrial applications in the Montreal protocol 1989. Today, atmospheric CFC mixing ratios are constant or even decrease again as a result of this international agreement (UNEP, 2009). Many VOX, naturally produced or man-made, are of significance due to their role in ozone-depletion as a source for halogen radicals or as greenhouse gases within the earth's atmosphere. Chlorinated and brominated species are predominantly involved in catalytic ozone depletion. Already at low concentrations they influence radiation budget and climate. Examples are naturally produced CH_3Cl , CH_3Br for stratospheric ozone depletion or SF_6 as the most potent greenhouse gas with a global warming potential 23.500-times that of CO_2 (IPCC, 2013).

Today, nearly 5000 naturally produced organohalogen compounds were isolated and identified (Gribble, 2010). Natural organohalogens refer to all classes of chemical compounds naturally produced that bear a halogen in their structure. Most compounds are chlorinated or brominated but a few also carry one or more iodine and fluorine atom. They are produced by living organisms such as terrestrial plants, fungi, lichens, bacteria insects, some higher animals and humans or are formed during natural abiotic processes such as volcanoes eruptions, forest fires and other geothermal processes (Gribble, 2003). Many of the naturally produced VOX, have been recognized and studied since the 1980s. MeCl and MeBr are known to have significant natural sources. Not all compounds of the group of natural organohalogens are volatiles and most identified organic halogen compounds were found in the marine environment (Ballschmiter, 2003; Moore, 2003; Gribble, 2010).

Table 1.2: Halide concentrations (mg/kg) in different environmental compartments (Gribble, 2009).

Halide	Oceans	Sedimentary rocks	Fungi	Wood pulp	Plants
Cl^-	19,000	10-320	-	70-2100	200-10,000
Br^-	65	1.0-3.0	100	-	-
I^-	0.05	0.3	-	-	-
F^-	1.4	270-740	-	-	-

Table 1.2 shows the distribution of halides in the environment, which is reflecting the distribution of organohalogenes occurring in nature. The relative importance of fluorinated compounds for geologic environments is emphasized.

The most recent comprehensive overview on naturally produced organohalogenes is available in the volume by Gribble (2010).

1.6. Geogenic organohalogenes

The studies on natural formation of organohalogenes in terrestrial environments mainly involve biotic activity. In the pedosphere, the dominating terrestrial environmental compartment, studies on abiotic organohalogen formation is not trivial due to the complexity of the system. It is the chemically reactive uppermost part of the lithosphere that interacts with the atmosphere, hydrosphere and biosphere. As soil microorganisms are omnipresent, direct flux measurements cannot differentiate between abiotic and biotic organohalogen production. Studies with model compounds have played a vital role in the revelation of abiotic organohalogen forming reaction mechanisms prevalent in soils (Schöler and Keppler, 2003; Huber et al., 2009).

In the terrestrial environment abiotic formation during diagenetic processes have been subdivided in three groups by Schöler and Keppler (2003), mainly referring to processes at ambient pressures and temperatures: (1) biomass burning, producing methylhalides, (2) early diagenetic processes in soils and sediments, producing VOX, halogenated acetic acids and total organic halogen and (3) volcanoes, accounting for a variety of VOX. The importance of hypersaline salt lakes in the emission of chlorinated volatiles has only recently been discovered (Weissflog et al., 2005; Kotte et al., 2012; Krause 2014) and the contribution of abiotic reactions in this context is still subject of study. With the exception of soils and volcanic emissions lithospheric organohalogenes have received comparatively little attention.

Although, providing potential precursor material, i.e. organic matter and halide as well as transition metals and surfaces for catalytic reactions, as well as a broad range of potentially suitable reaction parameters concerning temperatures and pressures, there are only few studies dealing with VOX from rocks and minerals. This is most likely owing to ‘fluid inclusionists’ that traditionally have petrological study objectives and conversely with environmental and organic chemists, that

apparently do not often perceive rocks as accessible environments. Gases are also known to slowly migrate from the earth interior or gas reservoirs and degas to the atmosphere along mineral grain boundaries; a process known as molecular diffusion or diffusive loss (e.g. Schloemer and Krooss, 2004). Effectively, VOX can be found predominantly within FIs of rocks and minerals that on the one hand archive the composition of the mineral forming fluid and on the other hand can become reaction vessels for secondary reactions.

Despite the fact that fluorine ranks 13th in order of abundance of the elements of the earth's crust, naturally occurring organofluorine compounds are comparatively rare (Banks et al., 1994). Presence of these compounds in the atmosphere and hydrosphere are mainly attributed to anthropogenic sources and a natural origin of compounds such as CCl_2F_2 and CCl_3F , has only in recent years been recognized. Their emission rates compared to anthropogenic sources is very low (Gribble, 2009; Harnisch et al., 2000) but due to their chemical inertness their enrichment in atmosphere or hydrosphere is likely. Same is true for the observation of tetrafluoromethane from FIs in natural fluorites and granites. The occurrence of halogenated VOX in FIs of rocks and minerals are summarized in Tables 1.3. Table 1.4 also reviews the available quantitative data on VOX and the perfluorated compounds NF_3 , SF_6 and CF_4 from FIs and compares them to atmospheric and volcanic gas concentrations. Additional tables of VOC and VOSC can be found in the appendix, Tables 6.10 and 6.11, respectively.

An interesting example for the emission of chlorinated species from sediments is the study of Weissflog et al. (2005), who reported the release of halogenated C_1/C_2 compounds as trichloroethene, tetrachloroethene and dichloromethane, tetrachloromethane and trichloromethane which were formed in surface sediment of salt lakes. Although they attributed the organohalogen occurrence to microbial activity, especially of archaic halobacteria, it appears plausible that these compounds when entrapped in FIs could also become archived in geologic salt deposits – and be released upon mining. Large amounts of an average 1.6 million t of mineral salts are distributed as de-icing salts on the roads every winter in Germany alone (Statista, 2014) releasing the entrapped gases.

Volcanoes are a major source of stratospheric hydrogen fluoride and hydrogen chloride and also significant amounts of methane. Stoiber et al. (1971) were the first to report the presence of organofluorine compounds, including some CFCs, in the volcanic gases from the fumaroles of the Santiaguito volcano in Guatemala. Additional to over 30 organic compounds tetrafluoroethylene,

hexafluoropropene, chlorodifluoromethane, chlorotrifluoroethylene, dichlorofluoromethane, trichlorofluoromethane, and 1,1,2-trichloro-1,2,2-trifluoroethane have been identified in that study. In solfataric gases of the Kamchatka volcanoes on the Siberian peninsula Isidorov et al. (1990, 1991) have identified dichlorodifluoromethane and reported dimethyl difluorosilane and at one vent concentrations of these organofluorines exceeded background levels by 400 times. Over 300 organohalogen compounds from volcanoes have been observed, predominantly fluoro- and chlorinated but also a few brominated ones. Jordan et al. (2000), reviewed the various studies. Generally, the studies agree that halogenated methanes are the predominant molecules emitted by volcanoes. However, in some samples of lava gas, chloroethyne, chloroethene and chlorobenzene showed comparable concentration levels as methyl chloride (Jordan et al., 2000).

The set of organic halocarbons produced by volcanoes thus include (poly-)fluorinated volatiles, but their concentrations are often at or below concentrations of ambient air (see also Table 1.4).

In the hydrosphere, SF₆ and other CFCs are of special relevance, since they are employed in dating young groundwater. Data obtained can be used to determine recharge rates of aquifers, to calibrate models of groundwater flow, evaluate contamination potential or determine remediation times and to obtain information on microbial or geochemical processes rates in aquifers (Busenberg and Plummer, 2008). Erratically high SF₆ values threw off a reasonable data interpretation and suggested a terrigenous source, for groundwater from fractured silicic igneous rocks, from some carbonate aquifers, from some hot springs, and groundwater from volcanic areas (Busenberg and Plummer, 2010; Koh et al., 2007).

Upon combustion of natural gas, 15% to 100% of the ambient levels of CF₄ have been reported from measurement of the exhaust gas (Harnisch and Eisenhauer, 1998).

Also, the sources for evenly distributed concentrations of 200 ng/L trifluoroacetic acid (TFA) throughout the world's oceans have yet to be identified (Frank et al., 2002) with Harnisch et al. (2000) suggesting the hypothesis that accessory fluorite in granites might be responsible.

Input of geogenic VOX to the atmosphere may take place via weathering, crustal degassing, diffusion, volcanic activity, mining and oil drilling operations, combustion of natural gas and oil and the use of road salt but the contributions from each segment is not further constrained.

Table 1.3: VOX from minerals. The term ‘grinding’ under treatment implies that these compounds were detected with the system presented in Chapter 2.

compound name	formula	structure	martix	treatment	reference
methyl chloride	CH ₃ Cl		halite, gypsum	heating, grinding	Sevensen et al., 2009; Bugla, 2010; Krieger, 2014
methyl bromide	CH ₃ Br		halite	heating, grinding	Sevensen et al., 2009; Bugla, 2010; Krieger, 2014
1-bromo-2-chloroethane	C ₂ H ₄ BrCl		halite	grinding	Krieger, 2014
1-chlorobutane	C ₄ H ₉ Cl		halite, gypsum	heating, grinding	Sevensen et al., 2009; Krieger, 2014; Bugla, 2010
1-bromobutane	C ₄ H ₉ Br		halite	heating	Sevensen et al., 2009
trichloromethane	CHCl ₃		halite, sylvinite,	grinding, heating	Isidorov, 1998; Krieger, 2014; Bugla, 2010
chlorobenzene	C ₆ H ₅ Cl		halite	grinding	Krieger, 2015
chloroethene	C ₂ H ₃ Cl		halite	heating	Bugla, 2010
dichloroethane	C ₂ H ₄ Cl ₂		halite	heating	Bugla, 2010
bromoethane	C ₂ H ₅ Br		halite	heating	Bugla, 2010
carbon tetrafluoride	CF ₄		fluorite, granite,	milling	Hamisch and Eisenhauer, 1998; Harnisch et al., 2000
sulfur hexafluoride	SF ₆		fluorite, granite,	milling	Hamisch and Eisenhauer, 1999; Harnisch et al., 2000
dichlorodifluoromethane	CF ₂ Cl ₂		fluorite, granite,	milling	Hamisch et al., 2000
trichlorofluoromethane	CFCl ₃		fluorite, granite,	milling	Hamisch et al., 2000
chlorotrifluoromethane	CF ₃ Cl		fluorite	milling	Hamisch et al., 2000
trifluoromethane	CHF ₃		fluorite	milling	Hamisch et al., 2000
nitrogen trifluoride	NF ₃		fluorite	milling	Hamisch et al., 2000
dichloromethane	CH ₂ Cl ₂		sylvinite, carnallite, halite, urtite	not specified	Isidorov, 1998
tetrachloromethane	CCl ₄		sylvinite, carnallite, halite, urtite	not specified	Isidorov, 1999

Table 1.4: Literature data on VOX, NF₃, SF₆ and CF₄ concentrations extracted from rocks and minerals in comparison to atmospheric and volcanic gas concentrations.

compound name	molecular formula	molecular weight	boiling point °C	atmospheric conc. pmol/mol	conc. in volcanic gases nmol/mol	extracted from rock pg gas/g rock
carbon tetrafluoride	CF ₄	88.01	-128	75 ^a	-	1-61000 ^c
nitrogen trifluoride	NF ₃	71	-129.1	0.5 ^a	-	✓ ^c
sulfur hexafluoride	SF ₆	146.06	-64	5.5 ^a	-	0.2-30000 ^c
chlorotrifluoromethane	CClF ₃	104.46	-81	3 ^a	-	0.5-460 ^c
trifluoromethane	CHF ₃	70.01	-82	~4 ^a	-	✓ ^c
dichlorodifluoromethane	CCl ₂ F ₂	120.91	-29.8	535 ^a	0.11-160 ^b	0.6-1200 ^c
trichlorofluoromethane	CCl ₃ F	137.37	23.7	255 ^a	0.03-78.9 ^b	✓ ^c
dichloromethane	CH ₂ Cl ₂	84.93	39-40	25 ^a	0.01-70 ^b	✓ ^d
methyl chloride	CH ₃ Cl	119.38	-24.2	528 ^a	0.61-200 ^b	500-161000 ^e
methyl bromide	CH ₃ Br	94.93	3.6	10 ^a	0.01-218 ^b	0-12600 ^e
1-chlorobutane	C ₄ H ₉ Cl	92.57	78	-	-	0-50900 ^e

^a Warneck and Williams, 2013^b Jordan, 2003^c Harnisch, 2000; Harnisch and Eisenhauer, 1998^d Isidorov, 1998^e Svenson, 2009

1.7. Behaviour of halogens in rocks and magma

From Table 1.5 it can be deduced, that in many cases fluorination is likely to dominate the halogenation processes in the lithosphere, due to the abundance of fluoride. However, amounts of organofluorines observed are relatively small. Table 1.5 shows that the bond dissociation energies from hydrogen and carbon for the hydrogen halides increase drastically from iodine to fluorine. Iodine forms radicals most easily, whereas for example the HF in volcanic gases is extremely stable and even at 1000°C no direct fluorination of hydrocarbons is likely to occur (Jordan et al., 2000).

In general, organohalogen compounds are chemically outermost stable (see Table 1.5) and this stability also explains the chemical inertness that raised concerns on CFC production.

Of all elements fluorine is the element of highest electronegativity, making it extremely reactive. The F_2 molecule is one of the strongest oxidants, therefore, when found in nature it is mostly bound in compounds, predominantly in halides. Even water is oxidized by F_2 to form hydrofluoric acid and oxygen.

The long suspected occurrence of molecular fluorine in antozonite, a variety of fluorite also known as stinkspar, has only recently scientifically been confirmed using NMR (nuclear magnetic resonance spectroscopy) (Schmedt auf der Günne et al., 2012), see also section 1.8.6 on radiochemical reactions. Fluorspar (CaF_2) besides fluorapatite ($Ca_5F(PO_4)_3$) and cryolite (Na_3AlF_6) are the economically most important fluoride minerals. Chloride is found in sea water and brines and in sedimentary halite ($NaCl$) and sylvite (KCl).

Table 1.5: Parameters influencing halogenation reactions for the different halogens and their distribution in geologic environments.

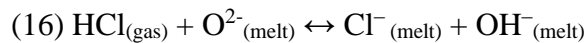
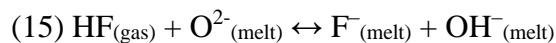
	F	Cl	Br	I
atomic mass ^a	18.998	35.453	79.904	126.904
electronegativity (Pauling) ^a	4	3	2.8	2.7
ionic radius (pm) ^a	1.33	1.81	1.96	2.2
C-X bond length C-X (pm) ^a	134	176	193	213
C-X bond dissociation energy (kJ/mol)	536	397	280	209
H-X bond dissociation energy (kJ/mol)	569.9	431.6	366.3	298.4
X-X bond dissociation energy (kJ/mol)	156.9	242.6	193.9	152.5
concentration (mg/kg)				
basalt ^b	50-300	50-200	0.050-2.5	0.004-0.011
andesites ^b	240-640	1000-1800	-	-
rhyolites ^b	400-640	600-1900	-	-
sedimentary rocks (as halide) ^b	270-740	10-320	1.0-3.0	0.3
continental crust average ^c	585	145	2.4	0.45
Fluid/melt partitioning coefficients ^b	<<1	8.0-10	3.7-17.5	104
Hydrogen halide concentration in volcanic gas (vol%) ^b	0.003-0.7	0.02-6	n/a	n/a

^a Lide, 2004

^b Jordan, 2000

^c Gribble, 2009

Due to the similar ionic radii of O^{2-} (140 pm), OH^- (132 pm) and fluoride (133 pm) (Lide, 2005), fluoride is a frequent isomorphous substituent in minerals such as amphiboles, mica and apatite (Wedepohl, 1995) and is readily soluble in silicate melts, up to more than 10 wt% (Carroll and Webster, 1994), so that is relatively enriched to a co-existing gas phase. The crystal lattices formed during early magmatic differentiation do not, with the exception of apatite, offer spaces for the incorporation of fluoride ions. Therefore residual magmas are often enriched in fluoride. Fluoride that cannot be incorporated in the crystalline phase accumulates in hydrothermal fluids, from where it is either deposited as fluorite or continues to react with the surrounding rock (Wedepohl, 1995). The dominating volcanic gases HCl and HF that are also major sources for atmospheric HF and HCl (Jordan et al., 2000), are dissolved in magma according to Holloway (1981) in analogy to water:



Like water, fluoride also depresses the melting temperature and decreases the density of a silicate melt (e.g. Holtz et al., 1993; Baker and Vaillancourt 1995; Webster et al., 1987). Infinite solubility of water in a F-, B-, and P-rich melt at shallow intrusion depth with $T \geq 720$ °C has been reported by Thomas et al. (2000). Their work and the studies of Veksler et al. (2004) and Dolejš and Baker (2007b) demonstrated that silicate, alkali-rich melts with high volatile content (H, F, Cl or B) coexist with a hydrothermal fluid down to low temperatures, e.g. 540 °C at 1 kbar before granite crystallization begins (Dolejš and Baker, 2004). Köhler et al. (2008) assumed that this effect of high fluoride concentration may have caused the extraordinary high abundance of fluoride in Ivigtut cryolite and fluorite with the melt still existent at 400–450 °C.

Contrary to fluoride, the larger ionic radii and smaller electronegativities of the heavier halides Cl^- and Br^- do not substitute significantly for oxygen in minerals or silicate melts (Aiuppa et al., 2009). The resulting low solubility of chloride in silicate melts also leads to an enrichment of chloride in aqueous fluids (Carroll and Webster, 1994) up to an alkali chloride concentration of 70% (Roedder, 1984). Thus, in volcanic systems fluoride and chloride behave differently and this can be seen in measurements of volcanic gases and melt compositions, see Figure 1.8. A detailed recent review

of data on halogens in volcanic matrix glasses and silicate melts was published by (Aiuppa et al., 2009) and is recommended for further reading.

In magmatic systems, as well as in early diagenetic environments, the formation of organohalogens depends not only on the available precursor compounds methane and halogen or halide. It is also greatly influenced by the presence of catalytically active transition metal compounds (Schöler and Keppler, 2003; Jordan et al., 2000).

It is therefore good to bear in mind, that fluids-rock permeation and interactions can chemically alter volcanic and adjacent host rocks (Reed, 1997). In turn, fluid composition can be altered and in some cases this entails dissolution, transport and precipitation of metals including the transition metals Sn, W, Mo, Cu, Au, Ag, Pt, Hg, Zn, the metallic members of the carbon family Sn and Pb and others (Vigneresse, 2009). Halogens influence the speciation and solubilities of ore metals in magmatic vapors, aqueous liquids and brines. Chloride is sufficiently abundant and acts as the dominant anion in metal-bearing hydrothermal ore-forming solutions (Seward and Barnes, 1997). Complex formation of chloride as a ligand in metal-ore-bearing hydrothermal systems with Na, K, Sr, Li, Rb, Cu, Zn, Sn, U in hydrothermal fluids or fluoride containing complex formation with Li, Rb, Cs, Be, Nb, Sn, U, some rare earth elements and other metals was reported based on experimental and modeling data. Extreme enrichment of alkali-fluorides can be achieved in magmatic-hydrothermal fluids during final magma differentiation in granites, according to melt and fluid inclusion composition (Aiuppa et al., 2009).

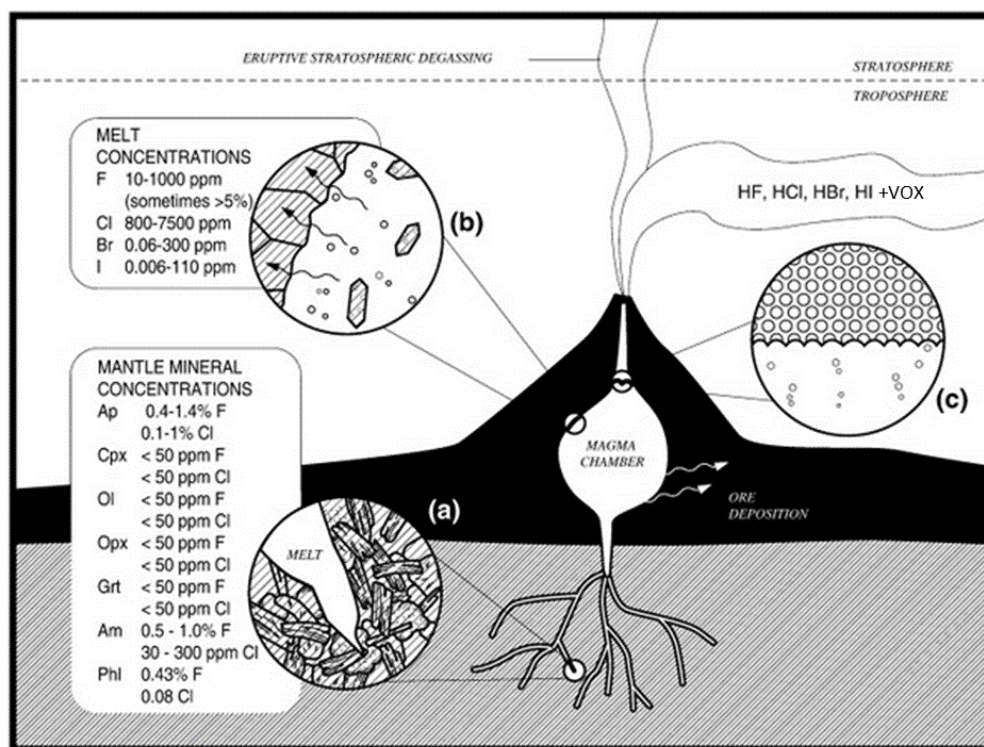


Figure 1.8: Schematic diagram of halogen behavior in mantle melt (a), during crystallization and melt inclusion entrapment in a volcanic magma chamber (b), through vesiculation and initiation of eruption (c) and the injection to the atmosphere. Mineral abbreviations: Ap=apatite, Cpx=clinopyroxene, Ol=olivine, Opx=orthopyroxene, Grt= garnet, Am=amphibole, Phl=phlogopite (modified from Aiuppa et al., 2009; with permission from Elsevier).

1.8. Halogenation reactions in geologic matrices

After having set the stage it is now time to gain more insight into the halogenation of hydrocarbons that might occur in terrestrial environments and geologic matrices. While for soils and sediments several studies on reaction mechanisms exist, and the natural occurrence of these reactions has been confirmed, most studies on halogenation pathways thought to proceed in geologic matrices are practically non-existent. The number of studies concerned with natural fluorinated organics from rocks and minerals is limited and the debate on corresponding formation pathways is largely dominated by speculation.

In this section, we will first have a look at halogenation reactions of relevance as known from the chemical industry and will then proceed from early diagenetic environments, to volcanic activity, to deep burial and metamorphic conditions. The different possible halogenation reactions, that will be presented briefly, will mostly have to be validated experimentally in the future to evaluate their pertinence to the respective geologic setting.

Figure 1.9 gives an overview of early diagenetic and lithospheric environments and processes that actually or potentially form VOX.

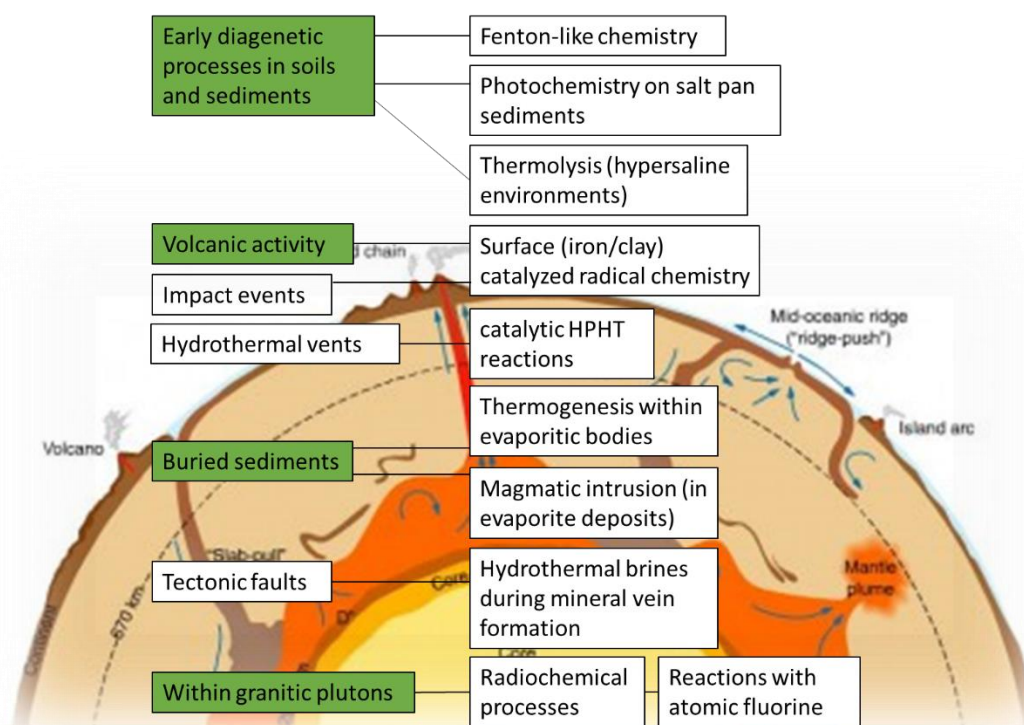
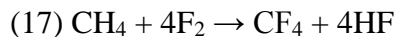


Figure 1.9: Conceptual overview of abiotic volatile organohalogen formation in the terrestrial environment. Green indicates environmental segments from which the occurrence of VOX has been confirmed.

1.8.1. Relevant halogenation reactions

Due to the reactivity of molecular F₂ fluorinated hydrocarbons can directly be produced via the free radical reaction

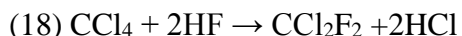


Fluorine can replace hydrogen in any linear or cyclic organic molecule. The replacement of the C-H (417 kJ/mol in CH₄) with C-F bonds (486 kJ/mol in CF₄), makes them shorter and stronger (Siegemund et al., 2000). Due to the violence of the reaction, it must be carefully controlled in the laboratory usually by diluting with inert gas.

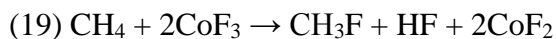
This reaction would spontaneously occur in the lithospheric context whenever F₂ and CH₄ are present, such as in FIs of fluorites.

SF₆ is directly synthesized from its elements.

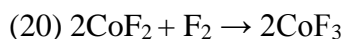
Commercial production of CFC involves nucleophilic substitution of alkyl chlorides with hydrogen fluoride in the liquid phase and in the presence of a catalyst, typically Sb(III)Cl₃. This reaction dates back to the reaction first described by Swarts in 1892, which was later improved for industrial purposes (Weaver, 1984, Siegemund et al., 2000). For example CCl₂F₂ is synthesized via



under addition of Sb(III)Cl₃, with pressure rising to 0.03 kbar after 2h for 24h in a steam-heated autoclave (Siegemund et al., 2000; Okazoe, 2009). The regenerative use of the catalyst is based on oxidizing fluorination reactions as in equation (17) with metal fluorides such as Ag(II)F₂ or CoF₃:



and the spent metal fluoride is regenerated with elemental fluorine



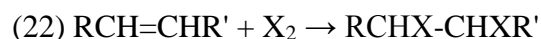
allowing for cyclic industrial production (Siegemund et al., 2000).

In a geologic setting several conditions would have to coincide: elevated temperature and pressures, abundance of HF (also HCl), methane and transition metals. Halogen-fluorine exchange, such as



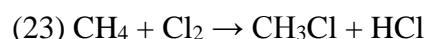
implies previous chlorination of methane. Hydrothermal ore forming magmas and brines with fluid-rock interactions/greisenation might just offer the right conditions for reactions of types (18) to (21). Biosynthetically produced organohalogen compounds, especially organochlorine, could also provide precursors for fluorination.

Next to the aforementioned substitution reactions, the electrophilic addition of fluorine, HF, or reactive nonmetal fluorides to unsaturated bonds is a known reaction mechanism. This reaction is also applicable to the other halogen reactions and proceeds via an intermediate halonium ion:

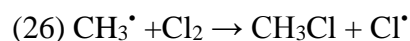
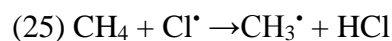
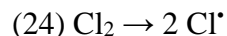


Volcanic activity is known to produce thermodynamically unstable alkenes and alkynes and they can also be a result of thermogenesis of organic matter, where this reaction type could apply.

Industrial production of organochlorine compounds relies almost entirely on chlorination of methane in thermal, photochemical or catalytic reactions. Although in principal the net reaction is the same as for fluorine (17)



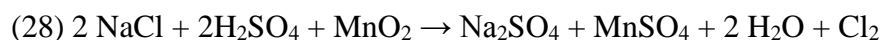
Thermal initiation of the radical chain reaction with $T = 300\text{--}350\text{ }^\circ\text{C}$ is used for the monochlorination. In more detail the chain reaction proceeds as follows:





with (24) initiation of the chain reaction, (25) and (26) chain propagation and (27) chain termination via recombination with $\text{M} =$ walls, impurities or O_2 (Rossberg et al., 2000). As has been shown in reactions (1) through (7) initial radical formation could also be started during catagenetic hydrocarbon formation.

A potential source for elemental chlorine in geologic settings could be the reaction in heated acidic brines:



Depending on pH, chlorine in aqueous solution exists as molecular chlorine, hypochlorous acid or hypochloride



while acidic conditions generate Cl_2 , alkaline conditions favor hypochloride in this reaction (Barcellos da Rosa, 2003).

Conditions of thermal generation of Cl-radicals together with methane are easily achieved in volcanic environments and upon subduction/burial along the geothermal gradient ($\approx 30^\circ\text{C}/\text{km}$) together with increasing lithostatic pressures. Early chain reaction termination in such a complex geologic setting might hinder this reaction type to proceed to significant yields. Within halite or sylvinite deposits this reaction type might be of special importance.

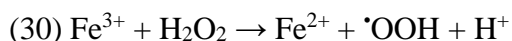
A photochemical Cl-radical formation is potentially applicable to hypersaline salt pan environments (see also section 1.8.2.). Hydrothermal ore-forming vein deposits could conceivably represent catalytic reactions.

Based on these assumptions methyl chloride could exist in a variety of minerals and geological settings.

1.8.2. VOX forming halogenation reactions in soils

The total iron concentrations in soils range from <1% to <20% with a median concentration of around 3% (Loeppert and Inskeep, 1996). Iron in soils exists predominantly in the ferric (III) and ferrous (II) oxidation state, as iron(III) oxide minerals (hematite, goethite, lepidocrocite, magnetite(III/II), maghemite and ferrihydrite), as structural components in layer silicates, or as iron (II) in primary or secondary minerals such as pyroxenes, amphiboles, pyrite and siderite. The concentration of soluble Fe in the aqueous phase is controlled by pH, redox potential, the concentration of organic complexing ligands, the solubilities of the mineral iron phases and the kinetics of their dissolution and precipitation (Loeppert and Inskeep 1996).

The Haber-Weiss-reaction (8) together with the so-called Fenton-like reaction, in which Fe³⁺ is reduced by hydrogen peroxide to ferrous iron



completes a catalytic iron cycle (Barb et al., 1951). The free radicals generated participate in secondary reactions.

Beside iron, other transition metals follow this reaction scheme to produce oxidizing agents with increasing reactivity in the following order: Ni²⁺ < Mn²⁺ < Fe³⁺ < Co²⁺ < Cr³⁺ < Cu²⁺ at circumneutral pH (Strlič et al., 2003).

The formation of terminal halogenated n-alkanes (Keppler et al., 2000, Krause, 2014), chloroethene (Keppler et al., 2002), chloroethyne (Keppler et al., 2006) and trihalomethanes (Huber et al., 2009) based on Fenton chemistry has been reported from model reactions and soil samples and generally correlate to higher iron contents in these studies.

Reactive halogen species (RHS) can be formed in hypersaline environments via Fenton reaction or photochemically. Krause (2014) put forward a concept for the possible production and interaction of RHS in organic matter halogenation in salt pans, which is summarized in Figure 1.10.

Aside from Fenton chemistry, photochemical reactions may play an important role for RHS production within surface sediments of salt lakes. Krause (2014) provided initial field data confirming the occurrence of Cl₂, as well as de VOX like chloromethane, dichloromethane, trichloromethane. The de-novo formation of these compounds supported the validity of parts of the assumed reaction pathway.

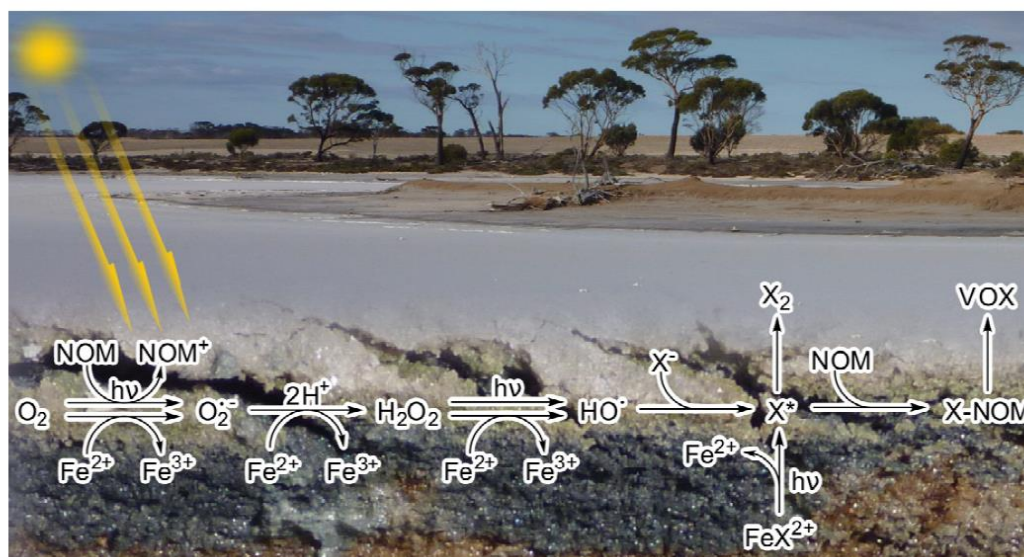


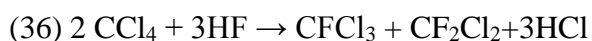
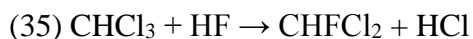
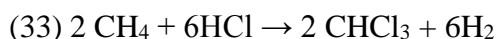
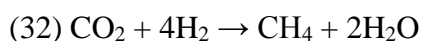
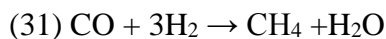
Figure 1.10.: Photochemical and Fenton-like reactions are proposed to interact in this scheme for VOX evolution in salt lake environments developed by Krause (2014). Aside the photochemical initiated auto-catalytic production of the superoxide radical anion, RHS with $X=Cl, Br$ or I is also produced in the reaction with photochemical activated of FeX^{2+} (Figure from Krause, 2014).

Another halogen formation procedure under ambient pressure and temperature and oxidative conditions of soils might be based on the activation of the C-H bond. Possible activation mechanisms involve a two-step procedure in which a cation from a soluble metal salt binds weakly to the C-H bond under equilibrium and successively is inserted between the C-H bond (Bergman, 2007). Oxidative additions in which a halogen is added to the C-H via activated solid metallic materials (heterogeneous catalysts) might have some significance for lithospheric environments. In biochemistry, several enzymes contain complexes of iron with a double bond to oxygen. In reaction with the C-H moiety they could yield a carbocation and an intermediate iron complex containing the hydroxyl group. If the hydroxyl transfers back or the iron complex oxidizes back it could continue reactions in a catalytic cycle (Bergman, 2007).

1.8.3. Volcanic VOX formation

Volcanoes produce a variety of volatile organohalogens mostly aliphatic chlorinated and/or fluorinated alkanes, alkenes and alkynes but also cyclic and aromatic halogenated compounds with methane and ethane derivatives being the predominant halogenation products.

Isidorov (1990) has proposed a set of reactions to account for the formation of chloro- and chlorofluoroalkanes:



Halogen distribution in fluids and melts (section 1.6) are in agreement with the abundance of HF and HCl for these reactions. Stoiber et al. (1971) suggested a thermogenic origin of methane from subducted sediments replacing (31) and (32). All reaction products have been measured from volcanic gas. Reaction (36) corresponds to the nucleophilic substitution (equation 18) used in the industrial manufacture of CFC. The presence of catalytic transition metal-halides is important.

However, Jordan et al. (2000) points out that the formation of organohalogens cannot proceed under magmatic equilibrium conditions since the compounds would not be thermodynamically stable. The discrepancy between measured and thermodynamic considerations could be resolved by considering the occurrence of hydrocarbons for halogenation reactions above magmatic equilibrium levels generated at shallow depth from basement sedimentary rocks. Large observed variability in concentration at one sampling location and the occurrence of the great variety of unstable short-chain organohalogens indicates a non-selective cracking producing

thermodynamically unstable reaction intermediates. Figure 1.11 shows a reaction sequence forming organohalogens during volcanic activity.

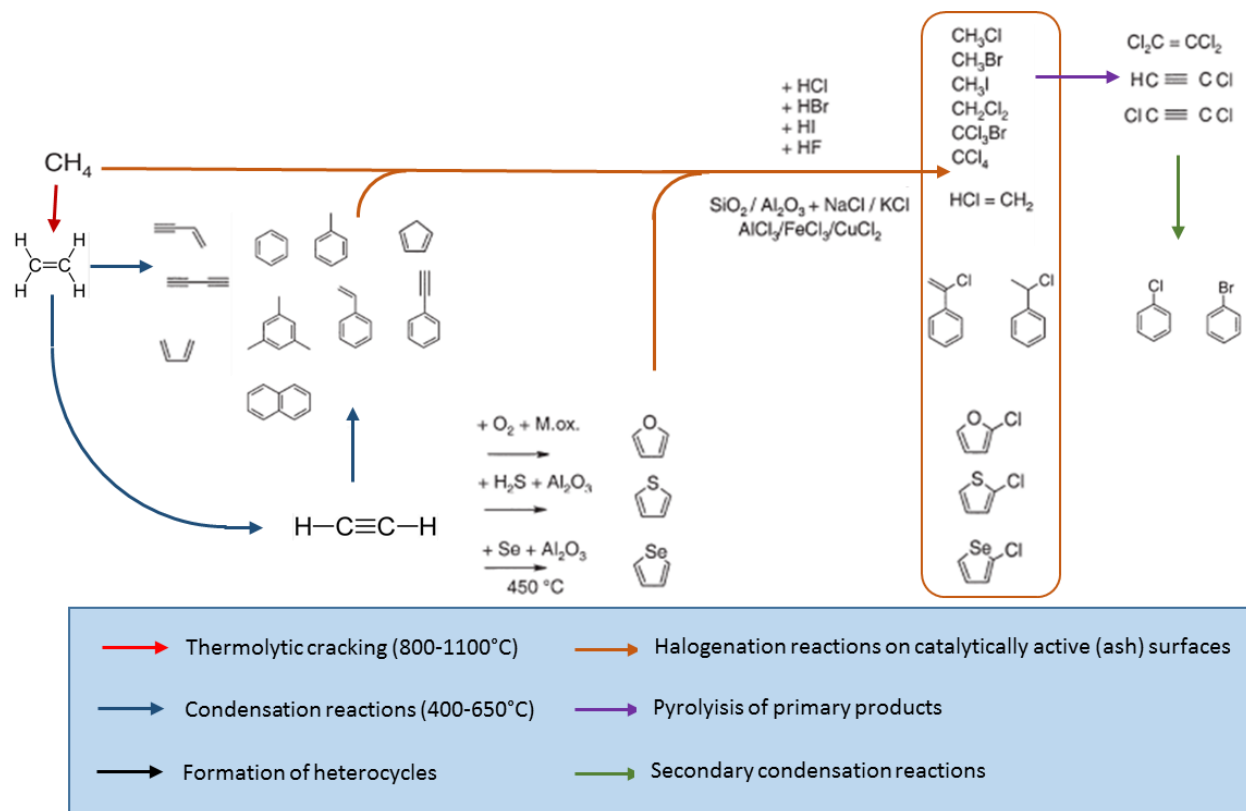


Figure 1.11: Reactions involved in volcanogenic organohalogen formation (adapted from Jordan et al., 2003).

1.8.4. Hydrothermal VOX formation

At submarine hydrothermal vents conditions are suitable for Fischer-Tropsch synthesis. Low temperature Fischer-Tropsch (LTFT) synthesis employs $219\text{-}260^\circ\text{C}$ and high temperature Fischer-Tropsch is carried out at $310\text{-}340^\circ\text{C}$ (Lamprecht et al., 2007). One can speculate that in a system of hydrothermal vents, with plenty of dissolved metals and in the presence of Cl^- from seawater, the catalysis from CO and H_2 over catalytic iron or copper as in LTFT to form saturated straight-chain hydrocarbons could also yield methyl chloride. However, no experimental data are available.

Other hydrothermal systems develop where tectonic activity causes strike/slip faults. As Schreiber et al. (2012) summarized, they offer reactive regimes characterized by periodically changing pressure and temperature conditions, varying pH values, clay minerals and a large number of metallic catalysts as well as supercritical and subcritical gases and high-salinity waters that are present. In the presented model for the origin of life in these systems, halogenations reactions could occur. Piezoelectric currents in mineralizing quartz veins could contribute to electrochemical production of halogenation agents. Again, no data are available but the model of Schreiber et al. (2012) might be referred to for the design of experiments on halogenation reactions in hydrothermal conditions.

1.8.6. Radiochemical halogenation/reactions with molecular fluorine

Kranz 1966, who investigated gases of hydrothermal fluorite samples from Wölsendorf, was the first to suggest radiochemical polymerization in the synthesis of simple organic molecule, including fluorinated derivatives.

Harnisch and Eisenhauer (1998) also proposed that the decay of uranium U^{238} and thorium Th^{234} provides α -particles for the necessary activation energy of SF_6 formation.

Isomorphic substitution in fluorite (Ca_2F_4) with $CaUO_4$ (oxidizing conditions) or UO_2 could be a source. Radionuclides are abundant in crystalline rock surrounding hydrothermal or accessory fluorites.

The impact of α -particles from radioactive products on the crystal lattice, called the atomic recoil, creates a momentum which can be high enough to disrupt the material. A vacancy (Schottky) defect can be formed in the crystal lattice. Frenkel and impurity defects result in cluster formation (Klein et al., 2002). Resulting clusters of Ca ions are known to cause blue and violet colors in fluorite. The presence of molecular F_2 has now been confirmed from ^{19}F -NMR spectra of fluorite from Wölsendorf, Bavaria (Schmedt auf der Günne et al., 2012). The typical fluorine smell observed upon crushing dark violet colored fluorite varieties can now be with confidence related to the occurrence of natural fluorine, which is to date a unique observation in nature. Schmedt von der Günne et al. (2012) also provided evidence, that the F_2 was produced naturally: the observed amounts of up to $0.46 \pm 0.06 \text{ mg } F_2 \text{ g}^{-1}$ fluorite were in agreement with the amount expected from the sample's uranium content and age of 200 to 300 Ma.

Figure 1.12 visualizes F_2 generation via radioactive decay in a fluorite crystal structure, which can then react with hydrocarbons in fluid inclusions or circulating hydrothermal fluids. In its molecular state F_2 is probably retained in structural cavities. It would thereby be isolated from the many reaction partners, and upon exposure to water or hydrocarbons would react quickly due to its high electronegativity.

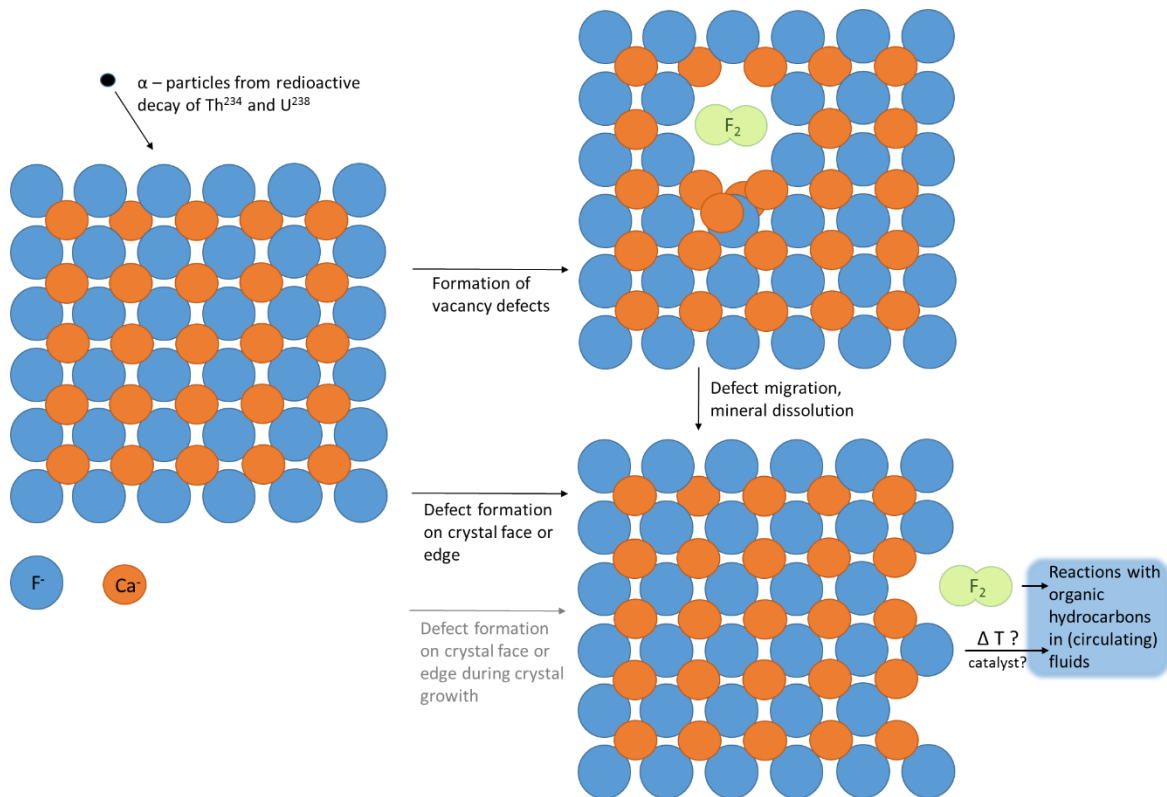


Figure 1.12: Schematic visualization of possible defect and molecular fluorine formation in the fluorite crystal structure caused by radioactive decay of neighboring radionuclides (based on the reports by Harnisch and Eisenhauer (1998) and Schmedt von der G nne et al. (2012)).

2

Method Development

A New Purge and Trap Headspace Technique to Analyse Low Volatile Compounds from Fluid Inclusions of Rocks and Minerals

Published in:

Mulder, Ines, Stefan G. Huber, Torsten Krause, Cornelius Zetsch, Karsten Kotte, Stefan Dultz, and Heinz F. Schöler. 2013. "A New Purge and Trap Headspace Technique to Analyze Low Volatile Compounds from Fluid Inclusions of Rocks and Minerals." *Chemical Geology* 358 (0): 148–55. doi:<http://dx.doi.org/10.1016/j.chemgeo.2013.09.00>

2.1. Introduction

Volatile organic compounds (VOC) released from fluid inclusions (FI) of rocks and minerals, especially the halogenated volatiles (VOX), are of pivotal importance for stratospheric and tropospheric chemistry. Currently there are discrepancies in the fundamental understanding of the sources and sinks for these compounds in the atmosphere. Here, we describe briefly the fundamental objectives of FI research, which provides a historical context in addition to the environmental focus of our application. It also compares previous methods in the area of FI and environmental research regarding the detection of VOX.

Fluid inclusions can be gaseous, liquid or solid and are present in practically all terrestrial minerals. They are formed either during crystal growth or later on in the minerals life along annealing cracks in the presence of fluid phases (Samson et al., 2003). The FI are only infrequently larger than 1 mm, in most samples their size ranges from 1 to 100 μm . The very small size fraction of FIs usually outnumbers all inclusions larger than 10 μm at least by a factor of 10 (Roedder, 1984). Current FI research spans a wide array of topics: phase relations and thermodynamic properties include the study of complex brines. Laser Raman techniques are increasingly employed in the investigation of mixed water/gas systems and with special emphasis on the analysis of single inclusions. Also, FI provide evidence about the character of early geological processes, are used in the study of modern (sub)-volcanic processes and supply information on ore formation. Frezzotti and van den Kerkhof (2007) summarized that about 20 % of published work on inclusions dealt with the use of melt inclusions to study the highly complex relationship between magma and fluids during crystallization. Bulk analysis of volatiles in FI, are predominantly concerned with the detection of O_2 , CO_2 , SO_2 , N_2 , H_2 , H_2S , HCl , HF , He , Ar , CH_4 and heavier hydrocarbons, which can be found in the literature as summarized by Salvi and Williams-Jones (2003). Typical contents of these compounds are reported to be in the ppb to ppm mass range, i.e. ng to μg per gram of mineral.

Mass spectrometric (MS) methods were mainly applied in noble gas analysis and detection of sulfur bearing compounds whereas gas chromatography (GC) was particularly used for the separation of hydrocarbons, as well as H_2 and N_2 (Salvi and Williams-Jones, 2003). Plessen and Lüders (2012) and Lüders et al. (2012) report the measurement of gas isotopic compositions of fluid inclusion gases (N_2 , CH_4 , CO_2) from 0.2 to 1 g of sample chips crushed with an on-line piston crusher followed by GC, an elemental analyzer and continuous-flow isotope ratio MS. The most recent

developments are in the application of laser ablation GC-MS, focusing on higher molecular weight hydrocarbons from single blue or yellow fluorescing FIs, and co-occurring molecular composition in order to gain insights on thermal maturity, paleo-oil charges and oil migration (Greenwood et al., 1998; Volk et al., 2010; Zhang et al., 2012). Zhang et al. (2012) summarized the GC-MS based procedures in this sector as follows: (1) offline mechanical crushing of (sedimentary) material in organic solvent to release hydrocarbons into solution and subsequent injection; (2) use of purpose-designed injectors that crush samples online via thermal decrepitation; (3) laser opening of selected inclusions with on- and offline GC-MS analysis.

Online crushing stages are employed before MS detection for the analysis of noble gases or stable isotope ratios. Principally, they consist of stainless steel cylinders with grains or cut cuboids of rock that are manually pounded several hundred times by a moveable piston (or ball) via a handheld magnet. For example, applications in the study of FIs from speleothems have been used to reconstruct paleoclimate (Dennis et al., 2001; Kluge et al., 2008) or in cosmochemistry (Scarsi, 2000). Less frequently, an alternative method is reported in which the sample is squeezed using a vice to release contained gases while in a copper tube under vacuum (Harmon et al., 1979; Scheidegger et al., 2006). Isidorov et al. (1993) detected chlorine and sulfur containing compounds from halite and sylvinitic mining emissions which they also partly measured after dissolution of the salt crystals by GC-MS headspace analysis. Most recently, Svensen et al. (2009) reported the extraction of CHCl_3 , CHBr_3 and 1-chloro- and 1-bromobutanes from halites using GC-MS and a heating procedure at 225 °C as well as a crushing procedure, but little details were reported on the latter one.

For the analysis of VOX, most expertise has been accumulated in atmospheric research. Advanced GC-MS systems with multiple traps and columns have been developed (Bahlmann et al., 2011; Miller et al., 2008; Sive et al., 2005). Crucial development was the employment of effective sample preconcentration traps. The low boiling point analytes of interest from air samples of up to several liters have to be enriched in order to detect their trace level amounts mostly in the ppt-range (mole fractions).

Little is known on the geogenic origin of CF_4 and SF_6 . The largest scientific community that has recognized and measured their natural occurrence is environmental physicists, who used CF_4 and SF_6 as age tracers in groundwater. Assumption of the underlying method was that both compounds are of purely anthropogenic origin and have gradually increased and partitioned into younger

groundwater since their industrial production in the 1950s. However, natural disturbances have been noted and reported, first by Busenberg and Plummer (2000). Literature on the topic is still scarce but the occurrence of SF₆ from basaltic aquifers (Koh et al., 2007), from granitic alluvium of the Mojave Desert (2008) and sedimentary aquifers of the North China Plain (von Rohden et al., 2010) have been reported, putting restrictions on the groundwater dating if SF₆ is taken as a tracer. Deeds et al. (2008) also mentioned CF₄ as of terrigenous origin and stated that fluxes of CF₄ and SF₆ when extrapolated from their measurements to a global scale could be consistent with the fluxes required to sustain the preindustrial atmospheric abundances of CF₄ and SF₆.

Busenberg and Plummer (2010) presented results on a new groundwater dating method using the environmental tracers SF₅CF₃, CClF₃ (CFC-13), SF₆, and CCl₂F₂ (CFC-12). However, Harnisch et al. (2000) reported values of up to 1200 pg g⁻¹ CCl₂F₂ released from fluid inclusions in fluorites and Jordan et al. (2000) reported detection of this compound from volcanic gas samples. An extensive screening of geologic materials has simply not taken place yet, so maybe even these newly developed methods encounter limitations in some natural environments where there is a terrigenous source of these compounds.

The studies of Harnisch and Eisenhauer (1998) and Harnisch (2000) are ground-breaking in VOX analysis from FIs of rocks and minerals. Harnisch and Eisenhauer (1998) demonstrated that CF₄ and SF₆ are commonly present in natural fluorites and granites, and the publication by Harnisch et al. (2000) provided a detailed description of their grinding procedure. They were using a grinding device emulating a “peppermill”-design in which samples were ground from 5 mm down to around 100 μm diameter and released gases were transported directly onto the preconcentration sample loop by using a vacuum. After desorption, analytes were separated using a packed column and detected with by MS. By using this technique they were able to detect CF₄, CF₂Cl₂, CFCl₃ and SF₆ from a number of natural samples and additionally CF₃Cl, CHF₃ and NF₃ from one fluorite sample. Levels of CF₄ were determined to be up to 5600 pg g⁻¹ and those of SF₆ reached 340 pg g⁻¹. On the one hand, their measurements, although in good agreement with old results from Kranz (1966), have apparently not been replicated by other groups or expanded to a larger set of samples. On the other hand, their papers are cited quite frequently, whenever authors acknowledge a natural origin in discussions on the atmospheric concentration of the corresponding compounds (e.g. Mühle et al., 2010).

In order to contribute to a larger scientific basis for natural background estimates of VOX, the major goal of this work was to develop a simple, inexpensive and robust method to detect VOX and organosulfur compounds from FIs. Objectives were to develop a grinding device that crushes mineral samples to a specific final grain size, to install a cooling trap that is capable of concentrating released gases with particularly low boiling points (as low as $-128\text{ }^{\circ}\text{C}$) prior to measurement and to assure high analytical performance of the GC-MS system by protecting it from mineral particles.

In this paper, we first describe an alternative purge-and trap GC-MS method to analyze the chemical composition of VOX from FIs using an adapted dynamic headspace approach that accommodates all types of minerals and rocks across the entire Moh's scale of hardness while maintaining high sensitivity.

2. Experimental Section

2.1. Grinding device

In order to analyze the volatile organohalogen and organosulfur compounds of FI using GC-MS the first step was to develop a grinding device that was able to crush and release the target gases from the rocks and minerals. Our approach was to create a purgeable grinding container mimicking a dynamic headspace vial, and at the same time, incorporate already existing infrastructure of our laboratory. The resulting grinding device consisted of a 80 mL tempered steel grinding bowl (Fritsch, Idar-Oberstein, Germany) equipped with a lid and a Viton seal ring. The lid was chosen in stainless steel and we constructed two brass orifices on top, which could be sealed by conventional crimp caps (diameter 8.4 mm) with Sil/PTFE septa (thickness 1.5 mm).

After inserting the sample and five tempered steel grinding balls (diameter 15 mm) to the bottom bowl the crimp cap sealed lid was pressed via a clamping plate onto the bowl. The Viton seal allowed for an air-tight closure. The whole fixture with grinding vessel and sample then fits into a regular planetary mill (Fritsch, Pulverisette 5).

In order to effectively grind samples, materials needed an initial particle size below 3 mm (preferentially between 2 and 3 mm), otherwise larger particles were not sufficiently ground to appropriate sizes.

Corresponding to the hardness of the minerals under investigation the grinding times were adjusted accordingly. Initially, tests were performed with quartz (Moh's hardness 7) and fluorite (hardness 4) samples for which grinding times, grinding intensities in revolutions per minute (rpm), amount of sample and amount of grinding balls were varied. The particle sizes of subsequently obtained fine powders were analyzed from suspensions of 50 mg 100 mL⁻¹ in deionized water using a ZetaPals (Brookhaven Instruments, Holtsville, NY) in multiple angle particle sizing mode. For the particle size determination, commercial quartz gravel (Quarzkies Natur, MK-Handel, Düren, Germany) of grain size 2 to 3.15 mm and of a fluorite of same grain size from the mine Marienschacht nearby Wölsendorf, Bavaria, Germany, were used. The particle size distribution was determined in the range from, 0.5 to 5000 nm. From the data of triplicate measurements mean values were calculated and found to be < 15 %. For easily soluble salt minerals, such as halite, this particle size determination was not carried out. Halite showed a ductile behavior upon intensive grinding with "smearing out" along the rim of the grinding bowls and clogging of the orifices. Therefore, we based the selection of grinding conditions observations made during the grinding procedure.

After setting the basic grinding conditions, temperature evolution during grinding operation was determined for quartz and fluorite. After different grinding times, the lid was taken off quickly and temperatures were determined instantaneously by an infrared thermometer (Voltcraft, IR 1200-50). Additionally, temperatures on the outer surface of the grinding vessel were recorded. Temperatures were recorded in triplicate from each 10 g of a commercially available Dead Sea salt (August Töpfer & Co. KG, Hamburg, Germany) was utilized.

2.2. Analytical system

The MAGNUM™ GC-MS system (Finnigan MAT, San Jose, CA) consists of three main components: the gas chromatograph (GC, Varian Model 3400), the ion-trap mass spectrometer (MS, Finnigan MAT, ITS40) and the data processing system and software (Saturn 5.4, Saturn 2000). Additionally, we employed a custom built temperature control unit (Newig GmbH, Ronnenberg, Germany) that was originally developed by Nolting et al. (1988) and also described more recently by Siekmann (2008) as well as the self-constructed inlet system comprising the sample preconcentration tube that bridged the GC injection port. All gas carrying components of

the setup consisted of 1/8-inch stainless steel tubing and 2 mm outer diameter Swagelok® compression fittings. Figure 1 provides a schematic of the analytical system.

2.2.1. Purge and trap unit

The regulation of the ultra high purity He carrier gas flow affects the measurement reproducibility. Helium flow is controlled by two 3-way solenoid valves (valve 1 and 2), two 2-way solenoid valves (valve 3 and 4) and one manual 2-way needle valve. Solenoid valves were obtained from Kuhnke AG, Malente, Germany (Micro-Solenoid Valves type 65). The first four valves are controlled by the external event relays of the GC computer. Under standby as well as desorption conditions, equivalent to a non-purge sequence, valves 1 and 2 are directly connected to each other and valve 3 is closed as represented by the solid lines in Figure 1. This means that the sample loop, i.e. the grinding vessel and connecting lines, are not purged by He, but instead the cooling trap made of glass lined tubing (GLT™) and GC columns are constantly flushed with He at a rate of 2.0 mL min⁻¹.

Analysis of a ground sample is started by piercing two stainless steel needles as inlet and outlet through the septa of the crimp caps on the grinding vessel. We used 16 gauge, point style hubless needles of custom length (10 cm; Hamilton Bonaduz AG, Bonaduz, Switzerland). To avoid rupture and leakage at the thin Si/PTFE septa employed, it is advisable to pre-pierce them with a thin needle before punching through with the 16 gauge needle. The cooling trap consists of a 215 mm long piece of GLT™ (SGE Analytical Science, Melbourne, Australia), which is bent in the middle to form a U-shaped section of the tube. This U-shaped part of the tube is installed above a Dewar vessel (80 ml, KGW Isotherm, Karlsruhe, Germany), and is submerged in liquid nitrogen during sample preconcentration. Liquid nitrogen was added manually before each measurement. A thermocouple connected to a temperature controller was attached to the submersible part of the GLT™ using PTFE-tape. The temperature control device monitors the temperature of the trap. During the sample preconcentration step valve 1 and 2 switches so that the He purges the grinding vessel (dotted lines, Figure 1). At the same time, valve 3 is opened to permit a high purge flow controlled by the flow controller (GFC17, Analyt-MTC), additionally to the existing flow through the GC column. Volatile compounds from the grinding vessel are purged for 6 min with a He flow at 10 mL min⁻¹, as regulated by the flow controller and enriched on the pre-cooled trap (-196 °C).

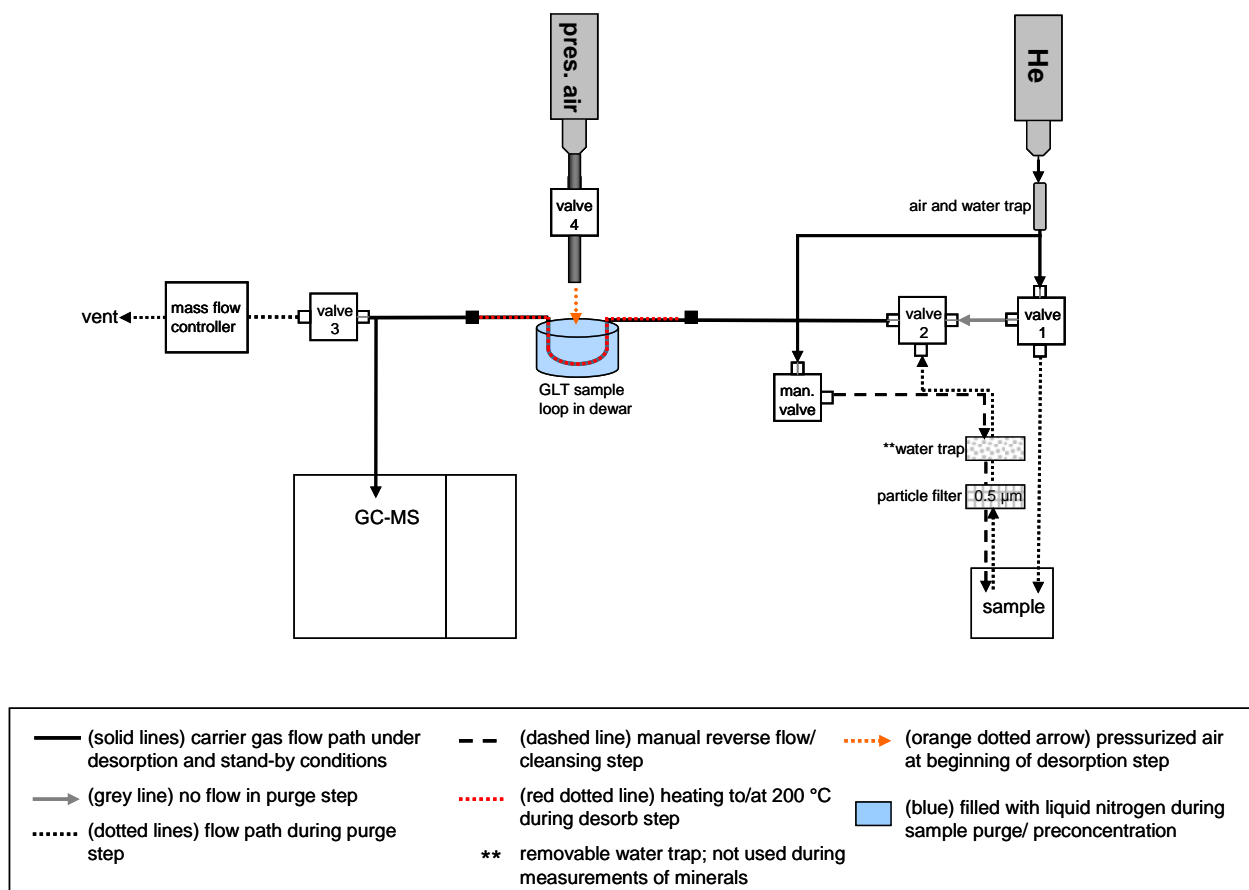


Figure 2.1: Schematic of the analytical system. The sample is attached by piercing through the sealing septa and sample is purged by the He carrier gas flow. Grinding of mineral samples is realized offline in a conventional planetary mill. The sample trap temperature is controlled via a thermocouple by the temperature control device. The thermocouple is attached at the deepest point of the U-shaped sample loop, but this is omitted in the scheme for simplicity. The resistance heating is attached to the GLT™ sample loop via copper clamps symbolized by the black squares and also regulated by the temperature control device.

An important aspect of this step in the process is the intercalated particle filter (Swagelok® Series F, mesh size 0.5 µm) that prevents fine mineral dust particles from entering the delicate GC-MS system. The sintered filter element should be exchanged every 20 to 30 measurements. Optionally, the scheme shows a (magnesium perchlorate) water trap. This has to be installed when measuring with a standard headspace technique (water vapour phase) or other sample requiring a moisture control system and is added here to demonstrate the versatility of the experimental setup. After

sample preconcentration is finished valve 4 is opened for 10 s and allows pressurized air to dissipate the liquid nitrogen from the Dewar vessel. A resistance heating that is controlled by the temperature control device is directly attached onto the GLT™ with two copper clamps, symbolized by the small black boxes in Figure 2.1. After liquid nitrogen is blown off, heating from -196 °C up to 200 °C is accomplished within 30 s and this temperature is held for 2 min. The optimum heating rate is regulated by the temperature control device, permitting on the one hand a fast desorption of the volatile compounds, but preventing the thermal decomposition of the trapped compounds. During the desorption sequence, valves 1, 2 and 3 switch back into the standby conditions as described above. While the measurement is running, the sampling line with the filter element was cleaned by opening the manual valve to allow He backflush.

2.2.2. GC-MS

After desorption the sample is transferred by the carrier gas flow through a 15 cm long retention gap (0.53 mm diameter fused silica capillary column, deactivated) perpendicular to the GLT™ directly onto the GC columns. A graphite ferrule is used for the connection between retention gap and GLT™, whereas a retention gap and two capillary columns were installed in series using quartz Press-Fit®-connectors (Mega s.n.c, Legnano, Italy). The first capillary column employed is a DB-624, ID 0.53 mm, df 3 µm, 30 m. The second capillary column is a BP-5, ID 0.32 mm, df 1µm, 60 m. Due to the choice and length of chromatographic columns in combination with the cold trap design, no further sample refocusing on the column or GC oven cooling was needed to achieve good retention of very low boiling point compounds such as CF₄ or SF₆.

The GC oven was programmed at 35 °C for 22 min, 35 °C to 150 °C at 5.5 °C/min, 150 °C are held 5 min, 150 °C to 210 °C at 30 °C/min, hold 10 min (Figure 2.2). The MS detector was operated at 170 °C with electron ionization of 70 kV. Signals were acquired between 11 – 50 min in scan mode for masses from 49-132 m/z at a scan rate of 0.17 s. Signal response and chromatographic performance of a reference gas mix (Crystal Mixture, Air Liquide) was controlled daily and electron multiplier voltage adjusted if necessary.

In order to achieve best analyte recoveries, the purge flow speed and time were varied and the measurement conditions were set for both, the grinding vessel and a 20 mL empty standard headspace vial.

Isobutene, 1,3-butadiene, *cis*-2-butene and *trans*-2-butene were contained in a mixed calibration standard (15 ppm in N₂, Crystal Mixture, Air Liquide). For optimization of purge flow and time 2.8 ng CF₄ (99.9 %, Sigma-Aldrich) and 0.7 ng of Crystal components were employed.

Calibration was performed subsequently according to optimum conditions using pure gas standards. The following chemicals were used: chloromethane (99.5 %, Sigma-Adrich), sulfur hexafluoride (5.0, Linde AG), carbon tetrafluoride (99.9 %, Sigma-Aldrich). Pure gases were diluted via injection into Erlenmeyer flasks, on top of which a thread for closure with screw caps and Sil/PTFE septum was mounted. Calibrations were performed at 25 °C.

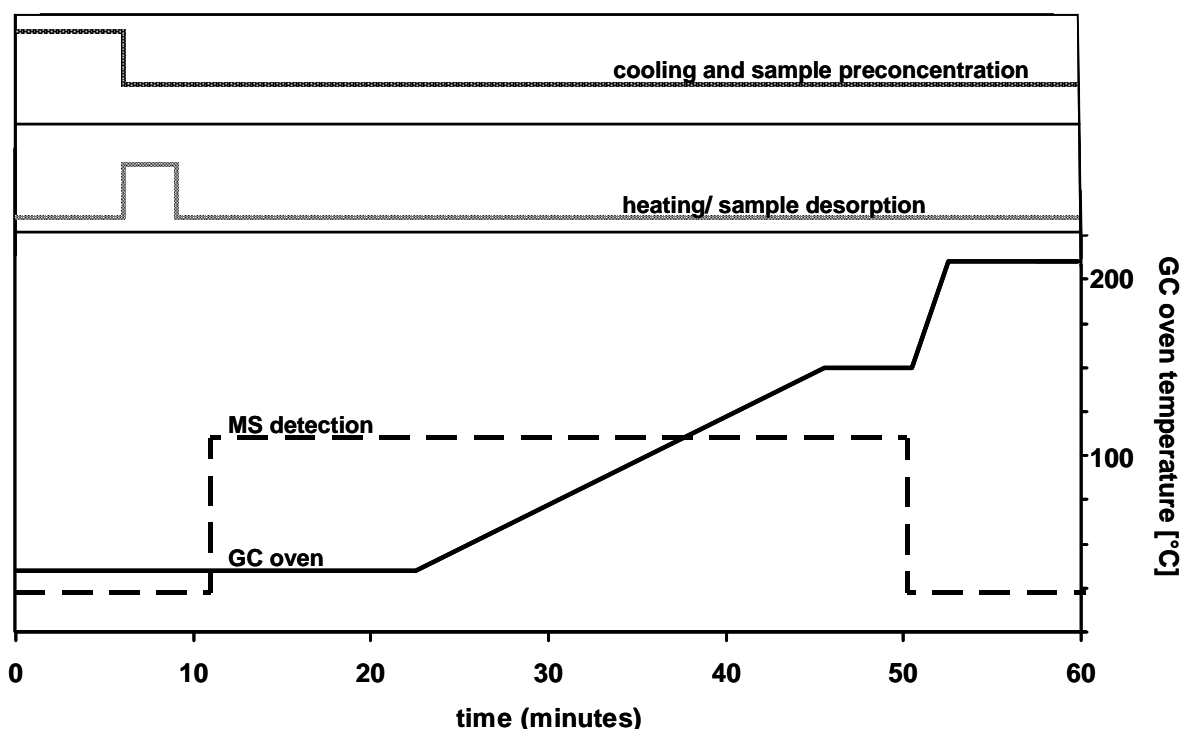


Figure 2.2: GC oven program and MS detection. (A) indicates the duration of the sample pre-concentration and (B) the desorption steps.

The solvent EPA 624 calibration mix 1 (Sigma-Aldrich) was used to determine retention times while the water trap was installed. Before samples were measured, mineral material was washed 3 times with bidistilled water or ethanol (p.a., Sigma Aldrich) and then evacuated at pressures below 10^{-4} mbar for at least 24 h in order to remove contaminants adsorbed to the mineral surfaces.

2.2.3. Measurement of samples

A 10 g mineral sample was measured in the closed grinding device before and after grinding. Samples were ground corresponding to their specific grinding conditions, e.g. 15 min at 400 rpm, 10 min at 400 or 5 min at 200 rpm for quartz, fluorite or halite, respectively. Sample results presented later originate from a purple-green banded hydrothermal fluorite from the mine Marienschacht, Wölsendorf, Germany, and a halite from a recent salt crust of the salt pan Lake Kasin, South Russia.

2.3. Results and discussion

2.3.1. Grinding procedure

Compared to previous crushing stages in FI analysis, our grinding is used in offline MS detection because of the need for chromatography and detection of trace amounts of volatiles. Hence, bulk released VOC composition is determined rather than the release of individual fluid inclusions. Crushing yielded mean average diameters of 1000 and 740 nm for quartz and fluorite, respectively. Response of particle size to selected grinding treatments is depicted in Figure 2.3. Quartz showed no further decrease of particle sizes after 15 min grinding time at 400 rpm, which was then chosen as the standard grinding condition for quartz and similar materials, such as granites. Fluorite summation curves of particle distribution clustered for the 10, 15 and 20 minutes grinding time at 400 rpm. Longer grinding times did not yield smaller particles, which is typically observed (Jefferson et al., 1997; Kano et al., 2000) with final grain sizes apparently depending on the choice of grinding method and the properties of ground material (Kumar et al., 2006).

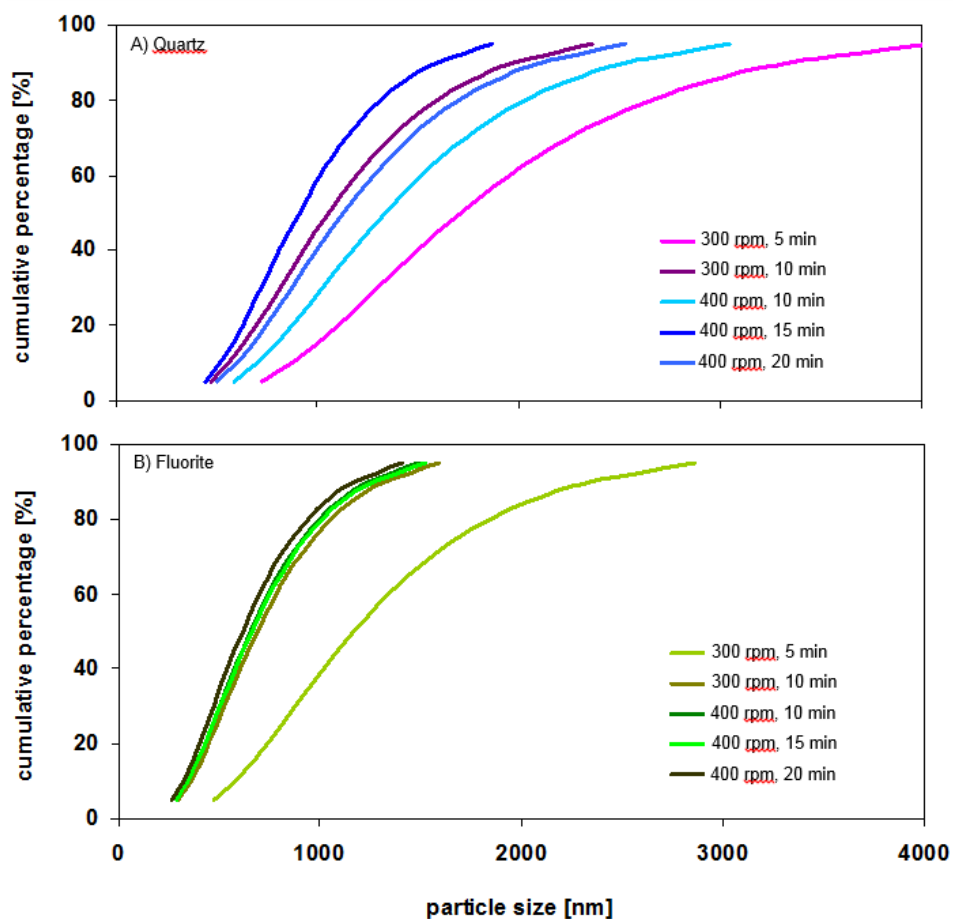


Figure 2.3: Particle size distributions obtained at grinding conditions using each 5 grinding balls and 10 g of sample. A) cumulative percentage curves for quartz and B) for fluorite at different grinding conditions. The legend indicates quartz (Q) and fluorite (F), grinding intensities in rpm (300 or 400) and grinding times (min).

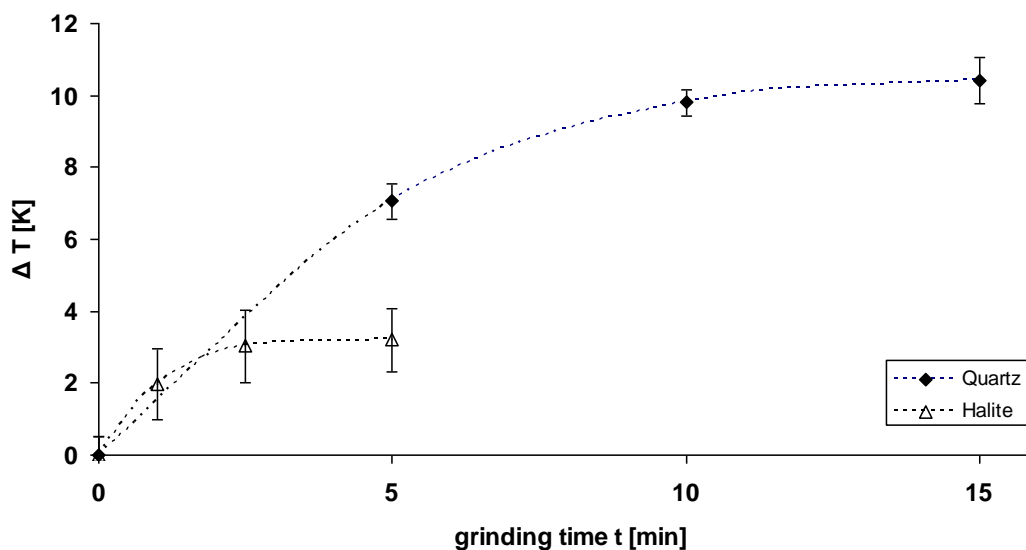


Figure 2.4: Temperature development inside the grinding vessel after different grinding times for quartz and halite.

Therefore, 400 rpm and 10 min were chosen as the standard grinding condition for fluorite and minerals of similar hardness, such as calcite or dolomite. Our grinding device avoids the tedious manual work done in the use of a crushing stage and ball. Also the cleaning of the grinding vessel is relatively easy as compared to the “peppermill”-design (Harnisch et al., 2000).

At the same time the whole analytical setup only needed minor adjustments in order to accomplish the detection of volatiles from FIs and can be easily adjusted for a variety of other applications.

The observation of temperature development within the grinding device during grinding was crucial in order to evaluate the potential risk of de-novo volatile compound formation. As seen in Figure 2.4, the interior temperature of the grinding chamber with sample and balls did not exceed $\Delta T = 10$ K for the quartz. However, an apparent plateau appeared to be reached. This can be explained by the high heat conductance of the tempered steel of $47 \text{ W m}^{-1} \text{ K}^{-1}$ (at 20°C).

After 15 min the maximum temperature difference on the outside of the vessel amounted to $\Delta 5$ K. This means that heat had been transported away from the grinding vessel's interior, heating up the whole steel container. For the halite sample, the obtained curve in Figure 2.5 shows a similar behavior, but temperatures on the outside of the vessel essentially remained constant, likely because of the higher deformation and plastic behavior of the salt. Energy input during grinding was lower as halite was only ground at 200 rpm (quartz at 400 rpm). After 5 min of grinding the temperature increase was less than half for the halites as compared to the quartz.

When calculating the energies released during impacts and friction of balls with sample and walls, time of heat conductance was considered to yield a linear energy development over time. The energies were calculated approximately based on the equation,

$$(37) Q = m \cdot c_p \cdot \Delta T$$

with Q being the heat energy (kJ/J), m the total mass of ground material, grinding balls and factored in the heated material of the grinding vessel, c_p the respective specific heat capacities (kJ/(kg K)) and ΔT the temperature difference (K). The calculated thermal energies released during grinding were 7.62 ± 0.47 kJ for quartz after 15 min and 0.87 ± 0.24 kJ for halite after 5 min. A larger error for the calculations for the halite crystal is probably due to its ductile behavior with energies being partly converted into deformation. Bond energies are for example 347 kJ/mol for C-C, 414 kJ/mol for C-H and 485 kJ/mol for C-F bonds (Mortimer, 2001). Although the values for the released energies can only be understood as approximations, they demonstrate that the energies developed within the grinding vessel are insufficient to break and form new covalent bonds. The grinding process should therefore not contribute to additional amounts of volatile compounds measured, thus we assume that the compounds measured after grinding are released directly from the fluid inclusions of the materials.

2.3.2. Chromatographic optimization

Results from the optimized measurement conditions are shown in Figure 2.5. First, the purge flow rate as regulated by the flow controller downstream of valve 3 (Figure 2.1) was varied for both the grinding vessel (a) as well as a regular empty 20 mL headspace vial (c) and purge flow as mL min^{-1} is plotted on the x-axis. The purge time was held constant at 6 min. The bars of the diagram in

Figure 5 show the response of each compound that was added in equal amounts each time. After 6 min with a purge flow of 10 mL min^{-1} CF_4 was recovered with highest intensities from the grinding vessel even though under these conditions the volume of the grinding vessel was not purged completely. Apparently, even at trapping temperatures of $-196 \text{ }^\circ\text{C}$ the adsorption of low boiling compounds is not absolute but can be optimized by adjustment of the purge flow. Recoveries for butenes were generally higher from the 20 mL headspace vial than from the grinding vessel. This may be caused by the different purge volumes and geometries of the purged containers and by the different boiling points of the calibrated substances.

As we were striving to optimize the system for the lower boiling compounds and butenes did not show significant increase with higher purge rates, the purge rate was set at 10 mL min^{-1} . When varying the purge times it was remarkable that with 4 min signals for all five compounds were too low to be detected. After 6 min highest values were observed for CF_4 , but recoveries for butenes between 6 and 10 min remained nearly constant from the grinding vessel (b). When looking at the headspace vial (d), clearly best results were achieved for the butenes after 6 min whereas CF_4 was not recovered at all, except for near detection limit amounts after 4 and 8 min.

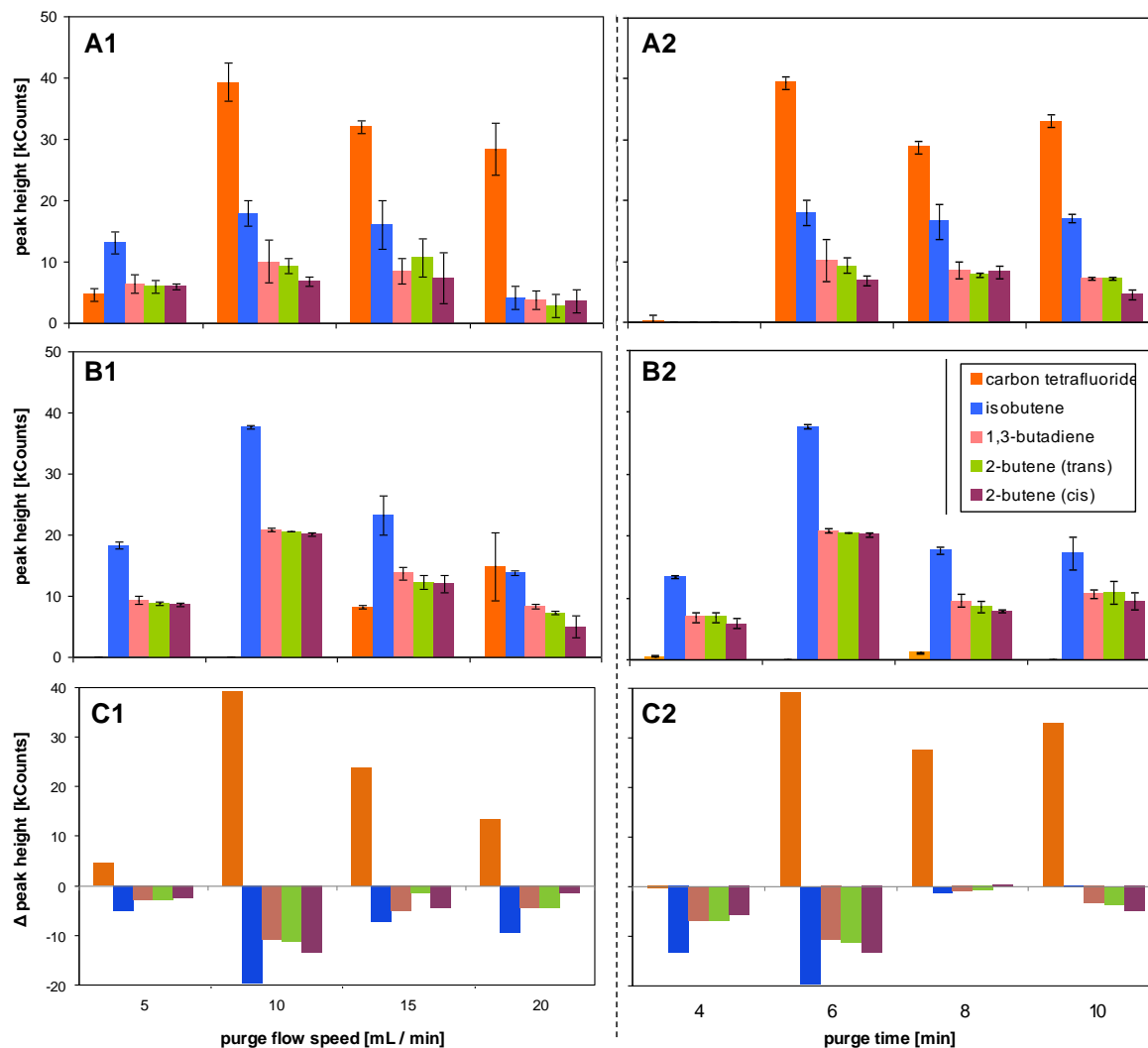


Figure 2.5: Chromatographic recoveries of 5 standards at different purge flow speeds and purge times. Results from grinding vessel are on top (A1 and A2) and from headspace vial in the middle (B1 and B2). Plots C1 and C2 show the difference between grinding vessel and purge time (A minus B). Purge flow speed was varied with a constant purge time set at 6 min (left). Subsequently, the purge flow speed was held constant at 10 mL min⁻¹ and purge times varied (right).

In general, purge time did not have such a distinct effect as purge speeds. However, best results were achieved after 6 min already. Hereupon, sample measurements were performed with 6 min purge time and 10 mL min^{-1} carrier gas flow. Detection limits with these conditions for the observed compounds are below 0.5 ng. The system installed at the University of Bayreuth employing a similar sample preconcentration applied to aerosol smog chamber experiments reached detection limits of 70 ppt for n-butanenes and other higher molecular weight hydrocarbons (Siekmann, 2008).

The two capillary columns combined with the specificity of the MS detection sufficiently resolved most compounds of interest. Prior to this work, only CF_4 and SF_6 were quantified in our set of fluorite and granite samples. Table 2.1 lists the analytes that have been detected from standard and sample measurements with the current system.

The use of the Viton (fluoropolymer) seal ring between grinding bowl and crimp cap lid was not found to additionally augment our samples with CHF_3 as was reported previously in the literature (Miller et al., 2008). Also grinding and analysis of FIs did not necessarily need to be performed under inert gas conditions as the concentrations of compounds released from mineral material by far exceed atmospheric concentrations. The 60 mL aliquot enriched from the grinding vial during the purge-and-trap sequence did not suffice for the detection of atmospheric volatile compounds as observed in blank measurements.

Two examples of the chromatograms after mineral grinding are shown in Figure 2.6. The Wölsendorf-fluorite shows peaks for CF_4 and SF_6 corresponding to 26.3 and 3.4 ng/g, respectively. This shows the effectiveness of the system to trap these low boiling point compounds. While Isidorov (1993) and Svensen et al. (2009) also reported the measurement of chloromethane after dissolution or heating of halite samples, this is the first time that the release of chloromethane after grinding can be reported. Its observation from fluorite is novel but in both cases its occurrence is conceivable as chlorine as chloride in brines and methane in gases of fluid inclusions are commonly observed.

Table 2.1: Selected analytes detectable with the purge and trap system from calibration standards, their boiling points and target qualifier ion masses. Release of carbon tetrafluoride, sulfur hexafluoride, methyl chloride and methyl bromide from FIs can be accounted for thus far.

compound name	boiling point (°C)	target ions (amu)
carbon tetrafluoride	-128	69, 50
sulfur hexafluoride	-64	127
methyl chloride	-24	49,50,52
chloroethene	-14	62, 64
methyl bromide	4	79, 94, 96
chloroethane	12,3	49, 64, 66
trichlorofluoromethane	24	66, 101, 103
1,1-dichlorethene	31,7	61, 96, 98
methylene chloride	40	49, 84, 86
trans-1,2-dichloroethene	48,7	61, 96, 98
1,1-dichloroethane	57,4	63, 65
chloroform	61	83, 85
1,1,1-trichloroethane	74	61, 97, 99
carbon tetrachloride	77	117, 119
benzene	80	77, 78
1,2-dichloroethane	83,5	62, 64
trichloroethene	87	95, 130, 132
1,2-dichloropropane	96	62, 63, 76
bromdichloromethane	90	83, 85, 129

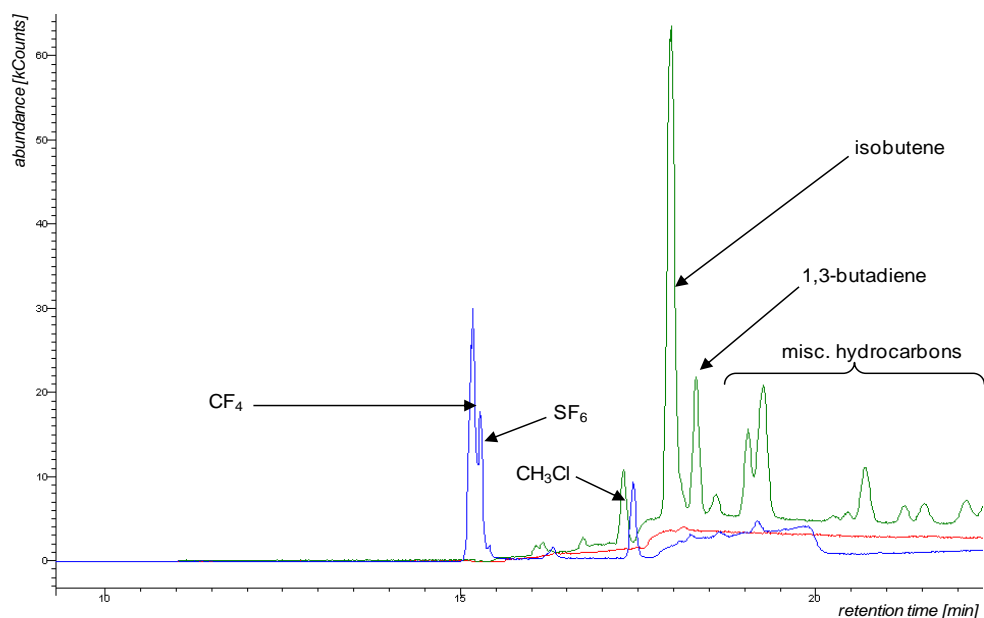


Figure 2.6: Examples of reconstructed ion chromatograms (RIC) obtained from fluorite (blue) and halite (green) samples after grinding. Blank measurement in red. Samples originate from mine Marienschacht, Wölsendorf, Germany (fluorite), and from a recent salt crust of the salt pan Lake Kasin, South Russia (halite).

2.4. Conclusions

Our GC-MS system together with the newly developed mineral grinding device allows for new compounds of interest in fluid inclusion research and at the same time maintains the high sensitivity of GC-MS measurements. Volatile compounds detected started at the very low boiling point of carbon tetrafluoride up to bromodichloromethane (Table 1), spanning a range of over 200 °C. The cold trap design constructed of the GLT™ column without further adsorbent material and installed directly before the GC columns made this possible. We report here for the first time the release of CH₃Cl from halites and fluorite following this grinding procedure as compared to previous mineral dissolution or heating experiments.

Mineral grinding as compared to the previous “Peppermill”-method by Harnisch et al. (2000) has been improved by a factor of 100, concerning final grain sizes. This also entailed a reduction of sample amount required. Initial measurements of mineral samples with this new system showed that it is able to reproduce SF₆ and CF₄ released from the FI as reported in previous studies by Harnisch et al. (Harnisch and Eisenhauer, 1998; Harnisch et al., 2000).

The adapted dynamic headspace approach accommodates not only all types of minerals and rocks but is still highly versatile. Conventional headspace applications are still feasible by inserting the water trap and since analytes are trapped prior to the GC column, the cold trap could easily be used with different GC configurations or different analytical techniques.

An expanding dataset based upon this method will help to gain new insights into the formation process of VOX found in FIs and their release to the environment upon weathering.

3

Sample Screening

Volatile organic compounds released from fluid inclusions of mineral and rock samples

3.1. Introduction

In order to apply the newly developed method, a set of various mineral and rock samples was assembled. This set includes, fluorites, halites, gypsum as well as quartz, granites, dolerite and basalt.

Quartz (SiO_2) belongs to the tectosilicates and has a Mohs' hardness of 7. It is the second most common mineral of the continental crust after feldspar. If quartz crystallizes below 573°C trigonal α -quartz is formed. At higher temperatures and pressures it changes its structure to hexagonal β -quartz. Quartz accounts for 30 wt% in granites and due to its mechanical and chemical stability it persists as detrital grains and is major constituent of many sediments (Langmuir, 1997). It is also present in many igneous and metamorphic rocks and the most common gangue mineral in hydrothermal veins, oftentimes as essentially the only mineral. In sandstone and its metamorphic equivalent quartzite is the major component. Chert and flint are hydrothermal quartz deposited on the sea floor or in limestone. Quartz varieties are numerous including gemstone, amethyst, citrine, smoky quartz rose quartz, chalcedony and agate to name a few. Milky quartz may be the most common quartz variety owing its milky white color due to minute FIs (Klein et al., 2002).

Basalts are the most important vulcanites as they build up the entire ocean floor. They are formed from molten mantle material and have a temperature of 1000 to 1300°C upon their extrusion. This temperature and the low SiO_2 -content lead to melts of low viscosity which is why basaltic volcanoes are less explosive. Main constituents of basalt are glass and the microcrystalline matrices, plagioclase and augite. Minor mineral constituents are olivine, orthopyroxene, ilmenite, magnetite, apatite and biotite (Markl, 2004). Dolerite is a rock-type chemically equivalent to basalt but of medium-grained texture. They are dominated by the minerals plagioclase and pyroxene but they can also contain olivine or quartz. They are typical found within dykes or as sills.

Fluorite, CaF_2 , crystallizes in the cubic crystal system and is of Mohs' hardness 4. It appears on various colours most commonly violet, blue, creamy yellow and green. It is a common and widely distributed mineral usually found in hydrothermal veins where CaF_2 precipitates first from acid solutions due to their low solubility (Klein, et al. 2002). But it also occurs in pneumatolytic deposits (e.g. accessory in granites), in pyrometasomatic rock (e.g. magmatic intrusions or skarn), in carbonatites and sedimentary from salt and fluorine-rich solutions (e.g. in dry lakebeds). Fluorites are frequently associated with lead-zinc bearing ores (Mississippi-Valley-Type) or with partly large

crystals together with quartz, calcite and barite as filling in veins. They are also common in vugs of dolomite and limestone. A renowned variety of fluorite is antozonite, historically known as stinkspar or fetid fluorite. Type locality for this dark violet or even black fluorite is Wölsendorf, Bavaria. These fluorites are rich in radioactive U^{238} which decays into β -emitting daughter nuclides. Experimentally, it was shown that radiation caused artificial calcium fluoride to turn violet by splitting into clusters of calcium ions and bubbles of fluorine gas. In 2012, Schmedt auf der Günne et al. (2012) finally proved that the stinky smell released from the stinkspar of Wölsendorf is indeed caused by F_2 . These fluorites are the only known natural place on Earth where elemental fluorine exists.

Halite, cubic crystals of NaCl with Mohs' hardness 2, is another representative of the mineral groups of halogenides. It occurs predominantly as evaporite and can be of marine or non-marine origin. The common model for its marine deposition is its formation in shallow coastal basins closed off or restricted by a topographical barrier toward the open sea and with restricted inflow of freshwater. Halite can occur in association with sylvite, and other Na-K-Mg-halogenides or sulfates like gypsum. Halite crusts from modern saline pans, referred to as playa, sahbkas, salt flats or salt pans, usually form in restricted drainage basins and under dry climatic conditions. They have undergone repeated episodes of flooding and desiccation resulting in characteristic syndepositional features such as dissolution textures and cements. Mud beds can contain displaced halite crystals. During diagenetic processes upon burial pore spaces are reduced via cementation and usually completely filled at burial depth of approximately 45 m (Casas and Lowenstein, 1989). The Salar de Uyuni in Bolivia is the largest contemporary salt pan covering an area of more than 10000 m^2 . Burial of thick beds of evaporite lead to the formation of salt domes or diapirs where the less dense salts rise up vertically into the overlying sediment strata. Rock salts are mined from salt domes and bedded deposits that are widely distributed throughout the world. The soft (Mohs' hardness 1.5-2) evaporate mineral gypsum $CaSO_4 \cdot 2H_2O$ (monoklin) together with the harder anhydrite $CaSO_4$ (orthorhombic, Mohs' hardness 4) is by far the most abundant mineral in natural deposits. This is because they are less-soluble and precipitate early during evaporation (Klein et al., 2002).

For this study, halite and gypsum samples were partly sampled during field campaigns to salt pans around the world. Other samples were obtained from third parties; either from mineral collectors or those samples were taken in the context of different research endeavours.

Major hypothesis for this work were that minerals contain volatile organohalogens in their FIs and that types and amounts of volatile compounds including organohalogens depend on the conditions during mineral formation. It is also expected that evaporites from salt pans can serve as source for organohalogens in soils, water and air as well as capture and archive gases trapped during mineral formation in the surroundings of their deposition.

The sample screening presented here was oriented mainly on routine environmental analysis. We did not seek to apply thermodynamic considerations of formation of rocks and minerals as is mostly the case in FI research but rather focused on the potential of VOC formation within geologic matrices. Formation time of inclusions during crystal growth (primary, secondary or pseudo-secondary) was thus neglected. The screening of samples also includes data on anion content, organic carbon content and x-ray diffraction data of samples.

Objective of the sample screening was to provide novel data on the chemical composition of fluid inclusions. A large number of samples was intended in order to allow for systematic observations among and between sample groups. This chapter also points out technical problems and discusses how to solve them.

3.2. Materials and Methods

3.2.1. Samples and their treatment

After breaking up solid crusts with a spade using stainless steel putty knives or by grabbing loosely assembled crystals with laboratory gloves from salt pan surfaces in South Russia, Southwest Australia, Bolivia, Mauretania, Namibia and South Africa, samples were collected into low density polyethylene (LDPE) plastic bags with zip locks. The samples were predominantly halites and gypsum minerals, thus soft materials. Other halite samples from drill cores or mines were provided by colleagues. Their crystals were usually up to 5 mm thick but often formed aggregates or crusts (see Figure 3.1). The samples were carefully broken down with a porcelain mortar and pestle. The final grain size ranged between 1 and 3 mm. The highly water soluble halides were immersed in ethanol (Supelco, 98%) within a glass beaker and covered with a watch glass. The vessel was then placed in an ultrasonic bath for 1 min. The washing solution was then decanted and the washing step was repeated three times or until the leftover supernatant was colourless. The cleaned minerals

were left in an open container overnight in a fume hood so that the employed ethanol could evaporate.

The fluorite used in this study were received from a private mineral collector and originated from the Wölsendofer fluorspar region of Upper Palatinate, Germany. Granites, a schist and a limestone stem from the Cambay river basin in North Gujarat, India, sampled by M. Wieser, Institute of Environmental Physics, University of Heidelberg. Dolerite sills and a synthetic Mid Ocean Ridge basalt (MORB) sample were provided by B. Black, Massachusetts Institute Technology and S. Dultz, University of Hannover, respectively.

These samples were first crushed into pieces of about 5 cm thickness using a large hammer. In the following, the samples were ground to yield grain sizes >3.15 mm using a jaw crusher followed by the vibrating cup mill. The size fraction of 2 to 3.15 mm was separated from the smaller particles. These materials of very low solubility were filled in a glass beaker, covered with ultrapure water (≥ 18 M Ω -cm, from a Purelab UHQ System, ELGA LabWater) and sonicated in an ultrasonic bath for 1 min. The washing water was then decanted and the washing step was repeated three times or until the leftover supernatant was colourless. The washed minerals were left in an open container in a desiccator to dry overnight. The hydrothermal quartz samples were provided by a campaign of U. Schreiber, University of Duisburg-Essen. They were sampled on the Archaean Yilgarn craton of Western Australia. Those designated SM were sampled at the 1.6 Ga old impact-generated quartz veins of the Shoemaker-Crater. Samples designated MU stem from hydrothermal quartz boulders from a 2.7 to 3 billion years old conglomerate near Murchison (Western Australia). Samples from Mesozoic hydrothermal quartz veins from High Taunus in Germany are designated HTV and were sampled by T. Kirnbauer, University of Bochum, and U. Schreiber (see above). The samples were partly prepared in external laboratories: samples were broken down with hammer and jaw crusher to a size of 3 to 5 mm. Approximately 100 g of material was then submerged in 100 mL HCl (14%) overnight. The acid was discarded the following day and the samples were covered with 100 mL bidistilled water. After the water was discarded the sample was subsequently rinsed 5 times with 40 mL bidistilled water. Samples were then washed three times with at least 20 mL ethanol and dried in an oven at 40 °C. This set of samples included a blind quartz sample which underwent the same treatment. Upon arrival they were subject to the same evacuation procedure as all samples and as outlined in the following.

In order to measure compounds released from the FIs of the minerals, we sought to minimize the amount of semivolatile gases adsorbed onto mineral surfaces. These adsorbed gases were removed within an ultra-high vacuum which also completely dried the samples, which was indispensable for GC-MS analysis. For this purpose a stainless steel cylinder was specially designed (see appendix Figure 6.1). Up to 6 samples could be placed on a rack and into the cylinder. The lid was then screwed on tight along the flange.



Figure 3.1: Impressions of samples and their processing. A and B shows the sampling of sample H45Bol on the Salar de Uyuni, Bolivia (pictures by K. Kotte). The orange colour indicates microbial activity and is caused by β -carotene as is typically produced i.e. by the halophilic microalgae *Dunaliella salina*. Pictures C to F illustrate the diversity within the set of halite samples. Pictures C to E are samples from salt pans: C is sample H45LD from Australia, D from Lake Elton in Russia, E from Botswana. F is a rock salt from a Siberian drilled core (provided by Sevensen) with its blue colour stemming from structural defects in the crystal structure. G to I show sample F1PS as received and prepared before and after grinding.

The lid was equipped with a stainless steel bellows valve which was attached to a high vacuum pumping station (for construction drawings of pumping station see appendix). After a pre-vacuum of $< 5 \cdot 10^{-2}$ mbar was reached the turbomolecular pump evacuating to $< 3 \cdot 10^{-3}$ mbar (limit of probe head) was started and ran for 24 h. After sample evacuation is completed the system is vented slowly with ambient air. The samples were taken out of the pumping station to be stored in a desiccator and kept away from the laboratories to avoid re-contamination.

Table 6.1 in the appendix contains a complete list of samples with information on characteristic sample features and sampling locations.

3.2.2. GC-MS

Volatile compounds from FIs were determined via GC-MS. First, the volatile compounds are separated chromatographically before entering the MS. The detection is induced by the ionization of incoming molecules via electrons with a kinetic energy of 70 eV. Thereby, compounds are broken down into smaller ionized fragments. The fragments then undergo a mass selection inside the ion trap. Time resolved mass distribution is obtained.

The analytical method and its development were described in detail in Chapter 2. However, some of the data presented here were obtained using the original analytical set-up first employed. Figure 3.2 depicts the original system together with the revised cold-trap design.

In short, after mineral samples were ground and the grinding chamber attached via stainless steel needles the released volatile compounds were carried out by a He purge gas stream onto the cold-trap. Here the analytes condense while the carrier gas and other permanent gases were vented to the atmosphere. The original cool trap consisted of a lying brass cylinder traversed by a 20 cm long glass lined tubing (GLT). Valves connected to the temperature control device allowed for a dynamic cooling of the trap to below -190 °C in a liquid nitrogen steam. If the temperature of the GLT dropped below a certain set point valves opened again to fill in new liquid nitrogen. Problematic with this cold-trap design was the high liquid nitrogen consumption. Another disadvantage was the fluctuating temperatures, which were not favourable for the retention of highly volatile compounds. For the revised cold-trap a GLT was bent to U-shape so that it could be cooled statically submerged in a 80 mL Dewar vessel filled with liquid N_2 . Pressurized air blew off the liquid N_2 before resistive heating facilitated sample desorption. Valve controlled, the

enriched VOCs were transported with the carrier gas stream via the 15 cm long GLT directly onto the capillary columns within the GC oven and detected in the ion trap MS.

Another substantial difference between the two experimental set-ups was the choice of the GC oven program. Figure 3.3 shows both temperature programs in comparison.

Originally, a GC oven cooling was installed to ensure proper separation of VOCs with very low boiling points. This cooling consumed a lot of additional liquid N₂. With the more efficient second cold-trap and the experience of the first measurements the later GC oven program started isothermal at 35°C for 22.5 min. Together with a replacement for the old BPX5 capillary column with a new one this program was found sufficient to separate most of the occurring volatiles. In Table 3.1 the influence of the two different experimental set-ups on retention time of analytes are listed. Note that the low boiling point analyte CF₄ at -128°C showed at first several peaks in a range of retention time. This was most likely due to the fluctuations occurring during the sample concentration as controlled by the temperature control device. Although the peaks for CF₄ and SF₆ were close together in the updated set-up, their identification and quantification was unproblematic. Another major advantage was the reduction of time needed for one measurement as can be seen in Table 3.1. Retention times and mass spectra were used to identify analytes of samples and those of commercial standards. If no standards were available the mass spectra were compared to the National Institute of Technology (NIST) mainlib database under consideration of respective retention times and estimated boiling points.

External multipoint calibration for all analytes was difficult due to lack of suitable gaseous calibration standards. Injections of a methanol based standards with known concentrations into the grinding chamber or the 20 mL headspace were used in parts but are in principle not the optimal option for this system. The absence of water, necessary to mimic conditions applied during measurements, enhanced the error and the MeOH interfered with the chromatography on a short term and lead to column-bleeding after several measurements. The use of diluted pure gases eventually served as standards for major analytes. The 1,3-butadiene peak of a gaseous hydrocarbon standard “crystal gas mix” (Air Liquid) served as a daily standard.

An interesting series of experiments, also referred to later on, was part of a bachelor thesis (Bugla, 2010). 2.5 g of samples are heated in a headspace vial for 24 h at 150 °C before measuring VOCs with the GC-MS. For more details on the GC-MS measurement and grinding procedure please refer to Chapter 2.

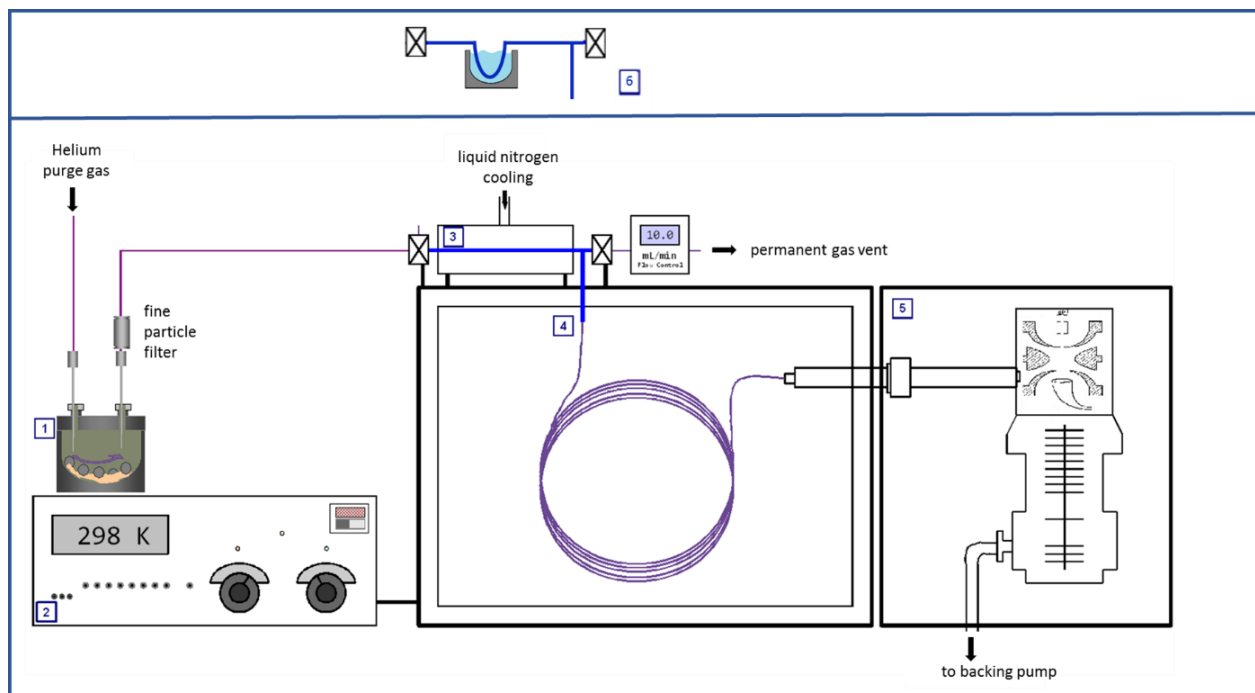


Figure 3.2: The original analytical set-up consisted of (1) the mineral grinding chamber, (2) a temperature control device, (3) the cylindrical cryo-trap with a liquid N₂-inlet, (4) the gas chromatograph equipped with two capillary columns and (5) an ion trap mass spectrometer (picture of ion trap design taken from Varian, ITS 40 Operation Manual). The revised set-up employed a different design of cold trap (6). The U-shaped glass lined tubing was submerged in liquid N₂ during cooling. Pressurized air blew off the liquid N₂ before resistive heating facilitated sample desorption.

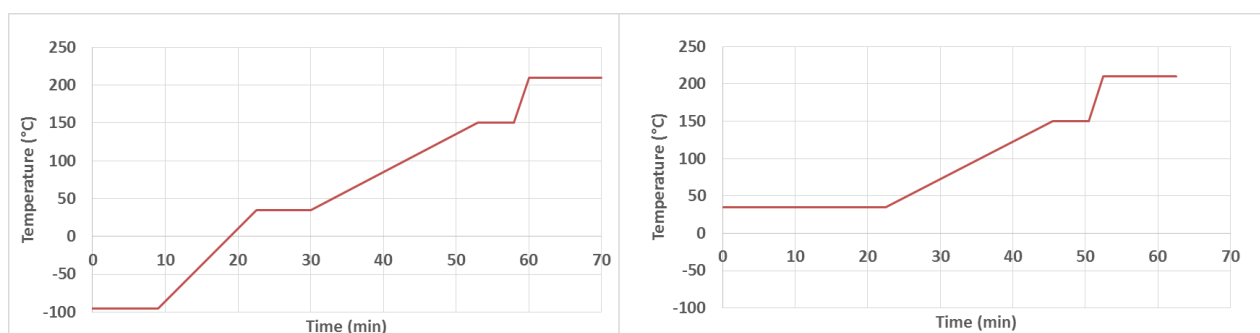


Figure 3.3: GC oven temperature programs for the “old” set-up (left) and the revised set-up with static cooling of the GLT trap (right).

Table 3.1: Selected analytes and their retention times under the old (retention time 1) and the updated experimental conditions (retention time 2). Retention times for 2-Butene marked with asterisk is a mean retention time value as isomers were not differentiated due to a lack of standards.

	boiling point °C	target ions amu	retention time 1 min	retention time 2 min
carbon tetrafluoride	-128	69, 50	10.5-12.5	14.8
sulfur hexasfluoride	-64	127	13.5	15.2
carbonylsulfide	-50	60	27.3	16.3
methylchloride	-23.8	49, 50, 52	31.7	17.5
2-butene (trans)	0.88	50, 52, 55, 56	33.1*	18.0
2-butene (cis)	3.72	50, 52, 55, 57	33.1*	18.4
methylbromide	38	79,94,96	37.6	19.7
benzene	80.1	77, 78	53.1	39.1

3.2.3. Ion chromatography

All halite samples were analyzed for Cl^- , Br^- and SO_4^{2-} via ion chromatography (ICS-1100, Dionex). This liquid chromatography method is used to separate and quantify ionic compounds mostly from inorganic salts.

As the mobile phase, an eluent consisting of a 4.5 mM Na_2CO_3 / 0.8 mM NaHCO_3 mixture is used at a flow rate of 1 mL/min. Samples are injected via the autosampler (AS90, Dionex) and pass through the guard column (AG23, Dionex) before separation. The analytical column (AS23, Dionex) employed as the stationary phase consists of a macroporous polymer, which has alkyl/alkanol quaternary ammonium ions as functional groups. The counter-ions (carbonate anion) from the mobile phase occupying the quaternary ammonium ions can be replaced with ions from the liquid sample. Depending on affinity to the stationary functional group carbonate anions are replaced by anions from the sample. The stronger their ionic binding to the stationary phase the longer sample anions are retained.

Before detection with a conductivity detector the signal is enhanced by passing through a self-generating suppressor which continuously provides H^+ . In this suppression step, the sample counter-ions are replaced by H^+ forming highly dissociative acids with the sample anions resulting

in an increased conductivity and better signal. At the same time, the eluent Na_2CO_3 is transferred into the weak acid H_2CO_3 which is hardly conductive, reducing the background.

The analytical system was operated with the software Chromeleon 6.80.

Usually, the sample is an aqueous solution e.g. of a soil sample. As our samples completely dissolved and contained high Cl^- -concentrations we used a dissolution rate of 1:3333 (sample/water). This was necessary to protect the stationary column and prevent Cl^- overload.

3.2.4. Carbon content

Carbon content of a set of halite samples was determined using a LECO SC-144DR, with a detection limit of 50 ppm. Samples are combusted in the analyzer at $1400\text{ }^\circ\text{C}$ in an oxygen current. The evolving CO_2 is then detected in an IR cell and carbon content output is given in percent taking into account the weight of the combusted sample. The set of samples analyzed comprised all samples from H1Elt to H27Gor as well as two gypsum samples G1Bas and G2Bas. Here, we used 0.5 g of halite sample for each measurement. A few samples were measured after they were ground and measured with GC-MS. Due to the scarcity of material and the destructive nature of this analytical technique several samples were also determined after they have been used for non-destructive total elemental analysis. Most samples were determined using crystals no larger than 5 mm thickness. As a control CaCO_3 was run every 10th to 15th measurement. As the samples consisted of halite crystals only, no inorganic carbonate contributed to the carbon contents determined with the analyzer. All carbon determined from this measurement is assumed to stem from organic matter in the sample.

3.2.5. Major and trace elements (XRF)

Major and trace elements of a selected set of samples were quantified via energy-dispersive XRF-spectrometry (x-ray fluorescence), a non-destructive method. From a glow filament (cathode) electrons are accelerated through a vacuum towards the primary target (anode). Upon electron impact the anode emits x-rays which then pass through an analyzer-crystal yielding monochromatic K_α -radiation. This monochromatic radiation is subsequently used to excite the sample elements. Fluorescence emissions are element specific. The detector measures the energies of the x-ray quanta and correlates them to wavelength after 2-point calibration.

The two instruments used here were custom made by Andrey Cheburkin and each was used for a different element range. For elements from Al to Mn a Co X-ray source (17 V, 1 mA) with a HPGe-detector called TITAN was employed. The second instrument consisted of a Mo X-ray source (37 V, 5 mA) and a Si(Li)-detector and recorded elements from Fe to Y (Z 26-39) as well as Pb (Z 82). It is described under the name EMMA (Cheburkin et al., 1997).

Powdered samples were filled to approximately 0.5 cm thickness onto a thin-film (Chemplex) in a sample holder. XRF measurements were conducted over 10 min for statistical certainty.

To verify calibration performance certified reference materials (CRMs) as external standards were used depending on sample matrix. A list of available CRM is given by Krause (2014). However, no CRM was available for halite matrices. A carbonate rock standard was the closest representative of the halite matrix and thus results from salt samples have to be seen as semi-quantitative. Lower limits of detection reside in the lower ppm range.

One objective of the XRF measurements was to investigate if samples are contaminated by the abrasion during the grinding procedure. Therefore some samples were also ground with an agate mortar and pestle and vibration cup mill as indicated in the results section.

3.2.6. X-ray diffraction

X-ray diffraction (XRD) relies on the principle of the diffraction of an incoming x-ray at the crystal lattice. Each mineral causes, depending on its lattice parameters and chemical composition, a unique diffraction pattern as a function of the incident angle of the x-ray beam. Minerals can thus be identified and characterized by these characteristic intensity maxima. Bragg's-equation explains the relationship of the incident angle of the x-ray beam θ to the diffracting planes of the crystal lattice

$$2 d \sin \theta = n \lambda,$$

where d is the spacing between diffracting planes, θ is the incident angle, n any integer, and λ is the wavelength of the beam.

For samples we used this method to test their mineralogical purity and to identify mineral mixtures qualitatively and quantitatively. Sample powders were mounted onto the sample holder and were then analyzed using a Bragg-Brentano powder-diffractometer with secondary-beam

monochromator (Philips XPert PW3020). The resulting peaks counts were registered between 10 and 70 on the 2-theta scale.

Data were plotted and evaluated using the Diffrac Plus EVA 13 (Bruker-AXS). If more than one mineral phase was present quantifications were carried out by the FPM Evaluation function of the program.

Not each individual samples was measured but rather samples representative for each sample type or sample location. If samples were visibly significantly different per location more than one sample was chosen for XRD.

3.2.7. Py-GC-MS

Pyrolysis is the thermal decomposition of materials. Commonly, data from Py-GC-MS are used as fingerprint to prove material identity or the identification of individual fragments can help to obtain structural information of larger molecules which are cleaved into smaller fragments.

GC-MS results from salt samples heated to 150 °C had shown a remarkable increase in emitted VOX (see results section). Therefore a sub section was analyzed by C. McRoberts at Queens University in Belfast, Ireland. The set of six untreated samples comprised H6Kas, H3Elt, H26Bas (Russia), H13Douwe (Mauretania), H42LD (Australia) and H27Gor (mine Gorleben, Germany).

A preliminary pyrolysis gas chromatography (Py-GC-MS) study showed that the supplied MeCl production was greatest for sample H3Elt out of the set of samples provided. Therefore this sample was used to investigate MeCl release at different pyrolysis temperatures.

Py-GC-MS was carried out using a CDS 5200 series pyrolyser in direct mode linked to an Agilent Technologies 5975 GC-MS system. Of each sample 6-7 mg were accurately weighed on a microbalance and pyrolysed at either 300 °C, 500 °C or 700 °C at a ramp rate of 20 °C/ms for 20 seconds. The pyrolysis products were separated on a Varian CP7550 PoraPLOT Q (12.5 m x 0.32 mm x 10 µm) capillary column with a split ratio of 50:1. The column was initially held at 30 °C for 1 min and then ramped at 10 °C/min to 200 °C with a constant flow rate of 3.0 mL/min. The MS was operated in the selected ion monitoring mode monitoring ions m/z 50 and 52 for chloromethane. The peak for chloromethane had a retention time of 2.9 min. Analytical grade NaCl was run as sample control.

3.3. Results and Discussion

3.3.1. Sample treatment and technical problems

As the results presented were obtained throughout the ongoing method development and improvements of the system were undertaken along the way, frequent calibrations were necessary. Also, as the initial calibration of the methanol based EPA 624 standard in the absence of water proved to be detrimental to the capillary column the use of gaseous standards was inevitable. Same was true for initial trials with hexafluorobenzene as a daily correction factor. Initially, pure gases for CF_4 , SF_6 and MeCl were used and diluted in a three steps via Erlenmeyer flask for calibration. MeCl dilutions were also applied partly for the daily correction factor. The handling was problematic due to frequent clogging of the syringe and in the case of the heavy SF_6 improper mixing. Also, these standards had to be prepared new every day. Own preparation of calibration standards in Helium filled Tedlar bags were not successful due to Helium loss through the walls of the bags. The use of 0.66 ng of the crystal gas standard and the 1,3-butadiene peak area as a daily correction factor was implemented successfully in advanced stages of the method development.

Figure 3.3 shows two blank chromatograms under conditions of high sensitivity of the electron multiplier and without air leaks. The red line shows a typical measurements from the empty grinding vessel with a norflurane peak from the Viton seal ring and a peak with $m/z=49$ and 50 at 20 minutes of unknown origin. The later peaks in the chromatogram were usually caused by the capillary column upon heating. The 20 minutes peak could be a compound like 1,3-butadiyne for example or a similar unsaturated hydrocarbon. A potential source for such a compound could be chemical ionizations of contaminants within the ion trap. Chemical ionization was a problem especially observed for the low boiling point compounds resulting in mass shifts by one unit. This occurred predominantly after a suite of samples, especially when salts were measured, which seemed to compromise the cleanliness of the ion trap. In an attempt to minimize signals in the blank measurement a 30 x 30 x 30 cm small glove box made from polymethyl methacrylate (Plexiglas) was built, in which the grinding chamber could be filled and closed under inert gas. However, as shown in the green chromatogram of Figure 3.3, the glue used in the construction of the box caused large chlorobutadiene and a multitude of other contamination peaks within an otherwise blank measurement. In general, working with samples in ambient air was sufficient for the experiments. Xenon, a compound occurring at concentrations of 87 ppb in the atmosphere, was recognized as a

sign of air leak at the grinding chamber during the purge step. Under air-tight measurement conditions the Xe concentration was below limit of detection in the grinding vessel. Contamination through abrasion within the chamber during grinding is discussed in section 3.3.5 of this chapter.

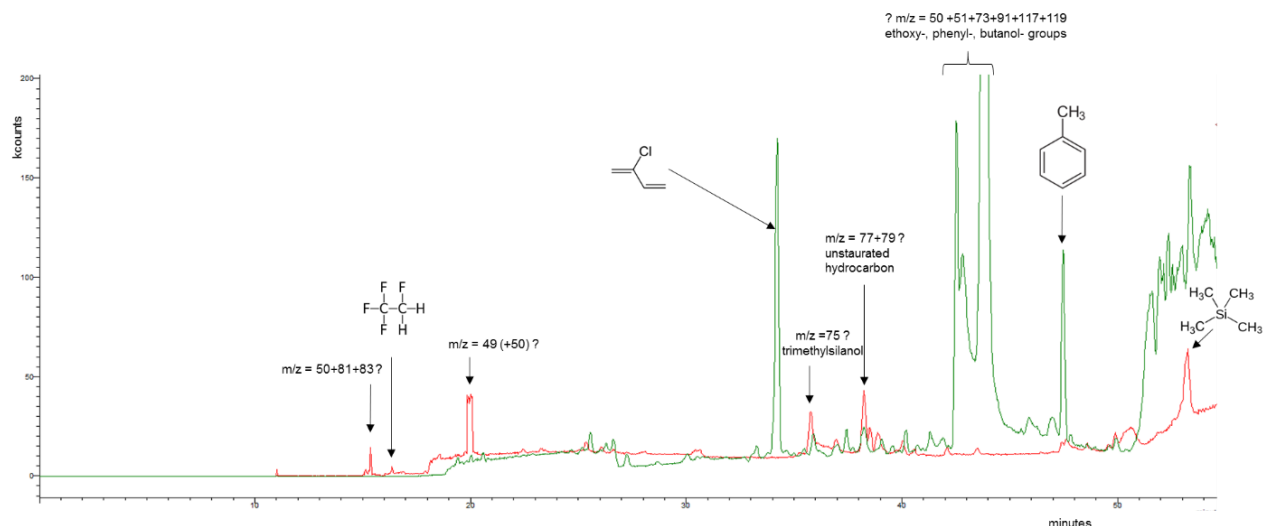


Figure 3.3: Blank chromatogram of the grinding chamber prepared under ambient air (red) and in the argon glove box (green).

3.3.2. GC-MS

Complete tables of results of VOC from mineral and rock samples can be found in the appendix, Tables 6.2 to 6.7. Those tables are subdivided by sample type and by time of measurement as to account for the different stages of method development. The results presented in Table 6.3 and Table 6.4a were obtained as part of the bachelor theses by Bugla, (2010) and Ubl (2011).

Figure 3.4 presents an overview of results of this sample screening. Although the number of measurements per sample group differed substantially, the samples were subdivided into the groups of halites, quartz, fluorites and volcanic glasses. Disregarding the amounts detected, occurrences of each VOC was counted and normalized by number of samples measured. Not included in Figure 3.4 are granites, gypsum and each one sample of schist, limestone and MORB. For the schist (G03MW), limestone (G04MW) and MORB no compound were detected. Only one out of the two

granite samples (G01MW) had a CF₄ content of 169 ng/kg. Two gypsum samples were measured and their VOC content resembled that of the halite samples. As the gypsum sample was taken at Lake Baskunchak, a close similarity to sample H26Bas is obvious, with VOCs present at slightly lower concentrations.

For all other samples Figure 3.4 reveals the occurrence of a multitude of compounds for halites and gypsum, whereas the compound diversity of fluorites and volcanic glass samples was lower. Clearly, the first conclusion is that the set of samples for the latter two need to be extended. Secondly, MeCl, carbonylsulfide (COS) and benzene were present in all sample groups. While small peaks of COS and benzene were also commonly observed in the control runs of the unground sample, MeCl was only detected after samples were ground, excluding the possibility that is a contaminant from the system. In fluorites and mafic rock (basalt/dolerite) however, the amounts detected were low. Surprisingly, the concentrations of MeCl in the quartz samples were partly as high as in the halites with 2.7 ng/g for sample MU4 and 1.5 ng/g for sample HTV115 (Figure 3.5). Also the fluorite sample F4PS with a value of 60 ng/kg (ppt) falls in the range of observed concentrations for many salts. While MeCl from halites has been previously reported in the literature (Isidorov, 1993; Svensen et al., 2009), this is a novel observation made for the fluorite and quartz samples. Similarly stunning is the occurrence of methyl bromide of up to 10 ng/g in quartz samples (Figure 3.5). Samples MU4 and HTV115 are special with regard to the diversity of compounds discovered after grinding. MU4 contained 2.7 ng/g of MeCl, 10 ng/g MeBr, 0.8 ng/g 1,1-dichloroethane and also showed peaks for carbon disulfide and trans-1,2-dichloroethane. Results for HTV115 were even more diverse: 1.5 ng/g MeCl, 7.5 ng/g MeBr, 0.5 ng/g vinylchloride, 0.3 ng/g but(adi)enes (consisting of isobutene, 1,3 butadiene, cis/trans-2-butene) and showed large peaks for carbon disulfide, carbonylsulfide, trans-1,2-dichloroethene and 2-chlorobutane (see table 5.7). This multitude of hydrocarbons and sulfurated and halogenated compounds indicate that conditions for their formation within the earth crust are favorable in parts. Although the results from sample HTV 115 are impressive the true origin of these compounds is unclear. It is possible that the compounds trapped stem from C_{org}-rich metasediments. In contrast, sample MU4 was sampled at a 2.7 to 3 billion years old conglomerate of the Yilgarn craton near Murchison (Western Australia). In this case, the analyzed quartz samples were formed in hydrothermal veins in early stages of the evolution of life and could have contributed in pre-biotic organic chemistry.

In contrast, almost no organic compounds have been detected inside FIs from impact-generated quartz veins of the Shoemaker-Crater (between 1.0 and 1.6 Ga). The absence of the compounds can be interpreted in agreement with the model put forward by Schreiber et al. (2012). It states that the prerequisites for the geochemical formation of organic molecules are a suitable carbon source (e.g. carbon dioxide), varying P/T conditions and catalysts. Pre-biotic organic molecules were earliest markers for a chemical evolution that have been formed in tectonic faults of Archaean cratons. According to the postulated model, rising hydrothermal fluids such as mineral-rich water and supercritical carbon dioxide in deep faults with contacts to the upper earth mantle offer conditions which allow for reactions similar to the Fischer-Tropsch synthesis. As the impact-induced hydrothermal system of the Shoemaker-Crater had no connection to the Earth's mantle, there was no contact to rising volcanic fluids. The results from FIs encapsulating hydrothermal fluids during the growth of these quartzes conserve the chemical composition predominating during the formation and distinguish them from other quartz samples.

When comparing halites and quartz samples in Figure 3.4 another observation that can be made is that the halites are dominated by hydrocarbons while quartz, mostly due to the inclusion within the two samples discussed above, exhibit a relatively larger fraction of halogenated compounds. Halite samples were predominantly sampled at surface sites, while the hydrothermal quartz samples underwent elevated temperature and pressure conditions. But with the omnipresence of alkanes, alkenes and maybe even alkynes (no verification by a standard yet) halites contain abundant precursor material that could be readily halogenated. Isidorov et al. (1993) detected chlorine and sulfur containing compounds from halite and sylvinite mining emissions which they also partly measured after dissolution of the salt crystals by GC-MS headspace analysis. Most recently, Svensen et al. (2009) reported the extraction of CHCl_3 , CHBr_3 and 1-chloro- and 1-bromobutanes from halites using GC-MS and a heating procedure at 225 °C as well as a crushing procedure, but little details were reported on the latter one. Samples H23Sib and H24Sib correspond to samples 194/3 and 194/4 reported by Svensen et al. (2009) and can directly be compared. Svenson et al. also reported benzene from the crushed sample at room temperature for both samples and also found methyl chloride, methyl bromide and chlorobutane in sample 119/4. The values for MeCl and MeBr for sample 194/4 were about 100-fold larger than our values but they heated to 275 °C as compared to 150 °C in the case of H24Sib.

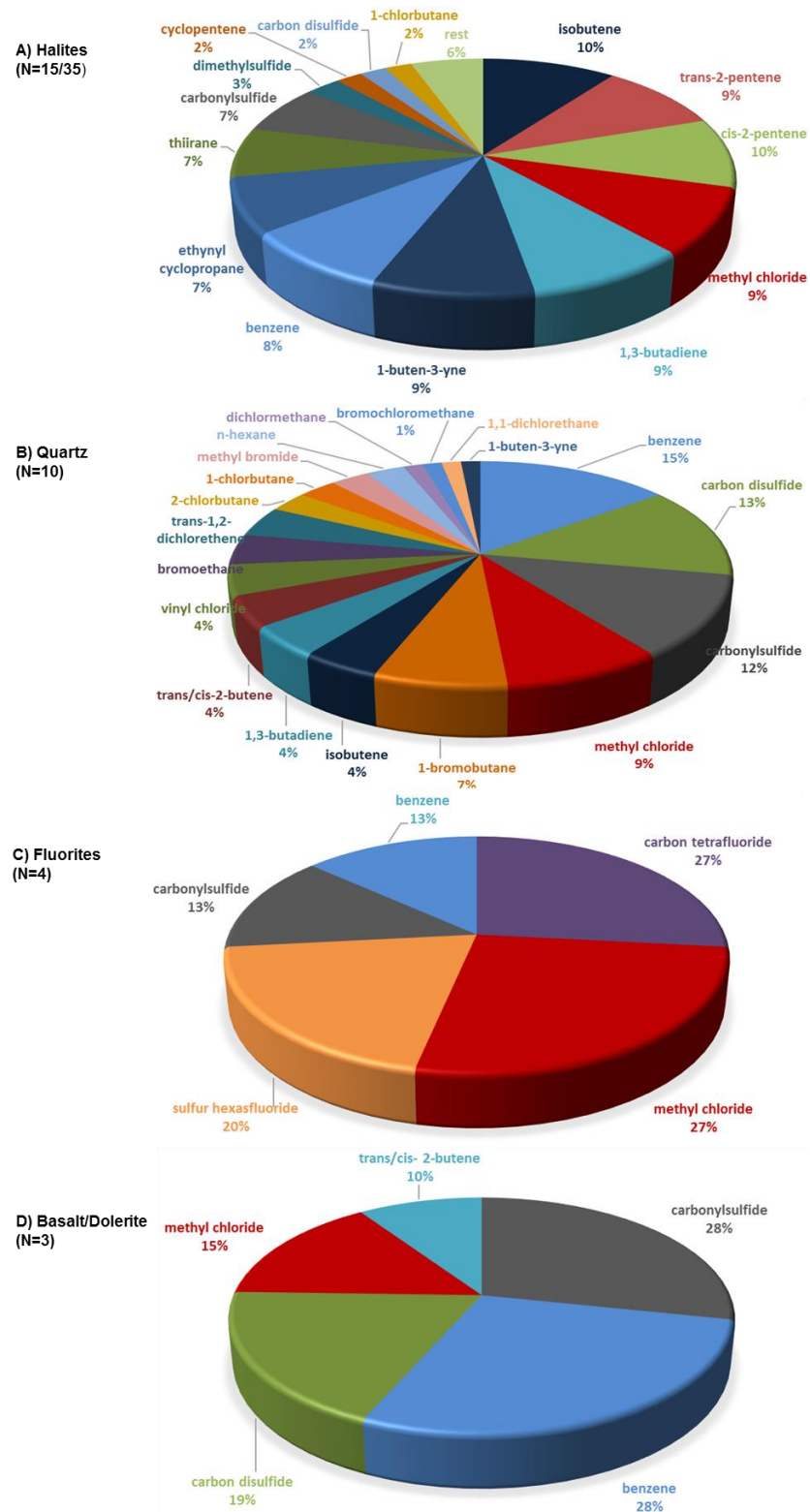


Figure 3.4.: Relative frequencies of VOC occurrence per sample group. The rest 6% of the halite samples comprise dichloromethane, n-hexane, 2-chlorbutane, 2,3-pentadiene, vinyl chloride and methyl bromide. N=35, inclusive data of Bugla (2010).

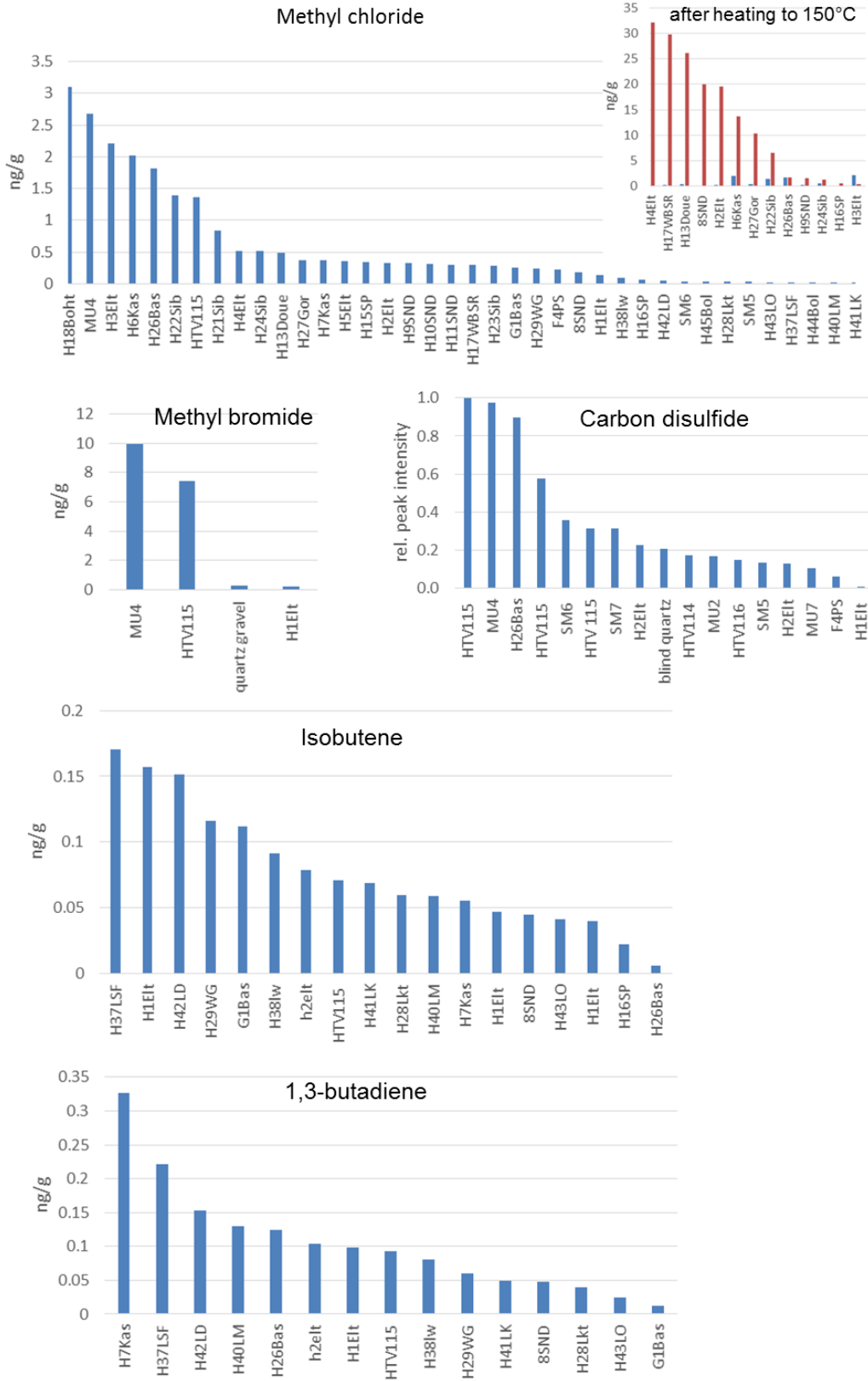


Figure 3.5: Selected VOC concentrations per gram of sample.

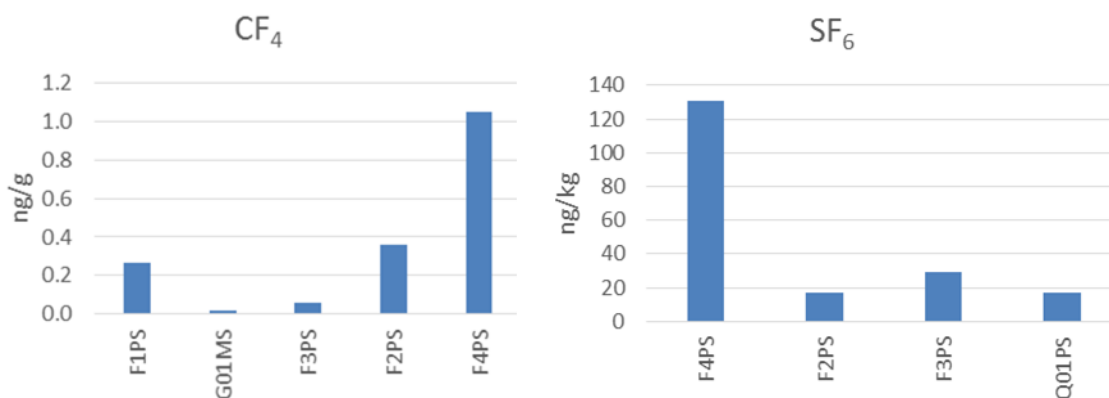


Figure 3.6: CF_4 and SF_6 concentrations of fluorite, granite and quartz samples (based on data by Ubl, 2011).

The tendency of increased VOX release upon heat for methyl chloride, methyl bromide and chlorobutane can be confirmed not only for the samples from Siberia but for all halite samples in general. The top right in Figure 3.5 shows that MeCl release after heating was partly more than 100-fold higher compared to the grinding procedure. Additionally, we found an increased formation of isobutene, bromomethane and trichloromethane upon heating as illustrated by the chromatograms of sample H6Kas in Figure 3.7., Beerling et al. (2007), modelled large amounts of total MeCl and MeBr of 63.6 and 0.8 Tg degassed during the intrusion of the Siberian Trap basalts into Permian salt beds. A MeCl/MeBr ratio of the same order of magnitude was observed for many halite samples.

As summarized by Wignall (2007), the discovery of mutated palynomorphs in end-Permian rocks led to the hypothesis that an O_3 depletion and increased terrestrial incidence of harmful ultraviolet-B ($\lambda=315-280$ nm) radiation might be responsible for the Permian-Triassic extinction event. The hypothetical synthesis and release of massive quantities of volatiles, especially organohalogens, in the Siberian Large Igneous province (SLIP) could have triggered O_3 depletion and allowed an increased terrestrial incidence of harmful UVB radiation is now a popular notion confirmed by many (Aarnes et al. 2011; Tang et al. 2013; Black et al. 2014). Also our results agree and strengthen this hypothesis as well as chlorination of hydrocarbons upon heating within salts as the general mechanism.

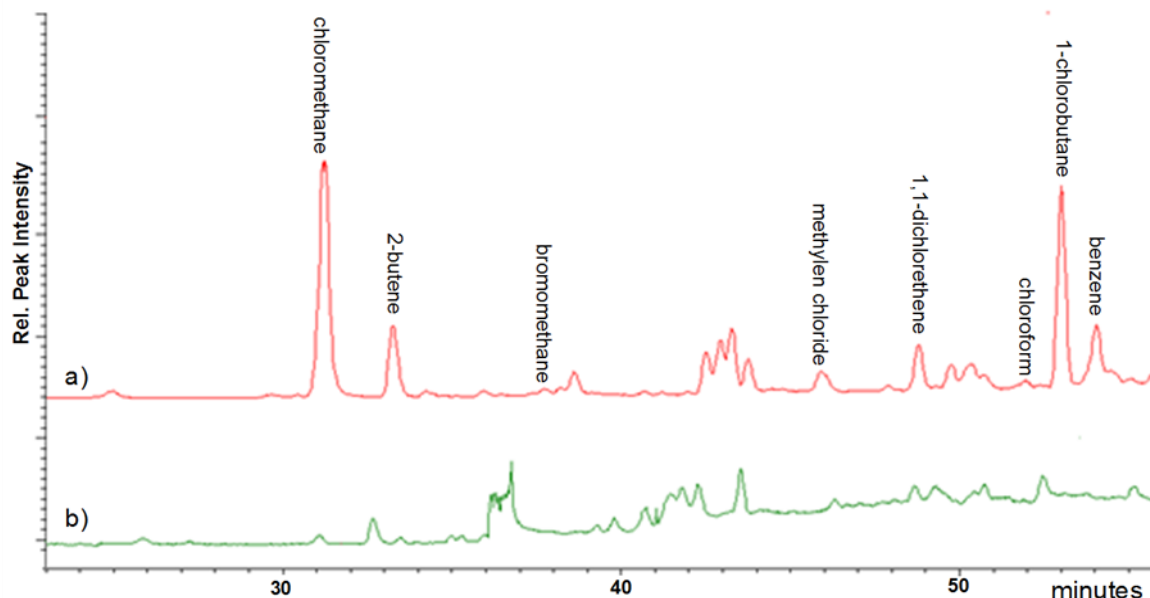


Figure 3.7: Chromatograms of sample H6Kas after heating (a) and after grinding (b).

Data of Svenson et al. (2007) on butanes and benzene, apparently common to FIs in salts, imply that these compounds are broken down upon heat and provide active organic matter (OM) precursor. Organic radicals could be formed upon heating and further oxidized to carbocations that are then subject to nucleophilic attack by gaseous chloride. Krieger (2014) confirms the widespread occurrence of methane, butane, benzene, toluene as well as chloromethane and carbon disulfide in halites. Furthermore, chlorobenzene and trichloromethane are added to the list of VOX observed in FIs of halite. Dimethylsulfide (DMS) and methanethiol were also found.

Another interesting set of samples related to the SLIP were samples P01BB, P02BB and P03BB provided by B. Black (Massachusetts Institute of Technology, USA). They measured S, F and Cl concentrations of dolerite sills, mafic tuffs, lava flows and picrites sampled in Siberia and based on their results estimated magmatic degassing from the SLIP to be ~6300–7800 Gt sulfur, ~3400–8700 Gt chlorine, and ~7100–13,600 Gt fluorine. The samples provided correspond to samples R06-07 and R06-09 presented in their publication (Black et al., 2012). For samples P01BB-P03BB sulfur, chlorine and fluorine concentrations of the melt inclusions corresponded to 0.13, 0.94 and 0.3 wt%, respectively. The question arose, if their elevated halogen content could contribute to VOX formation preserved also in gaseous FIs within the samples. Figure 3.4 and Table 5.2 indeed show peaks for methyl chloride, furthermore high carbonylsulfides and carbon disulfide peaks

which are in agreement with the occurrence of sulfur within the dolerite sill. However, no fluorinated compounds were detected. Unfortunately, restricting the FI data were analytical problems at the time of measurement. Measurement of sample R06-09 failed completely and the absence of e.g. SF₆ and CF₄ in R06-07 (=P01BB-P03BB) is doubtful.

The results for the Wölsendorf-fluorite F4PS showed peaks for CF₄ and SF₆ up to 19.1 and 2.1 ng/g, respectively. Lower values for the same sample were detected in August 2008 (Table 6.4), but these values might be underestimated due to an unidentified problem with leakage by the time. Our values lie within the range of observed quantities for CF₄ (0.002-61 ng /g and SF₆ (0-30 ng/g) from fluorite samples by Harnisch et al. (1998, 2000). We could not confirm the occurrence of CF₂Cl₂ and CFCl₃. In the sample from Wölsendorf Harnisch et al. (2000) also identified CF₃Cl, CHF₃ and NF₃. Possibilities why we did not detect those substances might be that they were present at quantities below detection limit in our sample. In principle our system setup should be able to retain them but separation might not be sufficient. We did, however, detect the presence of MeCl with 6 to 6170 pg/g in F4PS which was not reported previously. Halogenation reactions of organic precursor material (predominantly as methane homologue alkanes) may facilitate subsequent fluorination by fluoride-derived F⁻, HF or elemental F₂ possibly also via nucleophilic substitution as is one of the basic reaction mechanism of organofluorine compounds synthesis in industrial process (Dolbier, 2005; Schmedt auf der Günne et al., 2012). The occurrence of fluorinated compounds in Wölsendorf fluorites is also consistent with early results by Kranz (1966), who used mass spectrometry. His ion fragments of m/z 50 and 69 should correspond to the ions CF₂⁺ and CF₃⁺ from CF₄. The fragment with m/z 127 should correspond to SF₅⁺ from SF₆. There is a large natural variation within the set of samples, indicating that FIs are not evenly distributed. The inhomogeneity is reflected in the reported values that differ by a factor of 100 as well as by our data presented in Figure 3.6. A larger abundance of CF₄ compared to SF₆ was confirmed by our analyses. Results for sample F4PS, which was quantified in August 2011 (Table 6.4a), November 2011 (Table 6.4b) and August 2012 (Table 6.7) showed a low reproducibility owed to natural variance within the sample. Harnisch et al. (1998) argued, that SF₆ and CF₄ are formed mainly within fluorites and that granites contain only those amounts of these compounds that are contributed by the accessory fluorite (<0.1 wt%) present in these rocks. Our results on granite G01MW and G02MW, appear to agree with this hypothesis. However, we detected an amount of 17 pg/g SF₆ in a pure quartz sample. Although its exact sampling location is unknown, the Fichtel

Mountains, as part of the Bohemian Massif, began in the Precambrian and underwent the Variscan Orogeny. Possible processes which could have led to the capturing of SF₆ include, folding, high pressures and temperatures, circulating brines and partial melting. Speculating, that Fichtel Mountain's granite was the original source of this compound it must have been trapped when hydrothermal quartz precipitated. Accordingly, CF₄, which is more volatile and less soluble in water (Cosgrove and Walkley, 1981) as well as in n-alkanes (Hesse et al. 1996) may have degassed to the atmosphere and was thus not conserved in the FIs of the quartz.

Only two granite samples (G01MW and G02MW) were measured (Table 6.4a) though measurement conditions were not ideal (unidentified air leak). Together with samples G03MW and G04MW this set of samples was assembled during an investigation of elevated SF₆ in groundwater of the Cambay Basins, Northern Gujarat, India (Wieser, 2010). The use of SF₆ as tracer was problematic for their study on paleo climate, as SF₆ concentrations in groundwater were found to be abnormally high in some wells. A natural origin of SF₆ appeared to prevent the use of this tracer as a dating tool. A similar restriction on SF₆ groundwater dating was reported from the North China Plain (von Rohden et al., 2010) and the Odenwald region (Friedrich, 2007). Furthermore, high terrigenous concentrations of SF₆ have been measured in water from fractured silicic igneous rocks, carbonate aquifers, hot springs and from basaltic aquifers (Busenberg and Plummer, 2000; Koh et al., 2007). Kranz (1966) originally proposed the hypothesis of a radiogenic formation mechanism. Decay of uranium U²³⁸ and thorium Th²³⁴ was speculated to provide α -particles for the necessary activation energy of SF₆ formation. A correlation between terrigenous Radon and SF₆ was tested and obtained a first order linear correlation in crystalline rocks of the Odenwald (Friedrich et al., 2013). These authors found, that SF₆ was highly variable and not uniformly distributed throughout the crystalline study area, maybe hinting to the importance of fluorite accumulations in locally occurring hydrothermal veins. An understanding of the formation pathways is still subject to speculation. For more details on possible formation pathways please refer to Chapter 1.

Our data were not sufficient to contribute to an investigation of this problem. More samples and measurements are needed to allow for systematic observations together with a better characterization of the lithological facies.

Furthermore, other fluorine containing minerals such as tourmaline, apatite, biotite and topaz remain uninvestigated.

Finally, Table 3.2 presents results of exemplary calculations to estimate and compare the amounts of four selected compounds released by chemical weathering from fluorites and quartz of the continental crust to the atmosphere. Based on the mass of the continental crust of 2.09×10^{23} g (Yanagi, 2011) and a weathering rate for the continental crust of 9×10^9 t/a (Liu and Rudnick, 2011) contents of CF_4 , SF_6 from granitic and sedimentary fluorites as well as MeCl and MeBr from granitic quartz were estimated. 21% of the continental crust were assumed granitic (Harnisch and Eisenhauer, 1998), there of 30% quartz (Langmuir, 1997).

Table 3.2: Comparison of reservoirs and source strengths. Data on fluorite and quartz from the continental crust. Tropospheric data were taken, if not indicated otherwise, from Warneck and Williams (2012).

		fluorite		quartz	
		CF_4	SF_6	CH_3Cl	CH_3Br
concentration in mineral	pg/g	500	50	30	20
mass content continental crust	Tg	8485	848	509	339
mass content troposphere	Tg	0.96	0.14	4.4	0.14
chemical weathering of continantal crust	Gg/a	0.0365	0.0037	0.0022	0.0015
total sources (tropospheric budgets)	Gg/a	15^{\S}	$5\text{-}8^{\#}$	1700-1300	53.9-174*
tropospheric residence times	a	500000	3200	1	0.7

*Warwick et al., 2006

Maiss and Levin, 1994

§ Ehhalt et al., 2001

For the fluorite, Koritnig's (1951) data were used according to which granites contain $850 \mu\text{g/g}$ fluorine, with 45% of fluorine as fluorite, and sediments contain $300 \mu\text{g/g}$ fluorine, with 75% of fluorine as fluorite. Sediments made up 8% of the crust in the calculations. Amounts of hydrothermal fluorites and quartzes were neglected due to lack of corresponding literature values. All values were based on conservative and low values and thus results are systematically underestimated. This was intended due to estimative nature and poor experimental constraints on calculations.

Table 3.2. shows that the continental crust's reservoirs of SF_6 and CF_4 from accessory fluorites in granites is larger by a factor of 6000 to 8000 than the tropospheric reservoir, indicating a large emission potential from crust to atmosphere. The mass of atmospheric methyl bromide is about

200 times lower than the crustal quartz reservoir and the difference for methyl chloride was only about 100-fold. Although the compound reservoir of the crust is magnitudes larger than the atmospheric reservoir the source strength, i.e. the annual atmospheric release, to assess the emission potential of the crustal reservoirs, is more closely approximated by comparing the amounts released via chemical weathering from the crust to the reported known annual atmospheric emissions. The amount of SF₆ released by chemical weathering is 1000-times lower than that released by all other sources and that of CF₄ differed by a factor of about 500. Although now, that the emission potential of the continental crust is put into perspective, the tropospheric residence times indicate, that especially the budgets for SF₆ and CF₄ could be impacted due to their accumulation over time. Continuous diffusive loss of the compounds from the crust has not been considered so far. Values presented here rely on a prudent but also rather poorly constrained estimate. Furthermore, halites were left out of the equation. We know from the discussion above that MeCl is almost ubiquitously present in halites and that MeCl and MeBr are formed upon heating. Due to quick dissolution of surficial halite deposits, e.g. by sudden rain events, MeCl emissions probably impact local tropospheric loads. This aspect will also be a subject of Chapter 4.

In summary, results of GC-MS analysis revealed the presence of halogenated (chlorinated, brominated and even fluorinated) and sulfurated volatile compounds in FIs of most mineral and rock samples. Unsaturated n-alkyl chains and cyclic hydrocarbons, partly chloro- or brominated, were present in halites, hydrothermal quartz samples and fluorites. Carbon disulfide was the most commonly observed sulfurated compound, next to carbonyl sulfide. Halogenation reactions, especially the chlorination of methane, are widespread mechanisms in geologic matrices.

Except for the group of halites, more data are needed on each sample group. The halites will be the focus of the sample screening discussed in the following. In future investigations, special attention should also be given to carbonates and apatite, which were not studied by any group yet.

3.3.3. Ion Chromatography (IC)

Chloride values were very high as expected. In pure NaCl samples chloride should constitute 61 wt% and the values detected in the samples ranged from 48 to 61 wt% (for a complete list of results for Cl⁻, Br⁻ and SO₄²⁻ values see Table 6.8). As the chloride content was high and at the upper limits of detection these values are probably not reliable. XRD results, where available gave

indications of the mineral purity of samples and carbon analysis showed low contents of below 1%. It is not plausible to assume that the missing 13% (e.g. H3Elt) of the sample consisted of other mineral and organic matter. Although calibration of chloride was performed with the highest standard corresponding to the high Cl^- content of samples, the separation columns were not made for such excessive amounts but rather trace amounts.

Due to the high dilutions necessary to protect the chromatographic column bromide values which were detected in trace amounts in the order of ng/g, showed high relative standard deviations of almost 10 % on average. The detected amounts ranged from zero (for several samples) to 1,2 mg/g (H20Sib). Sulfate was present in all samples and ranged from 0.14 mg/g (H16SP) to 77.44 mg/g (H4 Elt). Bromide and sulfate were well suited to characterize the samples by location. No bromide was detected in samples from the Miocene salt deposits in Poland, samples from Lake Kasin in Russia and from Salar de Uyuni in Bolivia whereas South Russian halites of Lake Elton showed values between 130 and 290 ng/g Br^- , the very diverse salt lakes of South West Australia spanned a wide range from 30 to 270 ng/g Br^- and Siberian drill core samples showed remarkably high values of between 240 and 1197 ng/g Br^- . Highest sulfate contents were determined for Lake Elton samples and most of Siberian samples had a comparatively low sulfate content. With sulfate present and potassium and magnesium cations absent in the system thenardite, an anhydrous sodium sulfate mineral (Na_2SO_4), which occurs in arid evaporite environments could potentially be present according to the Jänecke diagram (Jänecke, 1918). However, XRD did not confirm the presence of this mineral phase as sulfate concentrations were too low (Table 6.8).

Figure 3.8 compares bromide results of our halite samples with data taken from Warren (2006). Overall, the observed values for bromide correspond well to literature data. Especially, the low values for the Bolivia samples (Warren, 2006; Risacher, 2000) are in good agreement with our observations. The values for our Siberian Permian halite are much higher than the values for the basal halite of Zechstein 2. However, the high values observed in our samples are not unique as the data on the Saline valley of California show. Values above 250 ppm in halite can be considered very high. As chloride is preferentially removed over bromide from an evaporating brine, only a small fraction of bromide is partitioned out into the halite crystal lattice. Thus, a large fraction of the bromide measured could stem from brines trapped in FIs. Bromide incorporated in the crystal structure increases with increasing temperature of the parent brine and speed of crystallization (Warren, 2006). Traditionally, bromide contents (or partition coefficients between crystal and

brine) of halite are used as an indicator for the source of the brine (Fisher, 1987; Risacher, 2000). Halite from a normal marine feed should contain from 50 to a maximum of 270 ppm bromide; halites formed in freshwater should contain around 500 ppm; recycled and re-crystallized halites, especially when freshwater-influenced should have bromide contents of 20 ppm or less. The degree of bromide spread values observed in our as well as literature data shows that it cannot always serve as a reliable indicator of the parent brine source. Variables such as differing salinity, dilutions, recrystallizations and back reactions in both marine and non-marine settings influence the Br⁻ content (Warren, 2006).

Correlations of bromide concentrations with MeCl and MeBr values from the GC-MS were tested. The best fit of a linear regression was obtained by bromide versus MeBr evolved after heating for 24 h at 150 °C which showed a clear positive correlation (Figure 3.9). After grinding, only from the blue rock salt sample H20Sib MeBr could be detected. The bromide contents therefore may give an indication for the MeBr formation potential upon exposure to heat. Conversely, the occurrence of MeBr from FIs in halite after grinding probably indicates, that the sample has been exposed to elevated temperatures upon burial and may provide an estimate on the initial bromide concentration present in the halite.

The regression coefficient of bromide versus MeCl after grinding (not shown) and heating was low. Similar correlations for chloride with MeCl and MeBr were not observed, most likely to problematic chloride analysis. Also the omnipresence of chloride suggests that the presence of suitable organic precursor would likely be the controlling parameter in MeCl-formation.

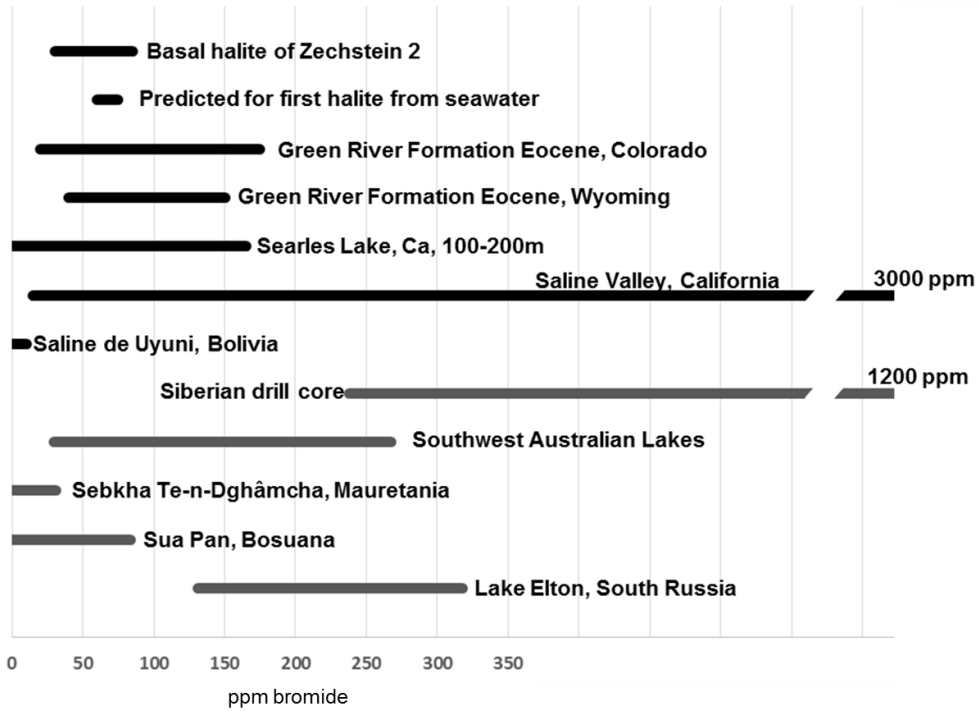


Figure 3.8: Comparison of bromide concentrations in halite. In grey own samples; in black data from Warren (2006).

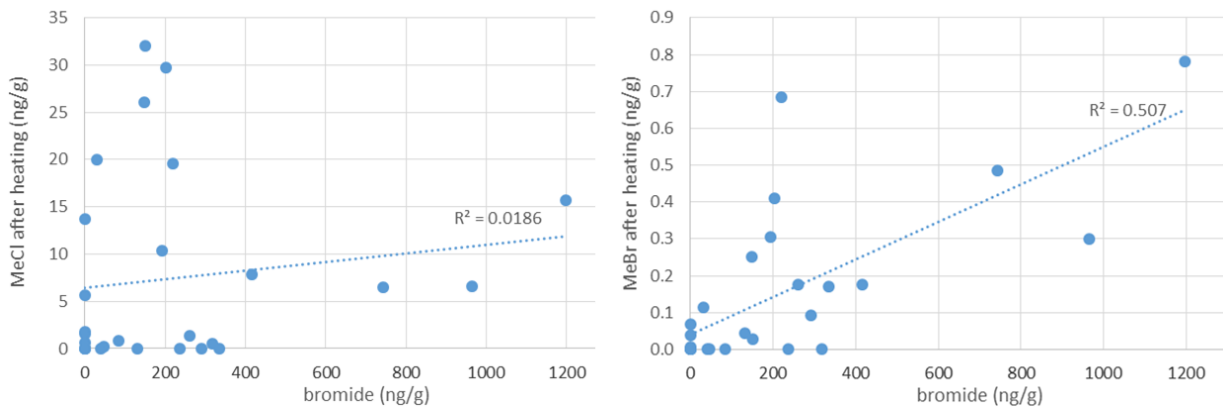


Figure 3.9: Correlation between bromide and MeCl (left) and MeBr (right) release after heating to 150 °C.

3.3.4. Carbon content

A complete table of results from the halite and gypsum samples that have been analyzed for carbon can be found in the appendix (Table 6.9). All samples show, as expected, a low organic carbon (C_{org}) content which was below 1% for all samples, and below 0.1% for most of the halites. It ranged from 0.1 mg/g (H12SND, G1Bas) to 9.0 mg/g (H18Boht) with a relatively high average concentration of 1.1 mg organic carbon per gram of sample as compared to reported values on rock salt 0.1 to 0.4 mg/g carbon (Grice et al. 1998; M. L. Bordenave and Durand 1993). The C_{org} values for more than half of our samples, however, falls in that range. A few extreme values of 9 mg/g (H18Boht) and around 5 mg/g (H14SP, H21Sib) were observed. In the case of H19Boht, this elevated value was likely caused by carbon from trona ($Na_3(CO_3)(HCO_3) \cdot 2H_2O$) that was detected with XRD (see Section 3.3.6.).

The analysis confirmed the abundance of organic carbon in the crystalline samples. The form in which the carbon occurs within the samples can be manifold and depend on deposition conditions: various microorganisms, detrital decaying plant and larger animal remains as well as humic substances or migrating crude oils with multitude of complex carbon containing compounds (see also Chapter 1). Methyl chloride, a VOX, detected in almost all halite samples, did not show an obvious correlation with the organic carbon content. After excluding the samples with C_{org} values > 1 mg/g from the correlation a trend of higher MeCl release after grinding with higher C_{org} concentrations is perceivable (Figure 3.9). For other compounds no such trend was observed. Benzene, which was present in many samples, is shown as another sample for a non-existing correlation.

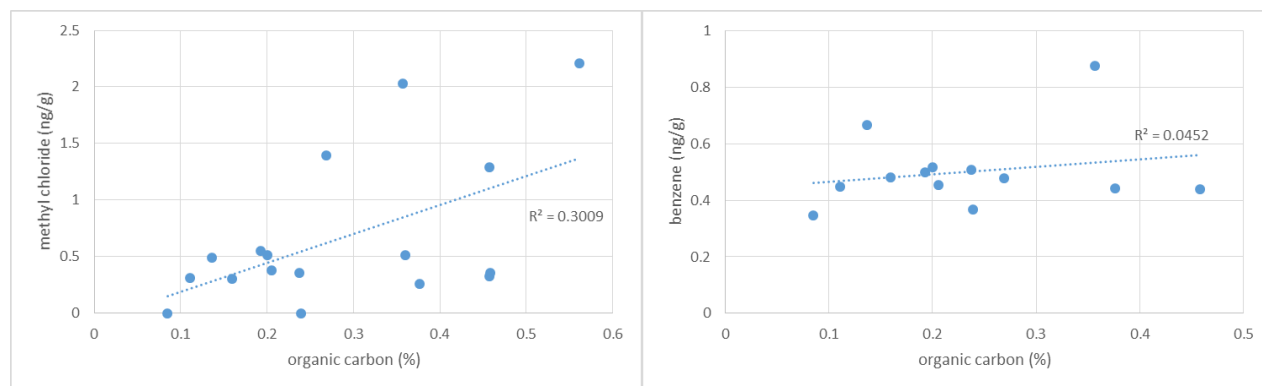


Figure 3.9: Correlation between C_{org} content and methyl chloride and benzene in FIs.

3.3.5. Major and trace elements (XRF)

Data obtained from XRF analysis are given in two tables. Table 3.3 contains results from a diverse set of samples including fluorites, granites, schist (G03MW), limestone (G04MW), quartz and gypsum. These samples were partly ground in different ways, i.e. manually with an agate mortar and pestle, in the grinding chamber or with the vibrating cup mill. Br content of all samples was below the detection limit of about 0.5 ppm, therefore it is omitted in table 3.3. Elevated levels of arsenic in F4PS are in good agreement with AsH₃ observation during GC-MS measurements.

Table 3.4 summarizes results for halite samples analyzed with XRF. Here, samples did not contain Pb, Ti, Cr, As or Ni. The elements Ga, S, Y, Si, Ca and Cl were also measured but values are not included in the tables. Their monitoring does not provide additional insights within this context, although Ti, Ga or Si could be of interest in further studies on potential catalytic reactions of organohalogen formation.

One objective of the XRF measurements was to investigate if samples are contaminated by the abrasion during the grinding procedure. Iron content of samples listed in Table 3.3 show a wide distribution with concentrations up to 9 wt % for sample G04MW. However, the difference in iron concentration between planetary mill ground and other grinding techniques is in the per mille range. Hence, abrasion of iron was not significantly determined for these samples. In contrast, after grinding within the tempered steel grinding vessel values for nickel significantly increased from zero to between 6.6 and 47.3 ppm, the latter being the extreme value for the quartz sample Q01PS. Apparently, Ni from the grinding chamber walls is abraded depending on the hardness of the minerals. As such, only gypsum samples contained low concentrations of Ni while halite contained no additional Ni after grinding in the grinding chamber (Table 3.4). Sample G03MW was the only sample containing high concentrations of Ni of around 46 ppm prior to grinding in the grinding vessel. A similar trend of increased trace amounts upon grinding can be observed for the elements Cu, Zn as well as Cr and Mn. Although the grinding chamber consists of hard tempered steel the grinding procedure for hard minerals clearly shows abrasion and iron is probably also abraded in corresponding trace amounts. The use of a highly durable zirconium oxide grinding chamber could possibly reduce the abrasion when hard minerals are ground.

Almost all halite salt samples contain traces of Br, Rb, Sr, K and Ca, whereas Mg, Zn and Cu are less ubiquitous. Sr and Rb are also present in all samples of Table 3.3. These elements can replace calcium in the crystal structure but a direct correlation to the calcium content of the samples is not

clear. Bromine concentrations, likely occurring as inorganic bromide, correlate to MeBr as observed with IC. However, XRF-bromine data deviate in parts substantially from bromide concentrations from IC measurements. Bromide partitions preferentially into the brine, i.e. depends also on FI distribution and natural samples show a high heterogeneity. Additionally, IC measurements had a high standard deviation of around 10% mostly due to the necessary dilutions. XRF data are single data points with unknown standard deviation. Therefore, IC data on bromide were preferred. Another interesting element was copper, which was found with 15 ppm in only one Siberian rock salt. Interesting aspect, because this sample H21Sib showed the highest iron concentration within the halite samples as well as dichloroethane release after grinding in the GC-MS measurement. Additionally, after heating H21Sib bromomethane and chlorobutane were found. The question arises, whether these elements play an important role in catalyzing geogenic halogenation reactions. Overall, XRF data, especially for the halite samples, demonstrate the heterogeneity of these natural samples.

3.3.6. Results XRD

Generally, results of XRD confirmed mineral identity as expected. Gypsum, halite and fluorite crystals were usually crystallographically pure or showed only minor traces of admixed quartz. Table 3.5 shows those samples, which had more than one mineral phase present or SiO₂ as the second phase exceeded 5wt%. The quantification was semi-quantitative.

Approximately 4 % of a Siberian drilled core sample were calcite. Halite and sylvite were jointly present in the drill core samples H19salt, H22Sib and H20bluesalt. Siberian halite-sylvite paragenesis dominates the sampling location. Trona was present in only one sample from a terrestrial salt pan of Botswana. Salt pans of Africa are known for elevated bicarbonate contents (Goudie and Cooke 1984) and trona has also been observed in Kenyan and Lybian locations.

Although a great variety of salt efflorescent minerals has been observed worldwide, Na⁺ is clearly the predominating cation on salt pans and Cl⁻ the predominating anion, followed by SO₄²⁻ and HCO₃⁻ /CO₃²⁻ (Goudie and Cooke 1984). In general our sample mineralogy of salt samples appears to fit well into the worldwide picture.

XRD has been found a suitable method to confide in mineral identity but is of even more importance when mineral mixtures or mineral soils with microcrystalline composition are studied.

Table 3.3: Major and trace elements of fluorites, granites, schist (G03MW), limestone (G04MW), quartz and gypsum as analyzed with XRF after ac = manual grinding with agate mortar and pestle, gr = grinding in tempered steel grinding vessel for GC-MS analysis, vc = grinding in vibrating cup mill (stainless steel). Checkmark=no quantification.

sample ID	Fe w%	Ni ppm	Cu ppm	Zn ppm	As ppm	Rb ppm	Sr ppm	Pb ppm	K w%	Cr ppm	Mn ppm
<i>LLD</i>	0.001	2	1.5	1	1	0.7	0.7	0.5	0.005	2	1.5
F1PS ac	0.42	-	-	15	2	22.3	68.4	70.5	-	-	-
F1PS gr	0.65	16.8	17.6	27	5	26.2	83.9	62.1	-	-	-
F1PS cm	0.50	-	26.8	41	0	61.5	60.4	63.0	-	-	-
F2PS ac	0.41	-	-	-	1	0.3	42.1	21.0	-	-	-
F2PS gr	0.50	6.7	-	-	1	3.3	40.1	9.3	-	-	-
F2PS cm	0.41	-	-	-	2	0.3	42.2	11.2	-	-	-
F3PS ac	0.41	-	-	-	-	1.5	34.0	5.5	-	-	-
F3PS gr	0.51	9.6	-	-	-	1.2	38.4	10.2	-	-	-
F3PS cm	0.43	-	-	-	-	0.7	34.7	9.0	-	-	-
F4PS ac	0.45	-	124.0	49	53	-	127.0	558.0	-	-	-
F4PS gr	0.49	6.6	93.9	43	45	2.2	155.0	913.0	-	-	-
F4PS cm	1.02	-	99.6	93	49	-	154.0	674.0	-	-	-
G01MW gr	2.84	35.8	17.4	64	-	272.0	48.1	34.4	2.8	389	384
G01MW cm	1.33	-	5.4	29	-	206.0	46.2	32.3	4.0	69	1035
G02MW gr	2.05	35.7	19.3	89	-	452.0	17.2	53.8	2.5	407	330
G02MW cm	3.36	-	5.1	60	-	162.0	157.0	25.4	2.8	30	770
G03MW gr	8.96	74.4	159.0	104	-	25.0	382.0	-	0.7	132	1650
G03MW cm	8.38	46.2	146.0	91	3	27.7	420.0	-	0.4	51	1182
G04MW gr	0.50	11.5	8.6	13	-	5.2	271.0	-	-	-	✓
G04MW cm	0.47	-	6.6	13	-	2.1	240.0	-	-	-	✓
Q1PS gr	1.42	46.7	23.8	12	2	3.5	18.3	2.0	0.2	671	172
Q1PS cm	0.47	-	5.8	10	1	3.9	8.2	8.8	0.2	90	190
G1Bas gr	0.56	3.0	-	11	n.a.	9.7	216.7	2.8	0.3	131	48
G2Bas gr	0.46	-	-	-	n.a.	-	189.7	-	-	-	9

Table 3.4: Major and trace elements via XRF analysis for halite samples.

sample ID	Fe w%	Cu ppm	Zn ppm	Br ppm	Rb ppm	Sr ppm	K w%	Mn ppm	Ca w%
<i>LLD</i>	0.001	1.5	1	0.5	0.7	0.7	0.005	1.5	0.002
H1Elt	0.40	-	11	435.1	5.9	30.0	0.4	9.9	0.41
H2Elt	0.40	-	9	119.9	1.2	2.5	0.3	7.6	-
H4Elt	0.40	-	9	83.0	0.8	18.2	0.2	4.1	-
H5Elt	0.43	-	11	179.0	3.5	69.1	0.2	22.8	0.84
H6Kas	0.41	-	8	17.9	-	52.0	0.2	16.6	0.36
H7Kas	0.40	-	8	7.1	-	14.5	0.2	20.5	0.12
H8SND	0.41	-	8	21.3	-	77.4	0.2	-	0.4
H9SND	0.46	-	10	7.4	1.0	94.6	0.2	16.9	0.59
H10SND	0.41	-	10	11.2	-	22.3	0.2	-	0.05
H11SND	0.43	-	8	48.3	0.3	126.0	0.2	-	0.59
H12SND	0.41	-	10	20.1	-	146.1	0.2	-	0.41
H13Doue	0.41	-	8	86.4	1.3	30.3	0.2	-	0.02
H14SP	0.41	-	10	118.9	2.4	10.1	0.2	-	-
H15SP	0.41	-	8	51.4	0.5	2.9	0.2	-	-
H16SP	0.43	-	9	53.9	0.9	8.8	0.2	-	-
H17WBSR	0.40	-	-	210.0	2.0	155.4	0.2	-	0.04
H18Boht	0.40	-	-	98.5	1.6	-	0.2	-	-
H19salt	0.41	-	-	1396.8	42.7	24.9	2.5	-	0.09
H20Sib	0.40	-	-	1293.3	27.9	6.7	2.4	-	-
H21Sib	0.57	15	-	403.6	5.6	14.4	0.2	-	1.54
H22Sib	0.40	-	-	886.7	19.4	46.8	1.7	-	0.17
H23Sib	0.40	-	-	279.0	2.3	4.4	0.2	-	-
H24Sib	0.40	-	-	346.1	4.7	1.9	0.2	-	-
H25Sib	0.40	-	-	492.2	7.1	4.7	0.2	-	-
H27Gor	0.40	-	-	208.3	3.0	63.4	0.2	-	-

Table 3.5: XRD evaluations of minerals with more than one phase present.

		H19Boht	H22 Sib	H20Sib	H21Sib	H18Boht	H13Doue	G1Bas
		wt %						
halite	NaCl		75.8	91.3	75.8	96	86.6	88
sylvite	KCl		24.2	8.7	24.2	-	-	-
calcite	CaCO ₃		-	-	-	4	-	-
trona	Na ₃ H(CO ₃) ₂ ·2H ₂ O		-	-	-	-	13.4	-
quartz	SiO ₂		-	-	-	-	-	28.2
gypsum	CaSO ₄ ·2H ₂ O		-	-	-	-	-	12
								71.8

3.3.7. Pyrolysis-GC-MS (Py-GC-MS)

GC-MS results from salt samples have shown a remarkable increase in emitted halogenated volatiles upon heating to 150 °C. The selected samples sent to be analyzed by Py-GC-MS were all characterized by MeCl release also after grinding. Samples H3Elt and sample H13Douwe had shown MeCl contents of 2.3 and 0.5 ng / g, respectively. Preliminary runs with Py-GC/MS yielded greatest MeCl production for sample H3Elt and this sample was utilised to investigate CH₃Cl release at different pyrolysis temperatures. However, sensitivity was a problem as only 6 to 7 mg were used for each run. The final temperature of 800 °C was chosen because NaCl can partly volatilize at higher temperatures (Zimm and Mayer, 1944). Analytical grade NaCl was used as a control yielding no CH₃Cl (Figure 3.10). In contrast to the analytical grade fine powder, H3Elt was ground or otherwise processed before Py-GC-MS. On the one hand, MeCl releases from H3Elt could be attributed to FI decrepitation caused by internal pressure increase with greatest releases between 300 and 500 °C.

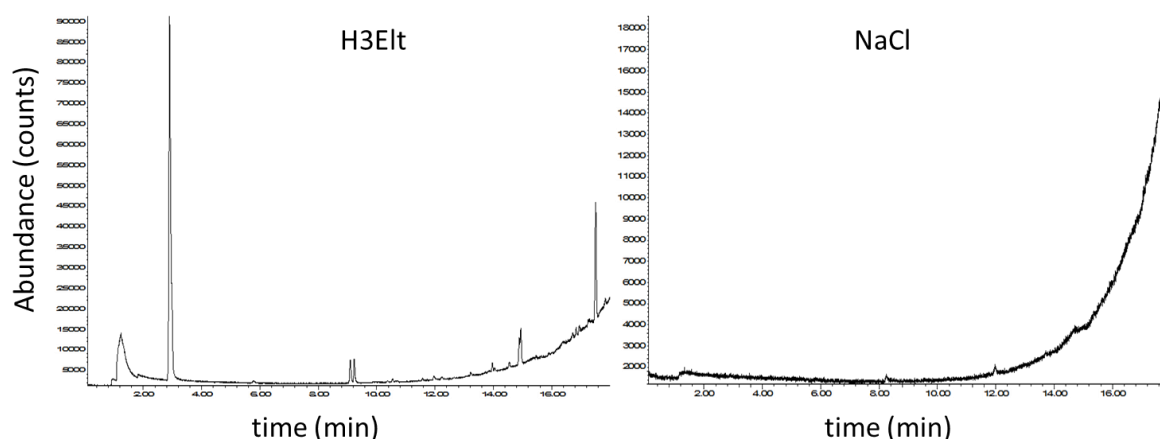


Figure 3.10: GC-MS chromatograms showing ions m/z 50 and 52, for sample H3Elt and analytical grade NaCl at pyrolysis of 300 °C. Note scales are different.

Table 3.6: Normalized peak area for CH₃Cl (ion current m/z 50) for sample H3Elt at different pyrolysis temperatures.

Pyrolysis temperature °C	Area for ion current m/z 50
300	594576
500	2393875
700	223468

On the other hand, the temperature window of 300 to 500 °C could also indicate ideal thermal production conditions for de-novo MeCl formation. With the observations made previously (see Figure 3.6 and 3.7) the second case appears more likely, but a calibration for these data in order to compare values of MeCl released are not available. Aside from MeCl, four other substances were observed in the chromatogram. While these analytes remain unknown their fragments of 50 and 52 m/z upon electron ionization point to 2-butene and benzene, but this cannot be confirmed as higher mass fragments have not been recorded in this study.

MeCl release was observed at all pyrolysis temperatures for sample H3Elt. Although MeCl production was not quantified it is possible to compare the mass normalized areas of the peaks to determine the relative amount formed (Table 3.6). MeCl production at 500 °C was 4-fold that of 300 °C. No increase was found upon pyrolysis at 700 °C which suggests that the carbon substrate and thus the CH₃ source, was utilized completely by 500 °C.

The Py-GC-MS tests mark only a beginning of possible experiments. More Pyrolysis-GC-MS results also to higher temperatures of 1200°C would be of interest to explore the impacts of igneous intrusions into adjacent rock salt beds. In order to be able to differentiate between adsorbed gases/humidity and decrepitating upon heating as well as identification of released fluids thermogravimetric-GC-MS might offer an alternative for better temperature resolved data. The data here presented demonstrate, that Py-GC-MS would be a good tool to narrow down optimal thermolytic MeCl formation conditions in FIs of halites with suitable experimental setups.

3.4. Conclusions

The analytical results from GC-MS prove the presence of a wide spectrum of volatile compounds from FIs trapped in various minerals.

MeCl was found to be an almost omnipresent compound occurring in quartz, fluorites, halites and dolerites. Initial heating experiments with halites using purge-and-trap GC-MS as well as Py-GC-MS demonstrated the important role of temperature in MeCl and VOX formation and aspects of this will be spotlighted further in Chapter 4.

The customized purge-and-trap GC-MS system for specialized FI analysis confirms the presence of SF₆ and CF₄ in fluorites. A better understanding of their formation in geological matrices would

improve the assessments of their role played in the atmospheric and hydrologic sector, i.e. in limitations to groundwater dating or balancing the atmospheric budgets.

Methyl bromide, dichloroethene and dichloroethane from quartz samples of the Archean Yilgarn craton in Australia give first insights into synthetic processes occurring in rising hydrothermal fluids in the upper crust. Vinyl chloride was found in a hydrothermal quartz from High Taunus. Assuming an abiotic genesis, these organic molecules are hypothesized to be involved in the formation of early prebiotic organic molecules. Generally, the differences of compounds trapped during the growth of these quartzes, conserving the chemical composition of the given fluid medium can provide information on the respective formation conditions.

IC analysis was a useful tool for halites but soluble minerals require a different setup. XRF is a more convenient tool for major and trace elemental analysis, when ionic speciation can be neglected. Bromide content of halites may be a potential indicator for the formation potential of MeBr.

The GC-MS technique here presented has been shown effective and yielded interesting results. However, continuing analytical and technical problems constricted the measurement of further samples. Except for the larger group of investigated halites, sample numbers were too low to allow for systematic observations among and between sample groups. Analytical problems have to be overcome. The use of a highly durable zirconium oxide grinding chamber and gaseous halocarbon standard mix are recommended to enhance analytical performance.

Based on these findings, future laboratory experiments can be designed in order to gain more insights on the formation mechanisms involved.

This sample screening can only mark the beginning and a realm of volatile compounds formed during geological processes archived in FIs waits to be discovered.

Case study

Thermolytic degradation of methyl methionine and implications for its role in DMS and MeCl formation in hypersaline environments

(Modified version) Submitted for publication:

Ines Mulder, Torsten Krause, Tobias Sattler, Christoph Tubbesing, Sabine Studenroth, Krzysztof Bukowski, Elliot Atlas and Heinz F. Schöler. 2014. "Thermolytic degradation of methyl methionine and implications for its role in DMS and MeCl formation in hypersaline environments." *Environmental Chemistry* (under review)

4.1. Introduction

Volatile organic halocarbons (VOX) and volatile organosulfur compounds (VOSC) occur both naturally and man-made and play an important role in photochemical processes of the lower atmosphere and information on the geogenic origin of these compounds will help to understand their global budgets and fluxes. A helpful tool to get a lead on possible geogenic VOX and VOSC formation is the study of gaseous composition of fluid inclusions (FIs) in rocks and minerals. These inclusions archive the conditions present at their formation. However, investigations concerned with the occurrence of VOX in fluid inclusions of rocks and minerals are scarce (Harnisch and Eisenhauer 1998, Svensen et al. 2009) and a more detailed overview can be found in chapter 3. VOSC from FIs of minerals except for sulfur dioxide, have not yet been reported.

Methyl chloride (MeCl) with an annual atmospheric burden of 4 to 5 Tg is the most abundant natural halocarbon in the atmosphere. It plays a significant role in chlorine-catalysed ozone destruction in the stratosphere (Keppler et al., 2005; Montzka et al., 2003). In 2000, Rhew et al., found that salt marshes, even though they constitute less than 0.1% of the global surface area, may contribute about 10% of the total MeCl and methyl bromide (MeBr) fluxes to the atmosphere. However, mechanisms of MeCl formation from these systems were not subject of these studies. A thermolytic production of MeCl from the methoxy group of plant pectin is known (Derendorp et al., 2012; Keppler et al., 2008).

Dimethylsulfide (DMS) is the major natural, mainly marine, source of organic sulfur in the atmosphere and contributes to both the tropospheric burden of sulfur as well as cloud formation via oxidation to acidic aerosols (Kloster et al. 2006). It is also known to act as an info-chemical for a wide range of organisms including mammals. Microorganisms that cycle DMS are widely distributed and were found in all kinds of environment: oxic and anoxic marine, freshwater and terrestrial habitats (Schäfer et al., 2010). Despite the importance of DMS that has been unearthed by many studies since the early 1970s, the understanding of the biochemistry, genetics, and ecology of DMS-degrading microorganisms is still limited. In marine and freshwater locations the occurrence of DMS is well documented and is attributed to several formation pathways including the degradation of the tertiary sulfonium compound dimethylsulfonium propionic acid (DMSP) and the metabolism of methionine (MET). These two processed are often linked. The main source for DMS from the ocean surface is DMSP which is formed from MET via hydrolysis within

phytoplankton (Sievert et al., 2007). Other known bacterial pathways of DMS formation include the bacterial methylation of thiols, especially in anaerobic sediments and the reduction of dimethylsulfoxide (DMSO) in marine and coastal environments (Kinsela et al., 2007). DMS is also produced during decay of algal mats and is a product of biotic methionine decomposition (Segal and Starkey, 1969; Zinder and Brock, 1978). Also other methylated sulfur compounds have been detected in a wide variety of environments like the atmosphere, soils, sewage sludge, salt marsh sediments and waters. In fact, in anoxic salt marsh sediments and anaerobic sediment volatile methylated sulfur compounds (DMS, DMDS, methanethiol (MSH)) have been found to be produced methanogenic from methionine (Kiene et al. 1986, Kiene and Visscher 1987). Despite the focus on DMS in many studies since the early 1970s, often dominated by aspects of its biological fate and questions of methylated sulfur compound metabolism, not all sources have been identified. Specifically, terrestrial DMS formation is not well understood. According to Watts et al. (2000) the mass budget of DMS is not balanced and more sources are needed.

MET, as one of two sulfur containing amino acids, could potentially serve as a precursor for MeCl and DMS in terrestrial salt pans. Of special interest is its derivative methylmethionine (MeMET) since it is widely distributed in nature (Bentley and Chasteen, 2004). This compound could potentially explain emissions of MeCl, which were observed from sediments of salt marshes as well as salt crystals. MeMET would contribute the necessary methyl-group for its formation.

Goals of this chapter is to present new data on VOCs released from salt samples from around the world and to put these into perspective of emissions from soil samples from a survey of salt lake sediments of SW Australia. Furthermore, we seek to contribute to a deeper understanding of the thermolytic degradation of MeMET and its role in the release of MeCl and VOSC from hypersaline environments. The investigation on the thermolytic formation pathways of these compounds and an extended scientific background on additional sources can help to refine regional atmospheric sulfur budgets as well as to the understanding of abiotic MeCl formation.

4.2. Materials and Methods

4.2.1. Chemicals

The following chemicals were used: EPA 624 calibration mix B (analytical standard; Supelco), sulfur mix (analytical standard; Spectrum Quality Standards), chloromethane (99.5%, Sigma-Aldrich), potassium chloride (99.5%; Merck), sodium hydroxide (99%; Aldrich), DL-methionine methylsulfonium chloride (= MeMET, 99%; Sigma), trimethylsulfonium bromide (97%, Aldrich), DL-methionine (99%, Fluka), trimethylsulfoxonium chloride (98%; Aldrich), dimethylsulfone (98%; Aldrich), DL-methionine sulfone (99%, Aldrich), DL-methionine sulfoxide ($\geq 99\%$), H₂O₂ (30 %; Sigma-Aldrich), iron(II)-sulfate heptahydrate (99 %, Sigma-Aldrich), iron(III) sulfate (99 %; Fe 21-23%; Riedel-de Haën), reagent grade sodium chloride (Baker). Type I ultrapure water (≥ 18 M Ω -cm) from a Purelab UHQ System by ELGA LabWater was used in all experiments.

4.2.2. Soil and salt samples

Soil and salt samples were sampled during campaigns of DFG research unit 763 to South Russia, Southwest Australia and Mauretania. The salt lakes taken in Australia are distributed in an area of about 120000 km² which is part of the Avon River catchment. The formation of salt lakes in this area was promoted by secondary salinization following deforestation (McFarlane and George, 1992).

South Russian salt lakes were sampled in the districts Volgograd Oblast and Astrakhan Oblast, in the northern steppe of the Caspian depression. Characteristically, they are outcrops of Permian salt domes.

The halite from Mauretania was sampled by Stefan Huber, Institute of Earth Sciences, University of Heidelberg, at the salt pan depression of Sebkhâ Te-n-Dghâmcha, 100 km north of Nouakchott/Mauretania.

Additionally, two halite samples from Miocene evaporites in Wieliczka and Bochnia Mines, Poland, were included. The sample of halite from Wieliczka (H29WG) was derived from the Upper Spiza Salts (Gruszczyn Gallery). The halite sample from Bochnia (H28Lkt) stems from a bed of crystal salts (Lichtenfeltz Gallery).

Properties and exact location of soil and salt samples are given in Table 4. 1.

10 g of salt samples were ground for 5 minutes at 200 rpm in the specifically designed grinding device that fits into a planetary mill (Fritsch, Pulverisette 5) and the released gases were subsequently analyzed using a gas chromatograph (GC, Varian, Model 3400) and an ion-trap mass spectrometer (MS, Finnigan MAT, ITS40). The capillary columns employed in the GC were a DB-624, ID 0.53 mm, df 3 μm , 30 m directly connected to BP-5, ID 0.32 mm, df 1 μm , 60 m. For more details on the dynamic injection and preconcentration by the customized purge and trap system as well as the grinding procedure please refer to Chapter 2.

For VOC detection from soil or sediment samples a Varian gas chromatograph GC 3400 linked to a Varian Saturn 4D with electron impact ionization and ion trap mass spectrometer was used. The GC was equipped with a DB-5, 60 m, ID 0.32mm, df 1 μm capillary column. With this system the measured samples compounds with boiling points of -24 $^{\circ}\text{C}$ to 200 $^{\circ}\text{C}$. Before analysis 1 g of freeze-dried and ground sample was transferred to a 20 mL air-tight headspace glass vial. The samples were shaken at 500 rpm for 24 h in the dark at 40 $^{\circ}\text{C}$ before measurement with the GC-MS system.

Table 1: Major anion and organic carbon content of halite and soil samples. The selected soil samples were chosen from a large set according to their relatively high organic matter content.

halite samples							
sample ID	sampling location	geographical position		Cl ⁻ g/kg	Br ⁻ mg/kg	SO ₄ ²⁻ g/kg	C _{org} wt%
H29WG	Wieliczka salt mine	N49°59'05.52"	E020°03'23.94"	612.9	30-80 ^[60]	2.9	n/a
H28Lkt	Bochnia salt mine	N49°58'13.0"	E020°25'54.7"	508.9	20-37 ^[61]	3.6	n/a
LD42	Lake Dune*, Australia	S33°04'58.58"	E119°38'18.13"	583.2	97.7	4.5	n/a
H2Elt	Lake Elton, Russia	N49°08'59.28"	E046°47'18.12"	549.8	220.1	18.1	0.09
H6Kas	Lake Kasin, Russia	N47°36'09.66"	E047°27'07.14"	573.7	0.0	3.1	0.13
H8SND	Sebkah N'Dramcha, Mauretania	N18°53'23.6"	W15°39'42.9"	533.6	30.0	8.5	0.06

soil samples							
profile depth cm	sample ID	geographical position		Cl ⁻ g/kg	Br ⁻ mg/kg	SO ₄ ²⁻ g/kg	C _{org} wt%
0-2	Lake Springfield*, Australia	S32°27'42.41"	E119°9'58.32"	172.7	309.6	38.5	2.12
0-2	Lake Orr*, Australia	S34°14'50.84"	E118°10'07.76"	139.6	156.5	38.9	1.47
3,5-6	Lake Dune*, Australia	S33°04'58.58"	E119°38'18.13"	83.2	118.6	35.0	2.24
0-2	Lake Hatter Hill*, Australia	S33°05'56.69"	E119°50'33.27"	258.9	595.1	58.9	4.01
0-2	Lake Kasin, Russia	N47°36'09.66"	E047°27'07.14"	30.3	0.0	6.4	0.32

*no official sample site name

4.2.3. Air samples

Air samples were taken in Australia accompanying soil sampling at the sites of Lake Dune and Lake Orr by T. Krause und H.-F. Schöler from the Institute of Earth Sciences, University of Heidelberg. Air was sampled about 3 cm above the surface taken with a membrane pump (KNF Neubauer, Freiburg, Germany) with a flow of 36 L min^{-1} . The air was pressurized into a stainless steel canister with a volume of 2 L and up to 2 bar. The canisters are electropolished on the inside and have a bellows-seal valve (Swagelok SS-4H-C1). Before sampling the canisters, they were evacuated to $<10^{-3}$ mbar. Canister samples were analyzed by T. Sattler (Institute of Earth Sciences, University of Heidelberg) with Elliot Atlas at the Department of Atmospheric Sciences, University of Miami, Florida, USA, using a multi-detector GC/MS/FID/ECD instrument (Agilent 7890 GC/5973 MSD) interfaced to a Markes Unity II Thermal Desorption Unit that included a CIA Advantage canister interface. A 0.8 L sample was introduced to the system at 80 sccm after an initial flush of 160 sccm. The sample flow was metered by a mass flow controller. The sample was enriched on an adsorbent trap (Markes UT17O3P-2S, Ozone precursor trap) held at -37°C . Prior to adsorption on the trap, the air sample was dried by passing through a $15'' \times \frac{1}{4}''$ stainless steel trap held at $-18 \pm 1^\circ\text{C}$, with additional drying in a $24'' \times .05''$ Nafion drier (MD-050-24-FS-2; Perma Pure, Toms River, NJ). To inject the sample, the tube was desorbed from the trap at 300°C using a backflush flow. The sample was split onto 2 analytical columns: 1) DB-624 ID 0.2mm, df $1.12\mu\text{m}$, 20m which was directed to the MS and ECD detectors, and 2) Al_2O_3 -PLOT column ID 0.25mm, df $5\mu\text{m}$, 30m which was directed to the FID. The temperature program of the GC started at -20°C and was heated after 3 min to 200°C with a rate of $10^\circ\text{C min}^{-1}$, 200°C was held for 4 min. A 1 m section of GS GASPRO column (0.32mm) was added to facilitate separation of ethyne from a co-eluting compound. The total sample flow was split approximately 2/3 to the FID column (525 sccm), and 1/3 to the MS/ECD (275 sccm). The effluent of the MS column was connected to a capillary splitter (Agilent G3183B). Approximately 70% of the sample (192 sccm) was sent to the MS, with 30% of the sample (83 sccm) directed to the ECD. Quantitation of MeCl and DMS concentrations of the samples was done by comparison to a working whole air standard that was calibrated against known mixtures, either directly or by dynamic dilutions.

4.2.4. Studies with MeMET and model substances

MeMET, as methionine methylsulfonium chloride, was employed to study the temperature dependence of its MeCl and DMS release at 30, 40, 50, 60 and 70 °C. Methionine, its derivatives and structurally related compounds, namely methionine sulfone (MET sulfone), methionine sulfoxide (MET sulfoxide), trimethylsulfoxonium chloride, trimethylsulfonium bromide, dimethylsulfoxid (DMSO) and dimethylsulfone (DMSO₂) were tested at 40 °C.

For each experiment 0.1 mmol of dry substance was shaken in a 20 mL air-tight headspace glass vials for 1 h in the dark at the defined temperature and then connected via two stainless steel needles to the GC/MS system as used for the soil samples.

For calibrations appropriate dilutions of the EPA 624 calibration mix B in 10 mL ultrapure water were used in the same 20 mL headspace vials.

All GC/MS measurements were done at least in triplicates.

4.2.5. Amino acids from soils

From three different soil samples (Elton II, T3-1 Usbekistan and Lake Hatter Hill) extracts of 4, 16 or 32 g of sample in 20 mL water were prepared by shaking for 20 min at 200 mot/min on an orbital shaker (brand model) in 50 mL Falcon tubes. Samples were then centrifuged for 15 min at 400 rpm. The supernatant was decanted and filtered with a 0.45 µm syringe filter. The samples were sent to be analyzed for free amino acids by ion exchange chromatography with on-line derivatization with standard ninhydrin method and UV spectroscopy (amino acid analyzer S 4300 Sykam, Fürstenfeldbruck, column: LCA K07/Li Sykam, Fürstenfeldbruck) by Dr. Uwe Schwarzenbolz in Prof. Henles Group, Department of Chemistry and Food Chemistry at Technische Universität Dresden.

4.3. Results and Discussion

4.3.1. Volatile compounds from salts, soil and air samples

This first section discusses the results obtained as part of the DFG Research Unit 763, which was concerned with natural halogenation processes in the environment. Volatile organic carbon (VOC) composition trapped in fluid inclusions of halite crystals deposited in recent salt pans or emitted from soil samples were analyzed using modified GC-MS set-ups.

The results of FI analysis are shown in Figure 4.1. The example chromatograms show an array of identified volatile compounds including various hydrocarbons, MeCl and in some cases DMS. They also represent typical observations made in a diverse set of halite samples from recent salt pans of Australia (H42LD), Mauretania (H8SND) and South Russia (H2Elt). The studied salt crystals were formed in the solutions of the salt lake environments, sometimes within hours. The FIs in these recent crystals studied are primary FIs formed during crystal growth. Generally, the size of FIs in most samples ranges from 1 to 100 μm . The very small size fraction of FIs usually outnumbers all inclusions larger than 10 μm at least by a factor of 10 (Roedder, 1984). The abundance of FIs in our salt samples was also evident by their milky appearance. These FIs represent trapped gases that were present in the salt forming solution during crystal growth. The chromatograms of samples H28Lkt and H29WG, however, display results for halites sampled at two mines in Poland. Here, primary FIs formed within the salt crystals during the Badenian Salinity Crisis (Middle Miocene 16.4-13.0 Ma) and then underwent burial, subduction and folding (Andreyev-Grigorovich et al., 2003). Radiometric age of the salt formations in Wieliczka and Bochnia was established to be 13.60 \pm 0.07 Ma (Leeuw et al., 2010). Further generations of FIs may have been included, e.g. from circulating brines. Furthermore, alterations of the FIs by temperature and pressure may have taken place but cannot be distinguished here. Interestingly, while almost all samples from halites contained MeCl, with concentrations between 0.05 ng/g to 0.6 ng/g, high signals for DMS were recorded only for the two samples of Badenian halite. The DMS peak of sample H29WG corresponds to about 0.54 ng/g. Based on Babel et al. (2004) the Badenian evaporite basin of the northern Carpathian foredeep may have consisted of several interconnected or temporarily disconnected sub-basins topographically separated from the ocean according to the salina basin model. Therefore, mechanisms of salt crystal formation for samples H28Lkt and H29WG are thought to resemble those of the recent salt crystals of this study.

In order to investigate possible mechanism of MeCl and DMS formation, results from FI studies are now compared to VOC observed in a large set of soil samples of the multifarious hypersaline lakes of SW Australia (Krause, 2014). Figure 4.2. shows MeCl along with VOSCs detected after wet incubation at 40 °C for 24 h. Next to DMS various VOSCs were observed, such as carbon disulfide, thiophene and methylthiophene. The observation of thiophene and methylthiophene from soils is novel, while emissions of its homologue furanoic compounds from soils (Huber et al., 2010) and hypersaline environments (Krause et al., 2013) are well known. Carbon disulfide and dimethyl disulfide (DMDS) were found with highest concentration with average concentrations of 115 ng/g and 100 ng/g, respectively. DMS was also present but less frequently observed. The predominance of DMDS as organosulfur compound next to carbon disulfide is surprising. Literature generally presents biogenic sources for VOSC emissions from soils clearly dominated by DMS and only with traces or minor amounts of DMDS (Yang et al., 1998; Warneck, 2000; Lomans et al., 1997). Sulfur compound concentrations in the Australian soil samples were high and their occurrence is in good agreement with the reducing redox milieu of the salt lakes.

Compounds that were not identified but are likely to be present under these conditions are carbonyl sulfide, sulfur dioxide and H₂S. Furthermore, methylated sulfoselenides were detected in some samples (not shown here). MeCl occurred frequently with an average concentration of 5 ng/g, which falls in the range of VOSC. The MeCl yields from soils are more than 50-fold higher compared to MeCl yields from halites. This can be explained with a higher organic matter content in soils. Rhew et al. (2000) have found large MeCl fluxes from salt marshes of up to 570 $\mu\text{mol}/(\text{m}^2 \text{ day})$. Based on a 24h production time under moist condition and elevated summer temperatures leading to topsoil temperatures of up to 55 °C (Kotte et al., 2012), a soil density of 1.3 g/cm^3 and 1 cm soil depth, our data are extrapolated to a MeCl production rate of 650 $\mu\text{mol}/(\text{m}^2 \text{ day})$ and would support those high fluxes.

The monitoring of concentrations of MeCl and DMS in air samples at Lake Dune and Lake Orr at the day of sampling is shown in Figure 4.3. Their values show differing quantities per site as well as over time. In the case of Lake Dune, highest values coincide with the highest temperatures of the day. For Lake Orr MeCl values are overall higher than at Lake Dune, however, only four measurements are available. MeCl in air samples was between 200 to 380 pmol/mol, which is less than the global atmospheric mixing ratio of 528 pmol/mol (Warneck and Williams, 2012). As local background concentrations most likely do not correspond to the global values, these MeCl values

locally could still mean that MeCl is emitted from soils. MeCl formation processes appear to be depending very much on local environmental conditions.

DMS values ranged from 30 to almost 100 pmol/mol, with Lake Orr showing high values between 80 and 100 pmol/mol. All DMS values observed fall in the range of global atmospheric mixing ratio reported between 20 and 150 pmol/mol.

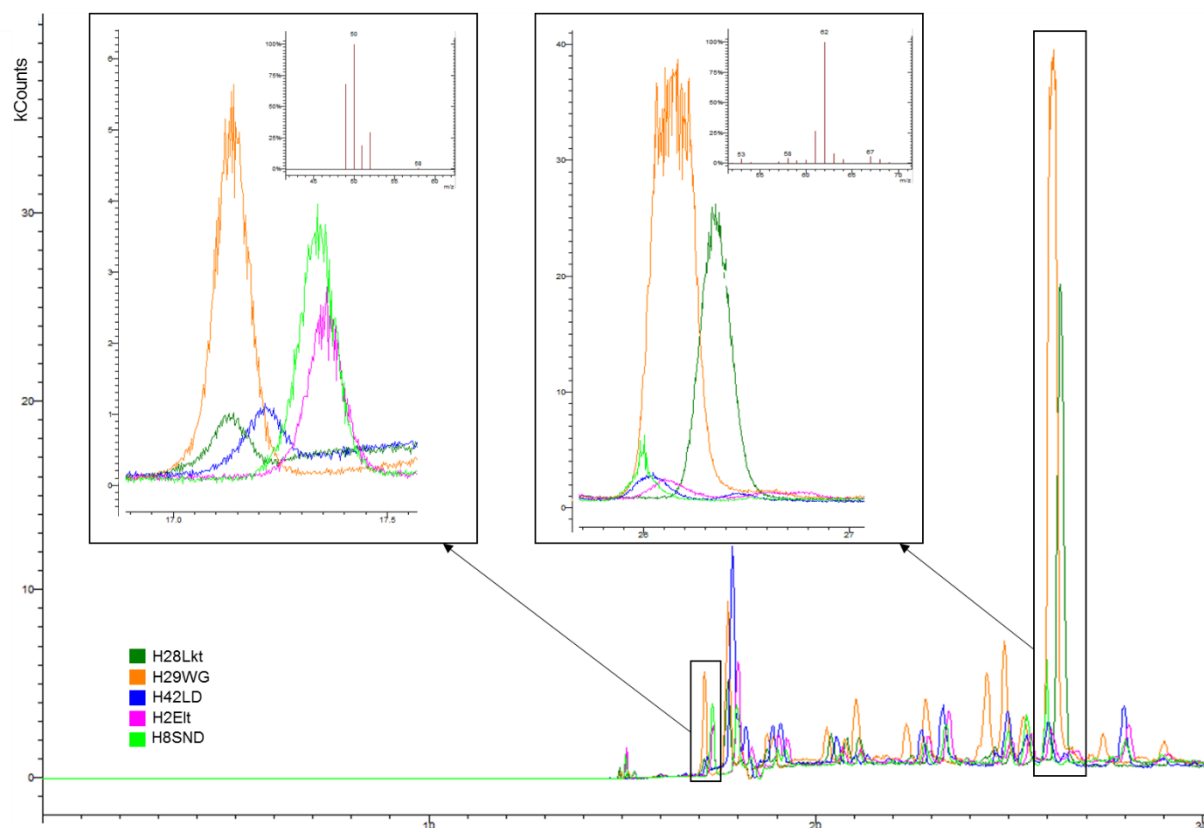


Figure 4.1: Chromatograms of five halite samples after grinding for 5 min at 200rpm in a steel vessel. The areas in the boxes show enlargements of the MeCl (left) and DMS (right) peaks including their observed mass spectra. MeCl was present at differing amounts in all five samples. While samples H28Lkt and H29WG displayed significant peaks for DMS the other samples did not contain DMS; the mass spectra of small observed peaks of the other samples did not fit that of DMS. Most other peaks in the chromatograms stem from short-chain alkanes, alkenes and further hydrocarbons.

4. Case Study: Thermolysis of MeMET yielding MeCl and DMS

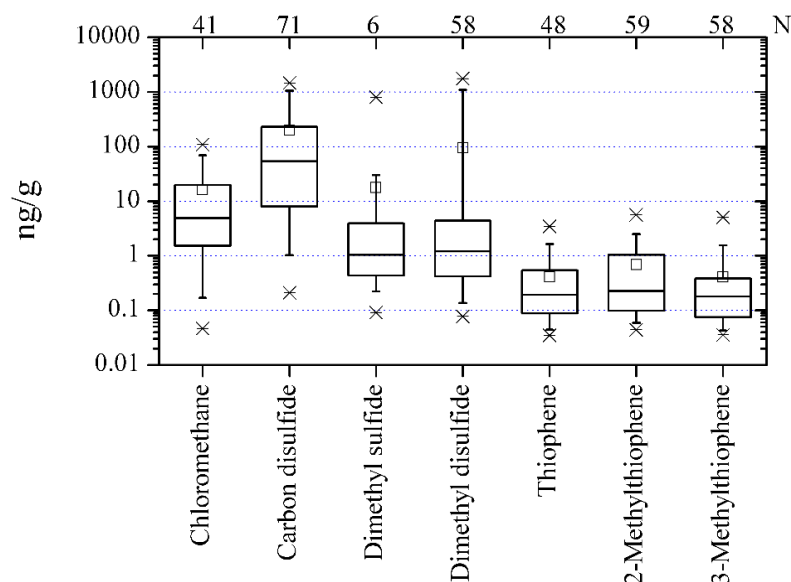


Figure 4.2: Results of sample screening for VOC from SW Australian salt lake soil samples (from Krause, 2014).

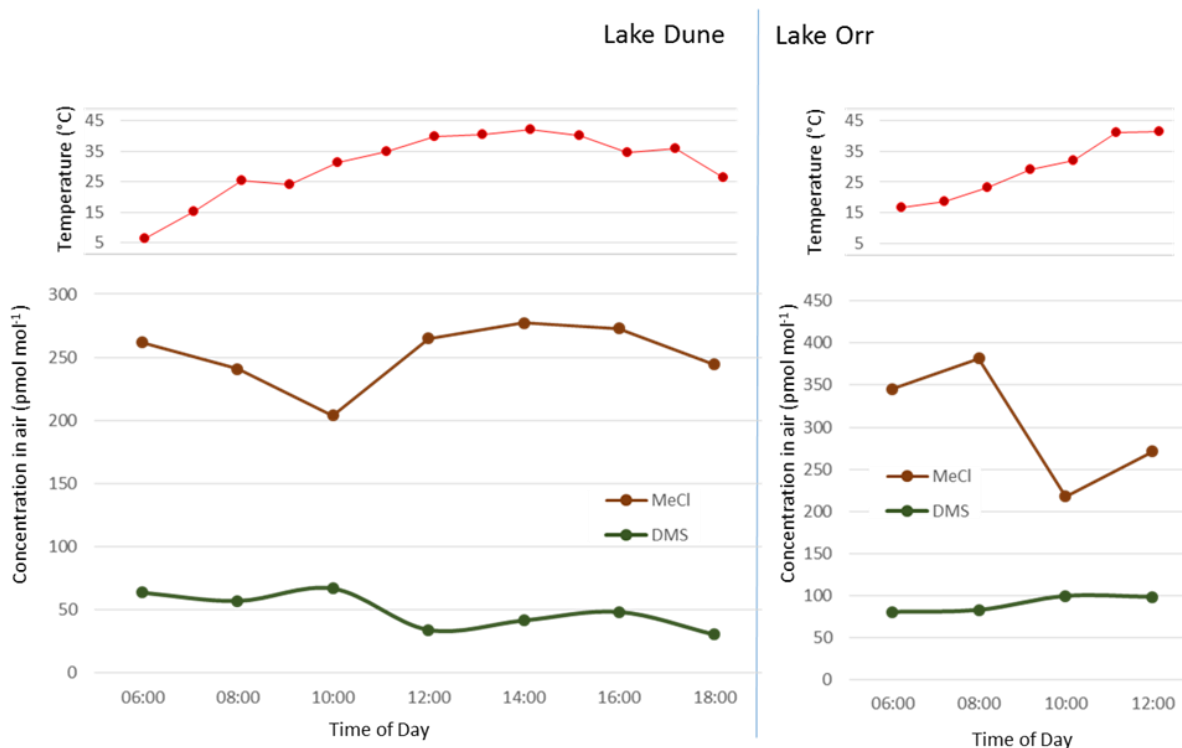


Figure 4.3: Diurnal variation of MeCl and DMS in sampled air on two different sampling sites and dates along with the logged air temperature.

However, local concentrations vary considerably depending upon environmental conditions such as availability of plant and animal dead matter, geochemical profile and weather. Overall, the locally confirmed presence of MeCl and DMS in air as well as soils and salt crystal samples gave rise to the question of a possible common formation mechanism of these compounds.

The observed compounds from salt lake soils, crystals and air are consistent with other emissions reported in literature, but those are commonly linked to microbial and plant activity such as the algae *dunaliella salina*, *spartina alterniflora*, *halobacterium* and other microorganisms (Rinnan et al., 2014; Attieh et al., 1995; Steudler and Peterson, 1984). Also, in the studied Australian salt lakes the fluctuating presence of water enables growth of aquatic plants and microorganisms. Plant residue, dead insects or larger animals were commonly observed at the sampling sites. This is important with regard to volatile sulfur emissions since living organisms produce the proposed precursor material.

The freeze-dried soil samples in our study were incubated in the dark before measurement. Within 24 h the volatile compounds were newly formed suggesting an abiotic mechanism involving the degradation of organic material. As fluid inclusion of salt crystals contained similar compounds we suppose that a similar mechanism may be responsible within the inclusions or that the FIs represent the situation of the solutions at the time of crystal formation. The presence of halophilic microorganisms even on ancient rock salt was reported (Denner et al., 1994; Stan-Lotter et al., 2002) and their amino acids could contribute to the needed precursor material for abiotic degradation reactions. The actual production of MeCl, DMS and other gases by these organisms within the salt cannot be excluded as a third formation pathway. In general, only few organisms are tolerant of the extreme conditions of hypersaline environments. However, due to lack of enemies and competitors these mostly very simple communities can flourish and produce up to 8-12 g m⁻² d⁻¹ carbon (Schidlowski, 1988).

In our trial for the presence of amino acid in soil only one of the prepared samples yielded sufficient signals. The chromatogram from Lake Hatter Hill (4 g of sample) is shown on top in Figure 4.4. For better comparison, the chromatogram of the smallest amino acid standard of 2,5 nmol) is shown on the bottom. The sample contains about 4,6 µmol/L lysine corresponding to 3,4 µg/g lysine in the soil. Ornithin was present at similar concentrations. All other amino acids were either below the detection limit of 4 µmol/L or peaks were not resolved due to high salt content. Methionine elutes at 36-38 min and the peak is clearly visible in the standard. Salt predominantly influences

peak resolution in the front part of the chromatogram and should not influence amino acid detection in general once amounts are high enough. However, no MET was found in the soil extract. In principle, this is not a surprise given the relatively high detection limit and the small amounts of free amino acid in soils ranging from 0.1 to 50 $\mu\text{mol}/\text{kg}$ (Jones et al., 2002).

Werdin-Pfisterer et al. (2009) summarized amino acid contents from different soils and methionine, if present, only represented 0,1 to 2.3 % of the total free amino acids detected. Also, the soils where MET was present were organic rich surface soils. The trial showed that amino acids could be detected in a soil sample, but high salt concentrations give rise to analytical problems. The detection of amino acids as free amino acids from soil extracts is described by Jones et al. (2002) and Martens and Loeffelmann (2003) but detection limits for free amino acids from soils are relatively high, between 0.5 and 50 $\mu\text{mol}/\text{kg}$. Therefore, MET is assumed to be present in salt pan environments due to the decay of algal mats, microbial communities, decaying insects and larger animals as well as leaves and other plant litter transported by wind.

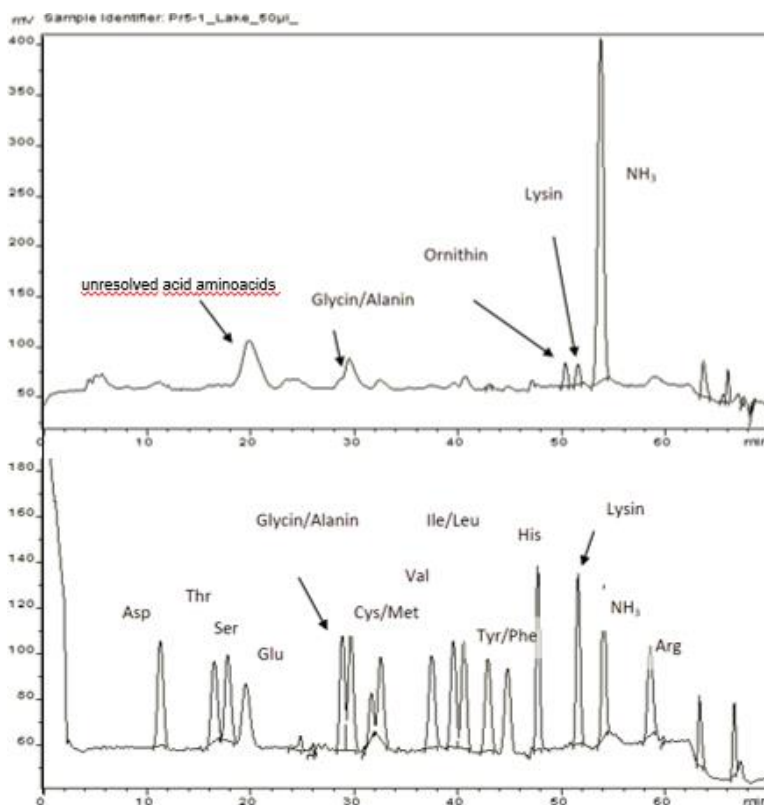


Figure 4.4: Chromatogram from Lake Hatter Hill soil (top) and the 2.5 nmol amino acid standard (bottom). The sample contains about 4.6 $\mu\text{mol}/\text{L}$ lysine (Uwe Schwarzenbolz, TU Dresden).

An amino acid derivative of interest is MeMET since it could serve as a precursor for both MeCl and DMS. We therefore decided to investigate the thermolytic degradation of MeMET to corroborate our assumption.

4.3.2. Temperature dependence of MeCl and DMS release from methionine methylsulfonium chloride

Figure 4.5 summarizes the results obtained after incubating pure methyl methionine chloride. The temperature interval from 30 to 70 °C was chosen as to include environmentally still relevant temperatures. Own observation confirmed that during the day salt and sediment surfaces of salt lakes can reach or exceed 50 °C. The top two diagrams show an exponential increase of MeCl and DMS with temperature. At temperatures above 60 °C small amounts of dimethyldisulfide (DMDS) were also observed. The temperature dependence observed for DMS was noted in an earlier study by Fall et al. (1988) who found a linear DMS increase between 5 and 35 °C from alfalfa and corn plants. Although this observation could correspond to the more linear regression at lower temperatures in our studies their reaction could also have been biotically mediated. Compared to DMS, there are more thermolytic data on MeCl formation available. Methyl halide production from plants is a known phenomenon and besides the enzyme-mediated reaction by methyl transferases from S-adenosylmethionine (Attieh et al., 1995) and abiotic release of MeCl from senescent or dead plant material in the temperature range 30-350 °C has been demonstrated (Hamilton et al., 2003). Hamilton et al. (2003) hypothesised that pectin as a plant structural component carrying methoxy groups could act as the methyl donor, which was confirmed by Keppler et al. (2008). In studies on the abiotic methyl halide production from vegetation temperature and halide content have been found to be the most crucial parameters (Hamilton et al., 2003; Keppler et al., 2008; Keppler et al., 2000; Keppler et al., 2005). Wishkerman et al. (2008) demonstrated an exponential increase of chloro- and bromomethane from saltwort material in the temperature range from 25 to 50 °C. While in the vicinity of salt pans halophytes are usually prolific, pectin as a precursor on the salt pans is not available due to lack of plant growth. The widespread presence of MeMET from microbial communities or algal mats however appears plausible. Additionally, these systems often fluctuate seasonally between wet and dry conditions and sufficiently hot temperatures as required for thermolysis.

Arrhenius plots for both DMS and MeCl (Figure 4.5, bottom) gives the logarithm of the kinetic constant, approximated by $\ln k$ in this case, against the inverse temperature. Straight lines were obtained here as is typical for a single rate-limited thermally activated process. The rearrangement Arrhenius equation to fit the plot is

$$(38) \ln k = -E_A / RT - \ln a$$

The activation energy (E_A) can now directly be determined from the slope of the Arrhenius plot (Atkins and de Paula 2008), in this case the calculated E_A for MeCl is 110.16 kJ/mol and 63.5 kJ/mol for DMS. These values are comparable to the data of Derendorp et al. (2012) whose E_A values for leave litter heated to temperatures between 30 and 50 °C ranged depending on plant species from 80 kJ/mol to 119 kJ/mol. The lower E_A for DMS means that this compound forms more readily than MeCl, which is in good agreement with the larger yields observed for DMS. The observed relationship of rising DMS from MeMET could potentially serve as an explanation for the DMS values obtained from the fluid inclusions of the mined salt and not from the recent salt samples (Figure 4.1). Assuming that those salts have been exposed to elevated temperatures during burial DMS could have been formed thermolytically.

Some observations reported in the literature may also be linked to a thermolytic production: Organic soils showed an increased DMS production upon rising temperatures as compared to soils with low humus content (Staubes et al., 1989). The observed diurnal patterns of DMS emissions (Warneck, 2000) may partly be explained by the coinciding temperature variation and the associated MeMET breakdown.

4. Case Study: Thermolysis of MeMET yielding MeCl and DMS

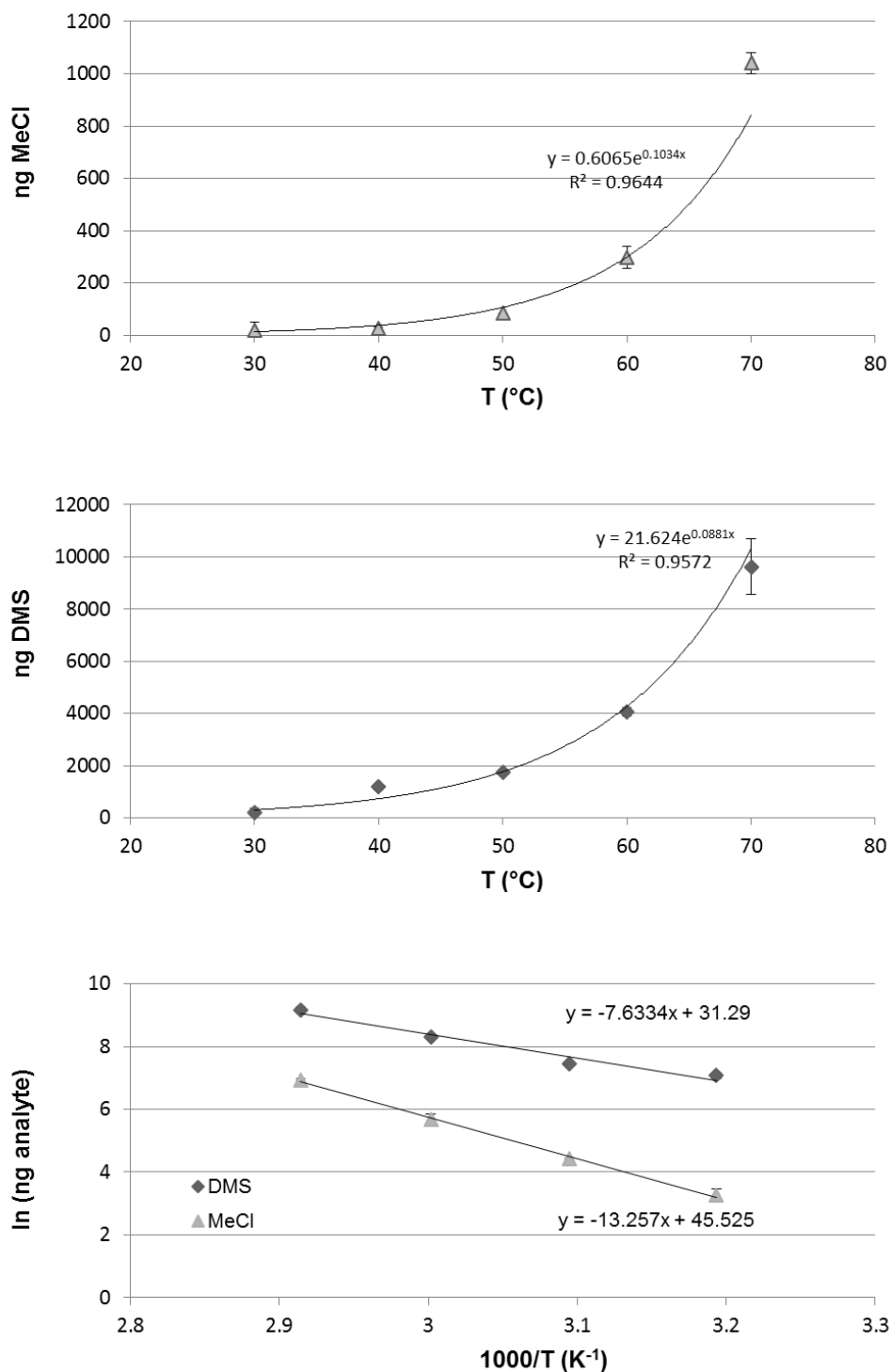


Figure 4.5: Exponential increase of MeCl and DMS release upon heating of 0.1 mmol MeMET at different temperatures for 1h. Arrhenius plots (bottom) for both compounds serve as basis for activation energy calculations.

4.3.3. Model substances and postulated reaction pathways for thermolytic DMS and MeCl generation

A set of structurally related compounds to MeMET was exposed to 40 °C for 1 h in order to gain further insights into the mechanism of DMS and MeCl formation under environmentally relevant conditions. Results obtained are summarized in Table 4.2. At 40 °C MeMET and trimethylsulfonium already serve as effective MeCl/MeBr and DMS sources. While MET, methionine sulfone and dimethylsulfone did not yield significant amounts of either compound, methionine sulfoxide surprisingly showed an elevated DMDS release and minor amounts of DMS. The release of methanethiol by methionine sulfoxide was also observed in the measurements, but was not quantified and is therefore not shown in the table. Trimethylsulfoxonium chloride showed highest MeCl but no DMS emissions. Initial tests with supplementation of NaCl or KBr indicate that higher temperatures (above 55 °C) would be needed to produce DMS and MeCl from MET. Note that all three compounds emitting significant MeCl or DMS amounts carry a positive charge on the sulfur atom lowering the activation energy for a C-S bond splitting.

From the 2 methyl groups at the sulfur moiety of MeMET either one DMS or two MeCl could be formed in the thermolytic reaction.

A possible explanation might be found in the reaction mechanism. If DMS is the leaving group, the remaining alkyl chain (polar homoserin) can form an α -amino- γ -butyrolactone ring (Yang and Hoffman 1984; Althoff, 2012), as can be induced from Figure 4.6. Alternatively, the remaining alkyl chain can rearrange to aminocyclopropane carboxylic acid (ACC) which is also linked to methionine via the ethylene biosynthesis in the Yang cycle (Yang and Hoffman, 1984).

When looking at the emission of MeMET, it can be argued that the DMS formation is thermodynamically favored over MeCl, which is in good agreement with the activation energies calculated from the Arrhenius plots above. Similarly, from trimethylsulfonium bromide once DMS is split off, MeBr would be the natural remainder. However, yields of DMS and MeBr are not equimolar indicating that the leaving methyl groups participate also in other reactions. Zinder and Brock (1978) have observed that the terminal S-methyl group of methionine was converted to CH₄, CO₂ and H₂S.

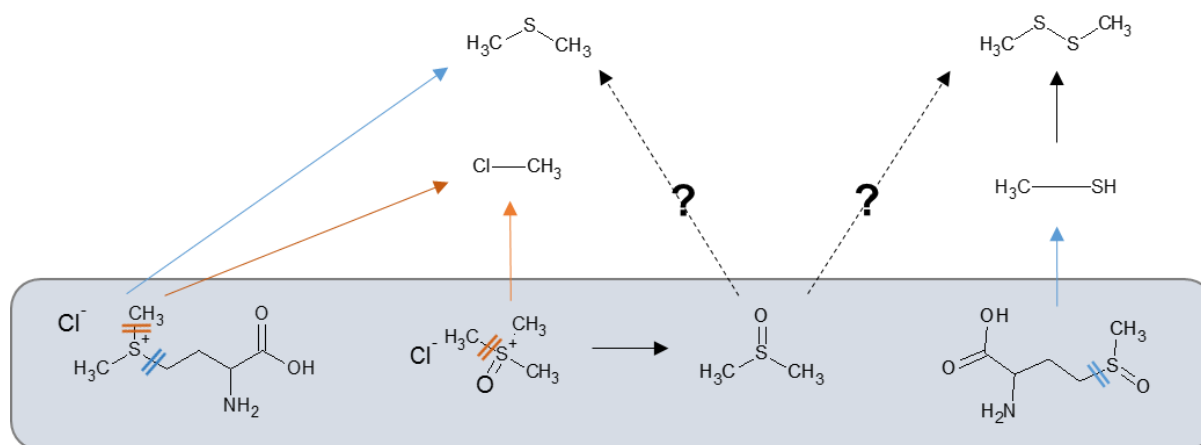
The formation of DMS has also been observed from the bacterial reduction of dimethylsulfoxide (DMSO) by a variety of microorganisms in marine (Simo et al., 2000) and coastal environments (Kiene and Capone, 1988; López and Duarte, 2004).

Table 2: MeCl, DMS and DMDS emissions of MeMET, MET and structurally related compounds after incubating 0.1 mmol of each substance in the dark at 40°C for 1h.

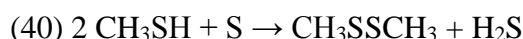
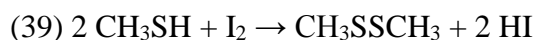
	MeMET		MET		MET sulfox.		MET sulfon.	
MW	199.7		149.21		165.21		181.21	
structural formula								
	ng	±	ng	±	ng	±	ng	±
MeCl	21.3	5.0	0.0	0.0	0.0	0.0	0.0	0.0
DMS	563.9	80.7	0.0	0.0	2.4	0.5	0.3	0.0
DMDS	0.0	0.0	0.0	0.0	41.1	2.7	0.0	0.0

	trimethyl sulfon.*		trimethyl sulfox.		DMSO		DMSO ₂	
MW	157.01		128.62		78.13		94.13	
structural formula								
	ng	±	ng	±	ng	±	ng	±
MeCl /MeBr*	7.6	0.7	88.8	5.4	0.0	0.0	0.0	0.0
DMS	804.5	197.8	0.0	0.0	2.5	1.5	0.0	0.0
DMDS	0.0	0.0	0.1	0.1	1.4	0.3	0.0	0.0

* bromide employed

**Figure 4.6: Postulated reaction pathways for the thermolytic degradation of methyl methionine and related compounds at 40°C. Compounds employed as educts are grey-shaded. Those are from right to left MeMET, trimethylsulfoxonium, DMSO and METsulfoxide. The methanethiol formed from METsulfoxide was measured but not quantified. Dashed lines are in doubt.**

When testing the potential of DMSO for thermolytic decomposition small amounts of DMS and DMDS were observed, but it is questionable whether they indeed stem from DMSO decomposition or whether they represent measured impurities. In general, DMSO under oxic conditions is more likely a reaction product. It is also the remainder after MeCl was emitted from trimethylsulfoxonium chloride and probably a dead end product to further reactions in this context. According to Janssen et al. (2013), the formation mechanism of DMDS has not yet been investigated. However, an enzymatic mechanism for the opposite direction from DMDS to MSH was presented by Smith and Kelly (1988) and they propose that DMDS formation is at least partly a result of oxidation of MSH to DMDS. Our detection of MSH, although not quantified, appears to be of importance. Also, the enzymatic formation of DMDS from methionine via MSH was documented by several authors (Ruiz-Herrera and Starkey, 1970; Challenger and Charlton, 1987). Already Challenger and Charlton (1987) discussed the fission of the methyl thiol group from α -keto-methionine, confirming the observation of this study. An abiotic removal of a methyl thiol group of MET sulfoxide followed by oxidation of MSH to DMDS is conceivable. DMDS can be produced by the oxidation of MSH involving iodine or elemental sulfur according to the following reactions:



Although these reactions are not likely from the here employed pure substances, they may be more important in natural systems. Höckendorf et al. (2012) conducted experiments with gas-phase hydrated radical anions involving DMDS and MSH. They found that, this reaction has



an exothermic reaction enthalpy of -94 kJ mol^{-1} . We suppose that upon oxidative stress and energy input via heating, this reaction might proceed in reverse. A hint of thermolytic DMDS production in nature was the observation that it was the major reduced sulfur-containing gas emitted from bushfires in Australia (Meinardi et al., 2003).

4.3.4. VOX and VSOC released from soils under experimental conditions of thermolytic study

Results from model compounds and the temperature dependence study confirmed that MeMET as well as trimethylsulfoxonium chloride and methionine sulfoxide served as effective precursors for the formation of MeCl and DMS. Additionally DMDS was observed from MET sulfoxide. The oxic conditions applied to our study of the model reactions would represent dried up salt lakes and salt pans that are heated up during the day. Selection criteria for the set of soil samples in the experiment described here was that they were sampled along with a salt crust, whose crystals had been analyzed and that MeCl and possibly DMS had been detected from the FIs in the salt crystal survey. The soil survey data as already presented in Figure 4.2 were performed from 1 g of freeze-dried soil in 10 mL of ultrapure water for 24 h. Now, 1 g of the five freeze-dried samples was exposed at 40 °C for 1 h without water in order to compare results from natural samples to our model reaction studies. Figure 4.7 shows the release of MeCl from all samples. Small amounts of DMS or DMDS were observed in only three samples. The measurements were then repeated with 10 mL water added to simulate conditions similar to a rainfall event. Even though the reaction time was again only 1 h, small amounts of DMS or DMDS were now detected in all samples. The sudden occurrence of CS₂ was remarkable as well as the high amounts detected exceeding those of DMS. To the contrary, results from soils and atmospheric measurements consistently showed higher DMS than CS₂ values (Warneck 2000).

Comparing the 24 h measurements (Figure 4.2), data from the literature and results obtained after 1 h, indicate that the CS₂ production may recede over time. The formation of CS₂ appears to be kinetically favored and based on our results we would expect rain-events after a dry period to cause short term spikes in the CS₂ concentrations. Staubes et al. (1989) reported that low humus and high moisture contents increased CS₂ and decreased DMS emissions released from soils and noted an increased release of both compounds in German soils after a thunderstorm event.

The effect on MeCl was less clear. While for three of the samples the MeCl release remained constant, Lake Springfield emitted slightly reduced amounts and emissions from the Lake Dune sample more than tripled. In principle, thermolytic processes have been confirmed to take place under dry conditions in the dry soil experiments as well as from the MeMET and model substance thermolysis. While the observed results for MeCl exceed DMS emission under dry conditions by far, these cannot be attributed to a sole thermolytic source in complex soils.

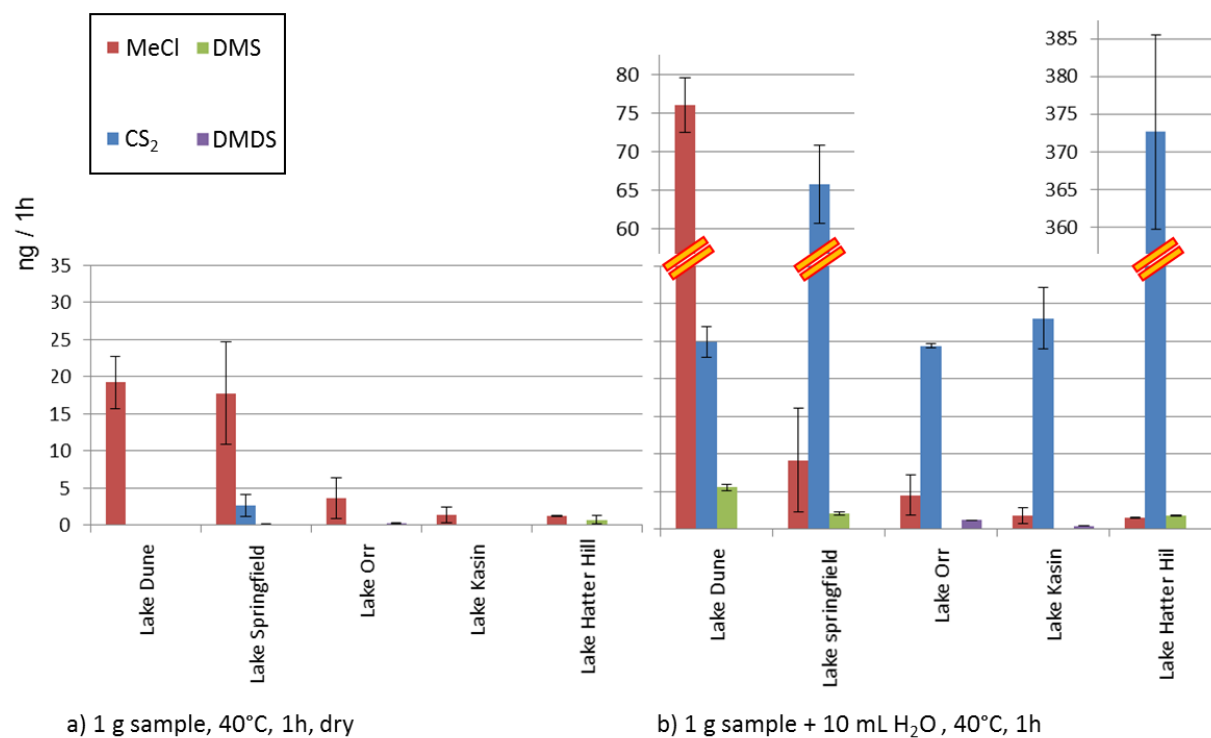


Figure 6: Comparison of MeCl and VOSC emissions of 1 g surface soil sample after incubation under dry (a, left) and wet conditions (b, right).

However, it was clearly demonstrated that thermolytic reactions take place even though the organic matter content of these soils is low.

When water is added, only 1 h of incubation is sufficient to produce MeCl and VOSC emissions that already fall in the concentration range observed after 24 h. Hence, an abiotic formation of these compounds appears likely.

In hypersaline environments, biotic precursor material is produced when conditions are favorable. Upon desiccation abiotic thermolytic emissions prevail and immediately after rainfall on previously dried-out land, abiotic aqueous reactions prevail. A re-wetting and drying-out cycle is typical for SW Australian salt lakes. Kotte et al. (Kotte et al., 2012) have reported high emissions of MeCl and MeBr from dry samples of similar environments in South Russia and Namibia. But also areas of regressing (salt) lakes such as the Aral Sea could contribute to thermolytic emissions. Hall et al. (2012) found elevated N₂O and CH₄ after amending Atacama Desert soils with water and organic carbon which was not conclusively linked to microbial production showing the

importance of abiotic reactions in soils. The abundance of abiotic mechanisms in hypersaline environments is also supported by our study, whereas data on the biogeochemical capacity of arid and hypersaline soils are scarce (Ruecker et al., 2014).

4.4. Conclusions

In this chapter, findings from field sampling campaigns with mechanistic studies of MeMET degradation were combined.

DMS and MeCl emissions were found to increase exponentially upon heating of MeMET and related compounds. At 40 °C. MeMET, trimethylsulfonium bromide and trimethylsulfoxonium chloride thermolytically formed MeCl and DMS under dry conditions at temperatures commonly measured on salt pan surfaces. Furthermore, MET sulfoxide has been shown to emit methanethiol and DMDS under these conditions.

Dry soils were clearly found to emit MeCl thermolytically despite their low organic matter content. DMS was also measured from natural samples. Together with data from model compounds a formation of these substances via temperature controlled MeMET decomposition appears plausible. However, the MeCl/DMS ratio from soils suggests other sources. Data from FIs of halites also support the hypothesis that temperature plays a crucial role in MeCl and DMS production. The abiotic production mechanism here proposed goes hand in hand with biotic activity during favorable conditions which provide the precursor material. Isotopic signatures might help to identify the exact source of the abiotically produced VOC in natural systems in the future. The occurrence of DMDS should be investigated further.

The new insights gained should help to get a clearer view on the relative importance on different formation mechanisms and to refine atmospheric VOSC and VOX budgets. In light of increasing desertification, anthropogenic salinization and the accompanying extension of salt lakes and salt lake influenced soils around the globe an understanding of these terrestrial sources for atmospheric chlorine and VSOC becomes even more important.

5

Summary and Conclusions

5.0 Summary and Conclusions

While the understanding and handling of the anthropogenic influence on Earth's climate is a challenge for science and society, the study of geogenic emissions as part of natural VOC emission sources is necessary to comprehend natural processes and their role for atmospheric chemistry. In this regard, the main goal of the work presented in this dissertation was the investigation of rocks and minerals for their VOX-formation potential. A central requirement was the development of a suitable method to release and detect VOX from FIs of the minerals under study (Chapter 2).

Major features of the newly developed purge and trap method are the purgeable grinding chamber to release gases from minerals and the efficient liquid N₂ cold trap for sample pre-concentration before GC-MS analysis.

The tempered steel grinding chamber effectuated the combination of mechanical grinding in a commercial planetary mill with the advantages of a headspace vial, i.e. via pierceable septa, for purge and trap sample preconcentration. The grinding procedures could be adapted according to the mineral's hardness and relatively low amounts of 10 g sample material produced sufficient amounts of measureable VOX, also due to an efficient grinding down to a final grain size of 1 μm (quartz).

The second essential feature of the method was the cold trap constructed of a glass lined tubing (™) without further adsorbent material and installed directly before the GC columns and MS detector. This in effect, made the detection of VOX released after grinding feasible. Volatile compounds detected ranged from the very low boiling point of carbon tetrafluoride up to bromodichloromethane, spanning a temperature range of over 200 °C.

Major advantages of this adapted dynamic headspace design is that it accommodates all types of minerals and rocks, while remaining versatile concerning analytical technique. Conventional headspace applications are still feasible with the GC-MS in use by inserting a water trap. Since analytes are trapped prior to the GC column, the experimental set-up could be used with different GC configurations or different analytical instrumentation, such as FID or IRMS.

Subsequent to the method development, the sample screening (Chapter 3) pursued the objective of expanding the data set on VOX released from FIs and deepen the scientific understanding of their natural abiotic formation pathways. A wide array of volatiles from various minerals could be documented. The presence of SF₆ and CF₄ in fluorites was confirmed, which is important with

regard to the role they play in the atmospheric and hydrologic sector as they may pose limitations to groundwater dating or balancing the atmospheric budgets.

Methyl bromide, dichloroethene and dichloroethane from quartz samples of the Archean Yilgarn craton in Australia give first insights into synthetic processes occurring in rising hydrothermal fluids in the upper crust. Vinyl chloride was found in a hydrothermal quartz from High Taunus. Assuming an abiotic genesis, these organic molecules are hypothesized to be involved in the formation of early prebiotic organic molecules.

Generally, the differences of compounds trapped during mineral growth can provide information on the respective formation conditions but sample sizes were too low to allow for systematic observations. Formation pathway of the aforementioned compounds in geological matrices remains subject of speculation and more research is needed. Improvements to the method in the future should include the use of a highly durable zirconium oxide grinding chamber and gaseous halocarbon standard mix to enhance analytical performance.

MeCl was found to be an almost omnipresent compound occurring in quartz, fluorites, halites and dolerites. Initial heating experiments with halites using purge-and-trap GC-MS as well as Py-GC-MS demonstrated the important role of temperature in MeCl and VOX.

In halites MeCl release was in some cases accompanied by DMS. This observation when combined with observations made in associated environmental compartments lead the way to mechanistic studies on MeCl and DMS formation from MeMET as a precursor material (Chapter 4). Hypersaline soil samples when incubated in headspace vials showed MeCl release and an array of VOSC including DMS and dimethyldisulfide (DMDS). MeCl and DMS were also present in air sampled immediately above the salt lake surfaces. An abiotic mechanism for their formation appeared conceivable due to the fast response of emission upon heating of freeze-dried samples at 40 °C.

The hypothesis that MeMET could serve as a precursor for both MeCl and DMS formation was confirmed. Based on the thermolytic degradation of MeMET the activation energies for MeCl and DMS are reported from their Arrhenius plots. The lower activation energy calculated for DMS means that this compound forms more readily than MeCl, which is in good agreement with the larger yields observed for DMS. This observation might also explain DMS values obtained from the fluid inclusions of the mined salt and not from the recent salt samples considering their exposure to elevated temperatures during burial where the DMS could have been formed thermolytically.

Structurally related substances to MeMET were analysed and methionine sulfoxide remarkably showed an elevated DMDS release and minor amounts of DMS and MeSH by methionine sulfoxide was also observed in the measurements. Finally, soil samples were tested again under thermolytic conditions of the model substances and the thermolytic processes appear to play an important role in salt lake environments during drying processes. The emerged abiotic production mechanism can only be understood in consecution of biotic activity during favorable environmental conditions providing the precursor material.

Hypersaline environments will likely gain more and more importance in their contributions to atmospheric VOSC and VOX budgets considering increasing desertification and anthropogenic salinization and thermolytic MeMET degradation is a plausible way to comprehend increased MeCl and DMS emissions under these conditions.

In summary, we implemented a customized purge-and-trap GC-MS system for specialized FI analysis confirming the presence VOX and VOC in a variety of minerals. The thermolytic degradation of the precursor MeMET to MeCl and DMS from MeMET was identified as one possible natural abiotic formation pathway. More data are needed to gain further insight into geogenic VOX formation as the analytical system is further improved.

This work demonstrates the potential of the method as new research topics emerged in the process of development. FI analysis via purge-and-trap GC-MS system presents a new tool to help deepen our understanding of the role of geospheric processes e.g. on aspects of the origin of life, trace gas dating of ground waters and balancing the atmospheric VOX budget. Isotopic studies could contribute significantly to future research.

With these developments and observations made the door was opened to future investigations in a still largely unexplored scientific terrain.

Acknowledgements

During my dissertation from 2008 to 2014 many people have assisted and accompanied me, and I would like to thank all of them!

First of all, I would like to express my gratitude to Prof. Dr. H.-F. Schöler, without whom this work and the wonderful time I had in Heidelberg would not have been possible. His patient way, knowledge of GC-MS and lots of hands-on technical support especially during the first year, finally made it possible to tackle the enthralling subject of volatile organohalogenes from fluid inclusions. I especially enjoyed the freedom and encouragement to pursue own projects. His input often facilitated fruitful collaboration with other researchers in and outside of the DFG763 research unit.

I thank Prof. Dr. U. A. Glasmacher for the co-supervision and second opinion of this work and especially for the support I received with regards to method development and sample compilation.

Thanks a lot to my former and current fellow Ph.D. students, who not only helped in all aspects of lab and field work but also made it worthwhile: Stefan Huber, Sabine Studenroth, Torsten Krause, Christoph Tubbesing and Tobias Sattler.

For a memorable trip to the salt lakes of South East Russia, interdisciplinary exchange and valuable discussions, I thank Karsten Kotte as well as Maren Emmerich and Robert Holla.

Thanks to Prof. Dr. Cornelius Zetzsch at BayCEER in Bayreuth, for the open doors and collaborations essential for the development of the analytical system. In this regard, I am also thankful for technical support and helpful discussions to Heinz-Ulrich Krüger (deceased), as well as to Gerhard Kilian, Andriy Cheburkin, Winfried Schwarz, Bernd Kober, Mario Trieloff, Andreas Thum and Christian Mächtle at the Institute of Earth Sciences in Heidelberg, Uwe Branczyk at the Institute of Physical Chemistry of the University of Heidelberg and Enno Bahlmann at University of Hamburg. I thank Barkley Sive, University of New Hampshire, for sharing details on the construction of the Cryo-Tiger.

I thank Sylvia and Stefan Rheinberger and Christian Scholz for their help with the IC and C_{org} measurements. When in trouble with computer problems Francis Cueto, Stefan Rheinberger and Torsten Krause saved the day for me.

Special thanks also to Stefan Dultz at the Institute of Soil Science in University of Hannover to welcome me in his labs to measure particle size distribution, for the field trip to Schiermonnikoog and valuable reflections on my research.

Thanks to Michael Burchard, for scientific support and discussions on the design of future experiments on halogenation of hydrocarbons under hydrothermal conditions and for presenting our poster at the AGU, 2012.

Likewise, I thank Marcus Greule, Prof. Dr. Frank Keppler and Frederick Althoff for the trials on methane from fluid inclusions at the Max Planck Institute of Atmospheric Chemistry.

Thanks to Uwe Schwarzenbolz, TU Dresden, for determining amino acid from halite samples, to Colin McRoberts at Queens University in Belfast, Ireland, for Py-GC-MS measurements on halites, to Harald Färber und Dirk Skutlarek, University of Bonn for the trials on trifluoroacetic acid on fluorite leachates and to Prof. Dr. Elliot Atlas together with Tobias Sattler for providing data from air measurements.

I thank Svenja Bugla and Marcus Ubl very much for contributing valuable measurements in their B.Sc thesis work. I thank my B.Sc. students Ji, Dominik, and Blanca for allowing me an excursion to soils. Thanks to Dominique and Maik for their inquisitiveness and interesting conversations.

Also thanks to Sonja Pabst, Alke Jugold, Bianca Oehm, Natalia Munoz, Felix Vogel, Tobias Kluge, Martin Wieser, Höpke Andresen and Stefan Wunderlich for discussions and help with measurements.

I owe many thanks to all contributors of mineral and rock samples to my study: Günther Schönlein, private mineral collector from Bamberg, Germany; Marek Dulinski and Krysztof Bukowski, from AGH University of Science and Technology, Cracow; Benjamin Black, MIT Massachusetts; Henrik Svenson, University of Oslo; Rainer Altherr and Michael Hanel, Karsten Kotte, Torsten Krause, Stefan Huber of the University of Heidelberg; Thomas Kirnbauer from the University of Bochum. Special thanks also to Ulrich Schreiber for samples and discussions, introducing new interesting aspects to the research on volatile organohalogenes from fluid inclusions.

Many thanks to Torsten Hoffman for assisting in administrative procedures and especially for keeping an eye on international transactions.

This work was supported in parts by the DFG Research Unit 763 Natural Halogenation Processes in the Environment - Atmosphere and Soil (HALOPROC).

I also thank the Clay Minerals Society of America for a Travel Grant and Ronald Bakker at the University of Leoben for his fluid inclusions workshop.

Last but not least: My dear family and friends, I thank you!

Bibliography

- Aarnes, I., K. Fristad, S. Planke, and H. Svensen. 2011. "The Impact of Host-Rock Composition on Devolatilization of Sedimentary Rocks during Contact Metamorphism around Mafic Sheet Intrusions." *Geochemistry, Geophysics, Geosystems* 12 (10): Q10019.
- Abrams, M. A. 2005. "Significance of Hydrocarbon Seepage Relative to Petroleum Generation and Entrapment." *Marine and Petroleum Geology, Near-Surface Hydrocarbon Migration: Mechanisms and Seepage Rates*, 22 (4): 457–77.
- Aiuppa, A., D. R. Baker, and J. D. Webster. 2009. "Halogens in Volcanic Systems." *Chemical Geology, Halogens in Volcanic Systems and Their Environmental Impacts*, 263 (1–4): 1–18.
- Althoff, Frederik. 2012. "Sources and Pathways of Methane Formed in Oxidative Environments." Mainz: Universität Mainz.
- Andreyeve-Grigorovich, S. Aida, N. Oszczytko, N. A. Savitskaya, A. Slaczka, and N. A. Trofimovich. 2003. "Correlation of Late Badenian Salts of Wieliczka, Bochnia and Kalush Areas (Polish and Ukrainian Carpathian Foredeep)." *Annales Societatis Geologorum Poloniae*, 73: 67–89.
- Atkins, P. W. and J. de Paula. 2008. *Kurzlehrbuch Physikalische Chemie*. 4. ed. Weinheim: Wiley-VCH.
- Attieh, J. M., A. D. Hanson, and H. S. Saini. 1995. "Purification and Characterization of a Novel Methyltransferase Responsible for Biosynthesis of Halomethanes and Methanethiol in Brassica Oleracea." *The Journal of Biological Chemistry* 270 (16): 9250–57.
- Bąbel, M. 2004. "Badenian Evaporite Basin of the Northern Carpathian Foredeep as a Drawdown Salina Basin." *Acta Geologica Polonica* 54 (3): 313–37.
- Bahlmann, E., I. Weinberg, R. Seifert, C. Tubbesing, W. Michaelis. 2011. A high volume sampling system for isotope determination of volatile halocarbons and hydrocarbons. *Atmospheric Measurement Techniques*, 4(10): 2073–2086.
- Baker, D. R. and J. Vaillancourt. 1995. "The Low Viscosities of F + H₂O-Bearing Granitic Melts and Implications for Melt Extraction and Transport." *Earth and Planetary Science Letters* 132 (1–4): 199–211.
- Ballschmiter, K. 2003. "Pattern and Sources of Naturally Produced Organohalogens in the Marine Environment: Biogenic Formation of Organohalogens." *Chemosphere, Naturally Produced Organohalogens*, 52 (2): 313–24.
- Banks, R. E., B. E. Smart, and J. C. Tatlow. 1994. *Organofluorine Chemistry: Principles and Commercial Applications*. Springer, pp. 644.

- Barb, W. G., J. H. Baxendale, P. George, and K. R. Hargrave. 1951. "Reactions of Ferrous and Ferric Ions with Hydrogen Peroxide. Part II.—The Ferric Ion Reaction." *Transactions of the Faraday Society* 47 (0): 591–616.
- Barcellos da Rosa, M. 2003. "Untersuchungen Heterogener Troposphärenrelevanter Reaktionen von Schwefel- und Halogenverbindungen." PhD Thesis.
- Barclay, S. A., R. H. Worden, J. Parnell, D. L. Hall, and S. M. Sterner. 2000. "Assessment of Fluid Contacts and Compartmentalization in Sandstone Reservoirs Using Fluid Inclusions: An Example from the Magnus Oil Field, North Sea." *AAPG Bulletin* 84 (4): 489–504.
- Barker, C. E., and M. J. Pawlewicz. 1986. "The Correlation of Vitrinite Reflectance with Maximum Temperature in Humic Organic Matter." *Paleogeothermics, Lecture Notes in Earth Sciences Volume 5*, pp. 79-93.
- Barker, C. E., Y. Bone, and M. D. Lewan. 1998. "Fluid Inclusion and Vitrinite-Reflectance Geothermometry Compared to Heat-Flow Models of Maximum Paleotemperature next to Dikes, Western Onshore Gippsland Basin, Australia." *International Journal of Coal Geology* 37 (1–2): 73–111.
- Beerling, D. J., M. Harfoot, B. Lomax, and J. A. Pyle. 2007. "The Stability of the Stratospheric Ozone Layer during the End-Permian Eruption of the Siberian Traps." *Philosophical Transactions of the Royal Society A: Mathematical, Physical and Engineering Sciences* 365 (1856): 1843–66.
- Bentley, R. and T. G. Chasteen. 2004. "Environmental VOSCs--Formation and Degradation of Dimethyl Sulfide, Methanethiol and Related Materials." *Chemosphere* 55 (3): 291–317.
- Bergman, R. G. 2007. "Organometallic Chemistry: C–H Activation." *Nature* 446 (7134): 391–93. Bodnar RJ (2003) Introduction to fluid inclusions. In I. Samson, A. Anderson, & D. Marshall, eds. *Fluid Inclusions: Analysis and Interpretation*. Mineral. Assoc. Canada, Short Course 32, 1-8.
- Black, B. A., J.-F. Lamarque, C. A. Shields, L. T. Elkins-Tanton, and J. T. Kiehl. 2014. "Acid Rain and Ozone Depletion from Pulsed Siberian Traps Magmatism." *Geology* 42 (1): 67–70.
- Black, B. A., L. T. Elkins-Tanton, M. C. Rowe, and I. Ukstins Peate. 2012. "Magnitude and Consequences of Volatile Release from the Siberian Traps." *Earth and Planetary Science Letters* 317–318, 363-373.
- Boerjan, W., J. Ralph, and M. Baucher. 2003. "Lignin Biosynthesis." *Annual Review of Plant Biology* 54 (1): 519–46.
- Bordenave M.L. 1993. "Applied Petroleum Geochemistry." Paris: Editions OPHRYS. pp. 531.
- Bugla, S. 2010. "Flüchtige Organische Verbindungen in Salzen." Bachelor-thesis, Rupert-Karls Universität Heidelberg.
- Bukowski, K. 1997. Zwartosc bromu w solach badenskich Bochni. *Przegląd Geologiczny*, 45: 819–821.
- Busenberg, E. and L.N. Plummer. 2000. Dating young groundwater with sulfur hexafluoride: Natural and anthropogenic sources of sulfur hexafluoride. *Water Resources Research*, 36(10): 3011-3030.
- Busenberg, E., and L. N. Plummer. 2010. "A Rapid Method for the Measurement of Sulfur Hexafluoride (SF₆), Trifluoromethyl Sulfur Pentafluoride (SF₅CF₃), and Halon 1211 (CF₂ClBr) in Hydrologic Tracer Studies." *Geochemistry, Geophysics, Geosystems* 11 (11): Q11001.
- Carroll, M. R., and J. D. Webster. 1994. "Solubilities of Sulfur, Noble Gases, Nitrogen, Chlorine, and Fluorine in Magmas." *Reviews in Mineralogy and Geochemistry* 30 (1): 231–79.
- Casas, E., and T. K. Lowenstein. 1989. "Diagenesis of Saline Pan Halite: Comparison of Petrographic Features of Modern, Quaternary and Permian Halites." *Journal of Sedimentary Research* 59 (5) 724-739.

- Challenger, F. and P. T. Charlton. 1987. "Studies on Biological Methylation. Part X. The Fission of the Mono- and Di-Sulphide Links by Moulds." *Journal of the Chemical Society* (84) 424–29.
- Charlson, R. J., S. E. Schwartz, J. M. Hales, R. D. Cess, J. A. Coakley, J. E. Hansen, and D. J. Hofmann. 1992. "Climate Forcing by Anthropogenic Aerosols." *Science* (New York, N.Y.) 255 (5043): 423–30.
- Cheburkin, A. K., Frei, R., and Shotyk, W. 1997. "An energy-dispersive miniprobe multielement analyzer (EMMA) for direct analysis of trace elements and chemical age dating of single mineral grains." *Chem. Geol.*, 135, 75–87.
- Cosgrove, B. A., and J. Walkley. 1981. "Solubilities of Gases in H₂O and ²H₂O." *Journal of Chromatography A*, 216: 161–67.
- Deeds, D. A., M. K. Vollmer, J. T. Kulongoski, B. R. Miller, J. Mühle, C. M. Harth, J. A. Izbicki, D. R. Hilton, and R. F. Weiss. 2008. Evidence for crustal degassing of CF₄ and SF₆ in Mojave Desert groundwaters. *Geochimica Et Cosmochimica Acta*, 72 (4): 999–1013.
- Denner, E. B. M., T. J. McGenity, H.-J. Busse, W. D. Grant, G. Wanner, and H. Stan-Lotter. 1994. "Halococcus Salifodinae Sp. Nov., an Archaeal Isolate from an Austrian Salt Mine." *International Journal of Systematic Bacteriology* 44 (4): 774–80.
- Dennis, P.F., Rowe, P.J., and Atkinson, T.C., 2001. The recovery and isotopic measurement of water from fluid inclusions in speleothems. *Geochimica Et Cosmochimica Acta*, 65 (6): 871–884.
- Derendorp L., A. Wishkerman, F. Keppler, C. McRoberts, R. Holzinger and T. Röckmann. 2012. "Methyl Chloride Emissions from Halophyte Leaf Litter: Dependence on Temperature and Chloride Content." *Chemosphere* 87 (5): 483–89.
- Dolbier Jr., W. R. 2005. "Fluorine Chemistry at the Millennium." *Journal of Fluorine Chemistry, Selected papers presented at the XIVth European Symposium on Fluorine Chemistry*, 126 (2): 157–63.
- Dolejš, D., and D. R. Baker. 2004. "Thermodynamic Analysis of the System Na₂O-K₂O-CaO-Al₂O₃-SiO₂-H₂O-F₂O⁻¹: Stability of Fluorine-Bearing Minerals in Felsic Igneous Suites." *Contributions to Mineralogy and Petrology* 146 (6): 762–78.
- Dutkiewicz, A., H. Volk, J. Ridley, and S. C. George. 2004. "Geochemistry of Oil in Fluid Inclusions in a Middle Proterozoic Igneous Intrusion: Implications for the Source of Hydrocarbons in Crystalline Rocks." *Organic Geochemistry* 35 (8): 937–57.
- Dutkiewicz, A., J. Ridley, and R. Buick. 2003. "Oil-Bearing CO₂-CH₄-H₂O Fluid Inclusions: Oil Survival since the Palaeoproterozoic after High Temperature Entrapment." *Chemical Geology, European Current Research on Fluid Inclusions*, 194 (1–3): 51–79.
- Etminan, Hashem, and Christopher F. Hoffmann. 1989. "Biomarkers in Fluid Inclusions: A New Tool in Constraining Source Regimes and Its Implications for the Genesis of Mississippi Valley-Type Deposits." *Geology* 17 (1): 19–22.
- Fall, R., D. L. Albritton, F. C. Fehsenfeld, W. C. Kuster, and P. D. Goldan. 1988. "Laboratory Studies of Some Environmental Variables Controlling Sulfur Emissions from Plants." *Journal of Atmospheric Chemistry* 6 (4): 341–62.
- Fiebig, Jens, Alan B. Woodland, Walter D'Alessandro, and Wilhelm Püttmann. 2009. "Excess Methane in Continental Hydrothermal Emissions Is Abiogenic." *Geology* 37 (6): 495–98.
- Fisher R.S. and S. D. Hovorka. 1987. "Relations between Bromide Content and Depositional Processes in Bedded Halite, Permian San Andres Formation, Palo Duro Basin, Texas" 2 (1): 67–82.

- Frezzotti, M.L., van den Kerkhof, A.M., 2007. "New results in fluid and melt inclusion research - XVIII European current research on fluid inclusions - Preface." *Chemical Geology*, 237 (3-4): 233-235.
- Friedrich, R. 2007. "Grundwassercharakterisierung mit Umwelttracern: Erkundung des Grundwassers der Odenwald-Region sowie Implementierung eines neuen Edelgas-Massenspektrometersystems." Dissertation. Universität Heidelberg.
- Garlicki A., and J. Wiewiórka. 1981. "The distribution of bromine in some halite rock salts of the Wieliczka salt deposit (Poland)." *Annales Societatis Geologorum Poloniae* 51 (3): 353-359.
- Giggenbach, W. F. 1997. "Relative Importance of Thermodynamic and Kinetic Processes in Governing the Chemical and Isotopic Composition of Carbon Gases in High-Heatflow Sedimentary Basins." *Geochimica et Cosmochimica Acta* 61 (17): 3763-85.
- Goldstein, R. H. 2001. "Fluid Inclusions in Sedimentary and Diagenetic Systems." *Lithos, Fluid Inclusions: Phase Relationships - Methods - Applications. A Special Issue in honour of Jacques Touret*, 55 (1-4): 159-93.
- Goldstein, R. H., and T. J. Reynolds. 1994. *Systematics of Fluid Inclusions in Diagenetic Minerals. SEPM Short Course 31*. Tulsa, pp. 199
- Goudie, A. S., and R. U. Cooke. 1984. "Salt Efflorescences and Saline Lakes; a Distributional Analysis." *Geoforum* 15 (4): 563-82.
- Gray, M. R., and W. C. McCaffrey. 2002. "Role of Chain Reactions and Olefin Formation in Cracking, Hydroconversion, and Coking of Petroleum and Bitumen Fractions." *Energy & Fuels* 16 (3): 756-66.
- Greensfelder, B. S., H. H. Voge, and G. M. Good. 1949. "Catalytic and Thermal Cracking of Pure Hydrocarbons: Mechanisms of Reaction." *Industrial & Engineering Chemistry* 41 (11): 2573-84.
- Greenwood, P. F., George, S. C., and Hall, K., 1998. "Application of laser micropyrolysis-gas chromatography-mass spectrometry." *Organic Geochemistry*, 29: 1075-1089.
- Gribble, G. W. 2003. "The diversity of naturally produced organohalogenes." *Chemosphere* 52(2): 289-97.
- Gribble, G. W. 2010. "Naturally occurring organohalogen compounds - a comprehensive survey" *Progress in the Chemistry of Organic Natural Products*, edited by: A. D. Kinghorn, H. Falk, J. Kobayashi, and W. Herz, Springer, Vienna, pp. 1-613.
- Grice, K., S. Schouten, A. Nissenbaum, J. Charrach, and J. S. Sinninghe Damsté. 1998. "Isotopically Heavy Carbon in the C₂₁ to C₂₅ Regular Isoprenoids in Halite-Rich Deposits from the Sdom Formation, Dead Sea Basin, Israel." *Organic Geochemistry* 28 (6): 349-59.
- Haber, F., and J. Weiss. 1932. "Über die Katalyse des Hydroperoxydes." *Naturwissenschaften* 20 (51): 948-50.
- Hall, S. J., W. L. Silver, and R. Amundson. 2012. "Greenhouse Gas Fluxes from Atacama Desert Soils: A Test of Biogeochemical Potential at the Earth's Arid Extreme." *Biogeochemistry* 111 (1-3): 303-15.
- Hamilton, J. T. G., W. C. McRoberts, F. Keppler, R. M. Kalin, and D. B. Harper. 2003. "Chloride Methylation by Plant Pectin: An Efficient Environmentally Significant Process." *Science* 301 (5630): 206-9. doi:10.1126/science.1085036.
- Harmon, R.S., Schwarcz, H.P., O'Neil, J.R., 1979. "D/H ratios in speleothem fluid inclusions: a guide to variations in the isotopic composition of meteoric precipitation?" *Earth and Planetary Science Letters*, 42: 254-266.

- Harnisch, J., and A. Eisenhauer. 1998. "Natural CF₄ and SF₆ on Earth." *Geophysical Research Letters*, 25(13): 2401-2404.
- Harnisch, J., M. Frische, R. Borchers, A. Eisenhauer and A. Jordan. 2000. "Natural fluorinated organics in fluorite and rocks." *Geophysical Research Letters*, 27(13): 1883-1886.
- Hatcher, P. G, and D. J. Clifford. 1997. "The Organic Geochemistry of Coal: From Plant Materials to Coal." *Organic Geochemistry* 27 (5-6): 251-74.
- Hesse, P. J., R. Battino, P. Scharlin, and E. Wilhelm. 1996. "Solubility of Gases in Liquids. 20. Solubility of He, Ne, Ar, Kr, N₂, O₂, CH₄, CF₄, and SF₆ in N-Alkanes N-C₁H_{2L+2} (6 ≤ L ≤ 16) at 298.15 K." *Journal of Chemical & Engineering Data* 41 (2): 195-201.
- Höckendorf, R. F., Q. Hao, Z. Sun, B. S. Fox-Beyer, Y. Cao, O. Petru Balaj, V. E. Bondybey, C.-K. Siu, and M. K. Beyer. 2012. "Reactions of CH₃SH and CH₃SSCH₃ with Gas-Phase Hydrated Radical Anions (H₂O)ⁿ⁻, CO₂⁻(H₂O)_n, and O₂⁻(H₂O)_n." *The Journal of Physical Chemistry A* 116 (15): 3824-35.
- Holloway, J. R. 1981. "Volatile Interactions in Magmas." In *Thermodynamics of Minerals and Melts*, edited by R. C. Newton, A. Navrotsky, and B. J. Wood, 273-93. *Advances in Physical Geochemistry* 1. Springer New York.
- Holtz, F., Dingwell D. B., and H. Behrens. 1993. "Effects of F, B₂O₃ and P₂O₅ on the Solubility of Water in Haplogranite Melts Compared to Natural Silicate Melts." *Contributions to Mineralogy and Petrology* 113 (4): 492-501.
- Huber, S. G., K. Kotte, H. F. Schöler, and J. Williams. 2009. "Natural Abiotic Formation of Trihalomethanes in Soil: Results from Laboratory Studies and Field Samples." *Environmental Science & Technology* 43 (13): 4934-39.
- Huber, S. G., S. Wunderlich, H. F. Schöler, and J. Williams. 2010. "Natural Abiotic Formation of Furans in Soil." *Environmental Science & Technology* 44 (15): 5799-5804.
- IPCC, Fifth assessment Report. 2013. "Climate Change 2013 - The Physical Science Basis." Intergovernmental Panel on Climate Change.
- Isidorov, V.A., E.B. Prilepsky, V.G. Povarov. 1993. "Photochemical and optically active components of minerals and gas emissions of mining plants." *Journal of Ecological Chemistry*, 2-3: 201-207.
- Jänecke, Ernst. 1918. "Vollständige Übersicht über die Lösungen ozeanischer Salze. IV." *Zeitschrift Für Anorganische und Allgemeine Chemie* 103 (1): 1-54.
- Janssen, A., P. L. F. van den Bosch, R. C. van Leerdam, and M. de Graaff. 2013. "Bioprocesses for the Removal of Volatile Sulfur Compounds from Gas Streams." *Air Pollution Prevention and Control*, C. Kennes and R. C. Veiga (eds.), 247-74. John Wiley & Sons.
- Jefferson, I.F., Jefferson, B.Q., Assallay, A.M., Rogers, C.D.F., Smalley, I.J., 1997. "Crushing of quartz sand to produce silt particles." *Naturwissenschaften*, 84(4): 148-149.
- Jeffrey, A. W. A., and I. R. Kaplan. 1988. "Hydrocarbons and Inorganic Gases in the Gravberg-1 Well, Siljan Ring, Sweden." *Chemical Geology, Origins of Methane in the Earth*, 71 (1-3): 237-55.
- Jones, D. L., A. G. Owen, and J. F. Farrar. 2002. "Simple Method to Enable the High Resolution Determination of Total Free Amino Acids in Soil Solutions and Soil Extracts." *Soil Biology and Biochemistry* 34 (12): 1893-1902.
- Jordan, A., Harnisch, J., Borchers, R., Le Guern, F.N. and Shinohara, H., 2000. Volcanogenic halocarbons. *Environmental Science & Technology*, 34(6): 1122-1124.

- Jorge, S., Coelho, C. E. S., and F. Radler de Aquino-Neto. 2011. "Analysis of Volatiles in Fluid Inclusions by Direct Online Crushing Mass Spectrometry." *Journal of the Brazilian Chemical Society* 22 (3): 437–45.
- Kano, J., H. Mio, and F. Saito. 2000. Correlation of grinding rate of gibbsite with impact energy of balls. *AIChE Journal*, 46(8): 1694-1697.
- Keppler F., and J. T. G. Hamilton. 2008. "Methoxyl Groups of Plant Pectin as a Precursor of Atmospheric Methane: Evidence from Deuterium Labelling Studies." *The New Phytologist* 178 (4): 808–14.
- Keppler F., and R. Eiden. 2000. "Halocarbons Produced by Natural Oxidation Processes during Degradation of Organic Matter." *Nature* 403 (6767): 298–301.
- Keppler, F., Borchers, R., Elsner, P., Fahimi, I., Pracht, J., and Schöler, H. F. 2003. „Formation of volatile iodinated alkanes in soil: results from laboratory studies." *Chemosphere*, 52, 477-483.
- Keppler, F., D. B. Harper, T. Röckmann, R. M. Moore, and J. T. G. Hamilton. 2005. "New Insight into the Atmospheric Chloromethane Budget Gained Using Stable Carbon Isotope Ratios." *Atmos. Chem. Phys.* 5 (9): 2403–11.
- Keppler, F., Borchers, R., Hamilton, J. T. G., Kilian, G., Pracht, J., and Schöler, H. F.: 2006. "De novo formation of chloroethyne in soil." *Environ. Sci. Technol.*, 40, 130-134.
- Kiene, R. P., R. S. Oremland, A. Catena, L. G. Miller, and D. G. Capone. 1986. "Metabolism of Reduced Methylated Sulfur Compounds in Anaerobic Sediments and by a Pure Culture of an Estuarine Methanogen." *Applied and Environmental Microbiology* 52 (5): 1037–45.
- Kiene, R. P., and P. T. Visscher. 1987. "Production and Fate of Methylated Sulfur Compounds from Methionine and Dimethylsulfoniopropionate in Anoxic Salt Marsh Sediments." *Applied and Environmental Microbiology* 53 (10): 2426–3
- Kiene, R. P., and D. G. Capone. 1988. "Microbial Transformations of Methylated Sulfur Compounds in Anoxic Salt Marsh Sediments." *Microbial Ecology* 15 (3): 275–91.
- Killops, S. D., and V. J. Killops. 2004. "Long-Term Fate of Organic Matter in the Geosphere." In *Introduction to Organic Geochemistry In Introduction to Organic Geochemistry*. Oxford: Blackwell Publishing. 117–65.
- Killops, S. D., and V. J. Killops. 2009. *Introduction to Organic Geochemistry*. Oxford: Blackwell Publishing. pp. 393.
- Kinsela, A. S., J. K. Reynolds, and M. D. Melville. 2007. "Agricultural Acid Sulfate Soils: A Potential Source of Volatile Sulfur Compounds?" *Environmental Chemistry* 4 (1): 18–25.
- Kissin, Y. V. 1987. "Catagenesis and Composition of Petroleum: Origin of N-Alkanes and Isoalkanes in Petroleum Crudes." *Geochimica et Cosmochimica Acta* 51 (9): 2445–57.
- Kissin, Y. V. 1998. "Catagenesis of Light Aromatic Compounds in Petroleum." *Organic Geochemistry* 29 (4): 947–62.
- Kissin, Y. V. 1998. "Primary Products in Hydrocarbon Cracking over Solid Acidic Catalysts under Very Mild Conditions: Relation to Cracking Mechanism." *Journal of Catalysis* 180 (1): 101–5.
- Klein, C., Hurlbut C. S., and J. D. Dana. 2002. *The 22nd Edition of the Manual of Mineral Science: (after James D. Dana)*. J. Wiley. pp. 647
- Kloster, S., J. Feichter, E. Maier-Reimer, K. D. Six, P. Stier, and P. Wetzel. 2006. "DMS cycle in the marine ocean-atmosphere system? A global model study." *Biogeosciences* 3 (1): 29–51.

- Kluge, T., T. Marx, D. Scholz, S. Niggemann, A. Mangini and W. Aeschbach-Hertig. 2008. A new tool for palaeoclimate reconstruction: Noble gas temperatures from fluid inclusions in speleothems. *Earth and Planetary Science Letters*, 269 (3-4): 407-414.
- Koh, Dong-Chan, L. N. Plummer, E. Busenberg, and Y. Kim. 2007. "Evidence for Terrigenous SF₆ in Groundwater from Basaltic Aquifers, Jeju Island, Korea: Implications for Groundwater Dating." *Journal of Hydrology* 339 (1-2): 93-104.
- Köhler, J., Konnerup-Madsen J. and G. Markl. 2008. "Fluid Geochemistry in the Ivigtut Cryolite Deposit, South Greenland." *Lithos* 103 (3-4): 369-92.
- Konnerup-Madsen, J., Rose-Hansen, J. and E. Larsen. 1979. "Hydrocarbon-Rich Fluid Inclusions in Minerals from the Alkaline Ilimaussaq Intrusion, South Greenland." *Schweizerische Mineralogische Und Petrographische Mitteilungen* 102: 642-53.
- Koritnig, S. 1951. "Ein Beitrag zur Geochemie des Fluor: (mit besonderer Berücksichtigung der Sedimente)." *Geochimica et Cosmochimica Acta* 1: 89-116.
- Kotte, K., F. Löw, S. G. Huber, T. Krause, I. Mulder, and H. F. Schöler. 2012. "Organohalogen Emissions from Saline Environments – Spatial Extrapolation Using Remote Sensing as Most Promising Tool." *Biogeosciences* 9 (3): 1225-35.
- Kranz, R., 1966. *Organische Fluor-Verbindungen in den Gaseinschlüssen der Wölsendörfer Flußspäte*. Die Naturwissenschaften, 23: 593-599.
- Krause, T., C. Tubbesing, K. Benzing, and H. F. Schöler. 2013. "Model Reactions and Natural Occurrence of Furans from Hypersaline Environments." *Biogeosciences Discussions* 11: 2871-2882.
- Krause, T., 2014. "Natural Occurrence of Volatile Mono-/Polyhalogenated Amd Aromatic/Heteroaromatic Hydrocarbons in Hypersaline Environments." Dissertation. University of Heidelberg.
- Krause, Torsten. 2014. "Natural Occurrence of Volatile Mono-/Polyhalogenated Amd Aromatic/Heteroaromatic Hydrocarbons in Hypersaline Environments." Dissertation.
- Krieger, Nadine. 2014. "Analyse von Fluid Inclusions in Permischen Notenliniensalzen aus dem Werra-Kalirevier." Master thesis, Universität Heidelberg.
- Kumar, R., I. F. Jefferson, K. O'Hara-Dhand, and I. J. Smalley, I.J. 2006. Controls on quartz silt formation by crystalline defects. *Naturwissenschaften*, 93(4): 185-188.
- Lamprecht, D., Dancuart L.P. and K. Harrilall. 2007. "Performance Synergies between Low-Temperature and High-Temperature Fischer-Tropsch Diesel Blends." *Energy & Fuels* 21 (5): 2846-52.
- Langmuir, D. 1997. *Aqueous Environmental Geochemistry*. Uppaer Saddle River: Prentice Hall, pp. 600.
- Leary, G. J. 1980. "Quinone Methides and the Structure of Lignin." *Wood Science and Technology* 14 (1): 21-34.
- Leeuw, A. de, K. Bukowski, W. Krijgsman, and K. F. Kuiper. 2010. "Age of the Badenian Salinity Crisis; Impact of Miocene Climate Variability on the Circum-Mediterranean Region." *Geology* 38 (8): 715-18.
- Lide, D. R. 2005. *CRC Handbook of Chemistry and Physics, Internet Version 2005*. Boca Raton, FL: CRC Press.
- Liu, X.-M., and R. L. Rudnick. 2011. "Constraints on Continental Crustal Mass Loss via Chemical Weathering Using Lithium and its Isotopes." *Proceedings of the National Academy of Sciences* 108 (52): 20873-80.

- Loeppert, R. H., and W. P. Inskeep. 1996. "Chapter 23 - Iron." In *Methods of Soil Analysis. Part 3 - Chemical Methods.*, Sparks, D.L. (ed.):xxi + 1390 pp. Soil Science Society of America Book Series 5. Madison, Wisconsin, USA: Soil Science Society of America.
- Lomans, B. P., A. Smolders, L. M. Intven, A. Pol, De Op, and C. van der Drift. 1997. "Formation of Dimethyl Sulfide and Methanethiol in Anoxic Freshwater Sediments." *Applied and Environmental Microbiology* 63 (12): 4741–47.
- López, Nancy I., and Carlos M. Duarte. 2004. "Dimethyl Sulfoxide (DMSO) Reduction Potential in Mediterranean Seagrass (*Posidonia Oceanica*) Sediments." *Journal of Sea Research* 51 (1): 11–20.
- Lüders, V., B. Plessen, and R. di Primio. 2012. Stable carbon isotopic ratios of CH₄-CO₂-bearing fluid inclusions in fracture-fill mineralization from the Lower Saxony Basin (Germany) - A tool for tracing gas sources and maturity. *Marine and Petroleum Geology* 30: 174-183.
- Markl, G. 2004. *Minerale und Gesteine - Mineralogie – Petrologie – Geochemie*. 1st ed. München: Elsevier, pp. 355.
- Markl, Gregor. 2004. *Minerale und Gesteine - Mineralogie – Petrologie – Geochemie*. 1st ed. München: Elsevier. pp. 355.
- Martens, D. A., and K. L. Loeffelmann. 2003. "Soil Amino Acid Composition Quantified by Acid Hydrolysis and Anion Chromatography–Pulsed Amperometry." *Journal of Agricultural and Food Chemistry* 51 (22): 6521–29.
- Mathez, E. A., and J. D. Webster. 2005. "Partitioning Behavior of Chlorine and Fluorine in the System Apatite-Silicate Melt-Fluid." *Geochimica et Cosmochimica Acta* 69 (5): 1275–86.
- McCollom, Thomas M., and J. S. Seewald. 2006. "Carbon Isotope Composition of Organic Compounds Produced by Abiotic Synthesis under Hydrothermal Conditions." *Earth and Planetary Science Letters* 243 (1–2): 74–84.
- McFarlane, D. J., and R. J. George. 1992. "Factors Affecting Dryland Salinity in Two Wheat Belt Catchments in Western Australia." *Australian Journal of Soil Research* 30 (1): 85.
- Meinardi, S., I. J. Simpson, N. J. Blake, D. R. Blake, and F. S. Rowland. 2003. "Dimethyl Disulfide (DMDS) and Dimethyl Sulfide (DMS) Emissions from Biomass Burning in Australia." *Geophysical Research Letters* 30 (9): 1454.
- Meinecke, J. L. G. 1823. "Ueber den Antheil, welchen der Erdboden an den meteorischen Processen nimmt." In *Journal für Chemie und Physik*, 38:194–228. Nürnberg: Schrag'sche Buchhandlung.
- Miller, B.R., R.F. Weiss , P. K. Salameh , T. Tanhua , B. R. Greally ,J. Mühle , and P. G. Simmonds. 2008. "Medusa: A sample preconcentration and GC/MS detector system for in situ measurements of atmospheric trace halocarbons, hydrocarbons, and sulfur compounds." *Analytical Chemistry*, 80(5): 1536-1545.
- Montzka, S. A., J. H. Butler, B. D. Hall, D. J. Mondeel, and J. W. Elkins. 2003. "A Decline in Tropospheric Organic Bromine." *Geophysical Research Letters* 30 (15): 1826.
- Moore, R. M. 2003. "Marine Sources of Volatile Organohalogens." In *Natural Production of Organohalogen Compounds*, edited by G. Gribble, 85–101. *The Handbook of Environmental Chemistry 3P*. Springer Berlin Heidelberg.
- Mühle, J., A. L. Ganesan, B. R. Miller*, P. K. Salameh, C. M. Harth, B. R. Greally, M. Rigby, L. W. Porter, L. P. Steele, C. M. Trudinger, P. B. Krummel, S. O'Doherty, P. J. Fraser, P. G. Simmonds, R. G. Prinn, and

- R. F. Weiss. 2010. Perfluorocarbons in the global atmosphere: tetrafluoromethane, hexafluoroethane, and octafluoropropane. *Atmospheric Chemistry and Physics*, 10(11): 5145-5164.
- Munz, I. A. 2001. "Petroleum Inclusions in Sedimentary Basins: Systematics, Analytical Methods and Applications." *Lithos, Fluid Inclusions: Phase Relationships - Methods - Applications. A Special Issue in honour of Jacques Touret*, 55 (1-4): 195-212.
- Neyens, E., and J. Baeyens. 2003. "A Review of Classic Fenton's Peroxidation as an Advanced Oxidation Technique." *Journal of Hazardous Materials* 98 (1-3): 33-50.
- Nolting, F., W. Behnke, C. Zetzsch. 1988. A Smog Chamber for Studies of the Reactions of Terpenes and Alkanes with Ozone and OH. *Journal of Atmospheric Chemistry*, 6 (1-2): 47-59.
- Okazoe, T. 2009. "Overview on the History of Organofluorine Chemistry from the Viewpoint of Material Industry." *Proceedings of the Japan Academy. Series B, Physical and Biological Sciences* 85 (8): 276-89.
- Parnell, J., Baron M., and H. Wycherley. 2006. "The Potential for Survival of Organic Matter in Fluid Inclusions at Impact Sites." In *Biological Processes Associated with Impact Events*, edited by C. Cockell, I. Gilmour, and C. Koeberl, 1-20. *Impact Studies*. Springer Berlin Heidelberg.
- Piccolo, A.. 2002. "The Supramolecular Structure of Humic Substances: A Novel Understanding of Humus Chemistry and Implications in Soil Science." In *Advances in Agronomy, Volume 75:57-134*. Academic Press.
- Plessen, B. and V. Lüders. 2012. Simultaneous measurements of gas isotopic compositions of fluid inclusion gases (N₂, CH₄, CO₂) using continuous-flow isotope ratio mass spectroscopy. *Rapid communications in Mass Spectrometry* 26: 1157-1161.
- Potter, J., and J. Konnerup-Madsen. 2003. "A Review of the Occurrence and Origin of Abiogenic Hydrocarbons in Igneous Rocks." *Geological Society, London, Special Publications* 214 (1): 151-73.
- Potter, Joanna, Andrew H. Rankin, Peter J. Treloar, Valentin A. Nivin, Wupao Ting, and Pei Ni. 1998. "A Preliminary Study of Methane Inclusions in Alkaline Igneous Rocks of the Kola Igneous Province, Russia: Implications for the Origin of Methane in Igneous Rocks." *European Journal of Mineralogy* 10 (6): 1167-80.
- Reed, M.H. 1997. "Hydrothermal Alteration and Its Relationship to Ore-Deposits." In *Geochemistry of Ore Forming Fluids, Volume 1*, Barnes, H.L. (ed.):303-66. New York: Wiley.
- Rhew, R. C., B. R. Miller, and R. F. Weiss. 2000. "Natural Methyl Bromide and Methyl Chloride Emissions from Coastal Salt Marshes." *Nature* 403 (6767): 292-95.
- Rinnan, R., M. Steinke, T. McGenity, and F. Loreto. 2014. "Plant Volatiles in Extreme Terrestrial and Marine Environments." *Plant, Cell & Environment*, May, n/a - n/a.
- Risacher F. and B. Fritz. 2000. "Bromine Geochemistry of Salar de Uyuni and Deeper Salt Crusts, Central Altiplano, Bolivia." *Chemical Geology* 167: 373-92.
- Roedder, E., 1984. Fluid inclusions. *Mineralogical Society of America Reviews in Mineralogy*, 12.
- Roedder, Edwin. 1962. "Studies of Fluid Inclusions; Part 1, Low Temperature Application of a Dual-Purpose Freezing and Heating Stage." *Economic Geology* 57 (7): 1045-61.
- Roedder, Edwin. 1984. "The Fluids in Salt." *American Mineralogist* 69 (5-6): 413-39.
- Rossberg, M., Lendle W, Pfleiderer G., Tögel, A., Dreher E.L., Langer E., and H. Rassaerts. 2000. "Chlorinated Hydrocarbons." In *Ullmann's Encyclopedia of Industrial Chemistry*. Wiley-VCH Verlag.

- Ruecker, A., P. Weigold, S. Behrens, M. Jochmann, J. Laaks, and A. Kappler. 2014. "Predominance of Biotic over Abiotic Formation of Halogenated Hydrocarbons in Hypersaline Sediments in Western Australia." *Environmental Science & Technology* 48 (16): 9170–78.
- Ruiz-Herrera, J., and R. L. Starkey. 1970. "Dissimilation of Methionine by *Achromobacter starkeyi*1." *Journal of Bacteriology* 104 (3): 1286–93.
- Russell, M. J., A. J. Hall, and W. Martin. 2010. "Serpentinization as a Source of Energy at the Origin of Life." *Geobiology* 8 (5): 355–71. doi:10.1111/j.1472-4669.2010.00249.x.
- Salmon, Elodie, Paul-Marie Marquaire, Françoise Behar, François Lorant, and Patrick G. Hatcher. 2009. "Early Maturation Processes in Coal. Part 1: Pyrolysis Mass Balances and Structural Evolution of Coalified Wood from the Morwell Brown Coal Seam." CERN Document Server. March 31. <http://cds.cern.ch/record/1169721>.
- Salvi, S., and A. E. Williams-Jones. 2003. Bulk analysis of volatiles in fluid inclusions. In: Samson, I., Anderson, A., Marshall, D. (Eds.), *Fluid Inclusions - Analysis and Interpretation*. Short Course Series. Mineralogical Association of Canada, Vancouver, pp. 247-278.
- Samson, I., Anderson, A., Marshall, D. (Eds.), 2003. *Fluid Inclusions - Analysis and Interpretations*. Short Course Series Volume, 32. Mineralogical Association of Canada, Vancouver, British Columbia, Canada.
- Scarsi, P. 2000. "Fractional extraction of helium by crushing of olivine and clinopyroxene phenocrysts: Effects on the (HE)-H-3/He-4 measured ratio." *Geochimica Et Cosmochimica Acta*, 64(24): 4263-4263.
- Schäfer, H., N. Myronova, and R. Boden. 2010. "Microbial Degradation of Dimethylsulphide and Related C1-Sulphur Compounds: Organisms and Pathways Controlling Fluxes of Sulphur in the Biosphere." *Journal of Experimental Botany* 61 (2): 315–34.
- Scheidegger, Y., M. Brennwald, V. Heber, R. Wieler, and R. Kipfer. 2006. „A first convincing step towards the application of dissolved noble gases in speleothem fluid inclusions to determine local meteorological conditions in caves." *Austria Geophysical Research Abstracts*, Vol. 8, 04382
- Schidlowski, Manfred. 1988. "A 3,800-Million-Year Isotopic Record of Life from Carbon in Sedimentary Rocks." *Nature* 333 (6171): 313–18.
- Schloemer, S., and B. M. Krooss. 2004. "Molecular Transport of Methane, Ethane and Nitrogen and the Influence of Diffusion on the Chemical and Isotopic Composition of Natural Gas Accumulations." *Geofluids* 4 (1): 81–108.
- Schmedt auf der Günne, J., M. Mangstl, and F. Kraus. 2012. "Elementares Fluor F₂ in der Natur – In-situ-Nachweis und Quantifizierung durch NMR-Spektroskopie." *Angewandte Chemie* 124 (31): 7968–71.
- Schöler, H. F., and F. Keppler. 2005. "Abiotic Formation of Organohalogens During Early Diagenetic Processes." In *Natural Production of Organohalogen Compounds*, edited by G. Gribble, 63–84. *The Handbook of Environmental Chemistry*. Springer.
- Schreiber, U., Locker-Grütjen O., and C. Mayer. 2012. "Hypothesis: Origin of Life in Deep-Reaching Tectonic Faults." *Origins of Life and Evolution of the Biosphere: The Journal of the International Society for the Study of the Origin of Life* 42 (1): 47–54.
- Schutter, S. R. 2003. "Occurrences of Hydrocarbons in and around Igneous Rocks." Geological Society, London, Special Publications 214 (1): 35–68.
- Segal, W., and R. L. Starkey. 1969. "Microbial Decomposition of Methionine and Identity of the Resulting Sulfur Products." *Journal of Bacteriology* 98 (3): 908–13.

- Seward, T.M., and H.L. Barnes. 1997. "Metal Transport by Hydrothermal Ore Fluids." In *Geochemistry of Ore Forming Fluids, Volume 1*, Barnes, H.L. (ed.):303–66. New York: Wiley.
- Sherwood Lollar, B., S. K. Frape, S. M. Weise, P. Fritz, S. A. Macko, and J. A. Welhan. 1993. "Abiogenic Methanogenesis in Crystalline Rocks." *Geochimica et Cosmochimica Acta* 57 (23–24): 5087–97.
- Sherwood Lollar, B., T. D. Westgate, J. A. Ward, G. F. Slater, and G. Lacrampe-Couloume. 2002. "Abiogenic Formation of Alkanes in the Earth's Crust as a Minor Source for Global Hydrocarbon Reservoirs." *Nature* 416 (6880): 522–24.
- Sherwood Lollar, B., G. Lacrampe-Couloume, G. F. Slater, J. Ward, D. P. Moser, T. M. Gihring, L. -H. Lin, and T. C. Onstott. 2006. "Unravelling Abiogenic and Biogenic Sources of Methane in the Earth's Deep Subsurface." *Chemical Geology, Special Issue in Honour of R.K. O'Nions*, 226 (3–4): 328–39.
- Siegemund, G., Schwertfeger W., Feiring A., Smart B., Behr F., Vogel H., and B. McKusick. 2000. "Fluorine Compounds, Organic." In *Ullmann's Encyclopedia of Industrial Chemistry*. Wiley-VCH
- Siekman, F., 2008. Freisetzung von photolabilen und reaktiven Halogenverbindungen aus salzhaltigen Aerosolen unter simulierten troposphärischen Reinluftbedingungen in einer Aerosol-Smogkammer. PhD Thesis, University of Bayreuth, Bayreuth.
- Sievert, S., R. Kiene, and H. Schulz-Vogt. 2007. "The Sulfur Cycle." *Oceanography* 20 (2): 117–23.
- Simo, R., C. Pedros-Alio, G. Malin, and J. O. Grimalt. 2000. "Biological Turnover of DMS, DMSP and DMSO in Contrasting Open-Sea Waters." *Marine Ecology Progress Series* 203: 1–11.
- Sive, B. C., Y. Zhou, D. Troop, Y. Wang, W. C. Little, O. W. Wingenter, R. S. Russo, R. K. Varner, and R. Talbot. 2005. "Development of a cryogen-free concentration system for measurements of volatile organic compounds." *Analytical Chemistry*, 77 (21): 6989-6998.
- Smith, Neil A., and Don P. Kelly. 1988. "Mechanism of Oxidation of Dimethyl Disulphide by *Thiobacillus Thioparus* Strain E6." *Journal of General Microbiology* 134 (11): 3031–39.
- Sposito, G. 1989. *The Chemistry of Soils*. Oxford University Press. pp. 317.
- Stan-Lotter, H., M. Pfaffenhuemer, A. Legat, H.-J. Busse, C. Radax, and C. Gruber. 2002. "Halococcus Dombrowskii Sp. Nov., an Archaeal Isolate from a Permian Alpine Salt Deposit." *International Journal of Systematic and Evolutionary Microbiology* 52 (5): 1807–14.
- Stasiuk, L. D., and L. R. Snowdon. 1997. "Fluorescence Micro-Spectrometry of Synthetic and Natural Hydrocarbon Fluid Inclusions: Crude Oil Chemistry, Density and Application to Petroleum Migration." *Applied Geochemistry* 12 (3): 229–41.
- Statista. 2014. "Streusalz-Verbrauch Auf Straßen in Deutschland | Statistik." Accessed October 18. <http://de.statista.com/statistik/daten/studie/282120/umfrage/streusalz-verbrauch-auf-deutschen-strassen/>.
- Staubes, R., H.-W. Georgii, and G. Ockelmann. 1989. "Flux of COS, DMS and CS₂ from Various Soils in Germany." *Tellus B* 41B (3): 305–13.
- Stuedler, P. A., and B. J. Peterson. 1984. "Contribution of Gaseous Sulphur from Salt Marshes to the Global Sulphur Cycle." *Nature* 311 (5985): 455–57.
- Stoiber, R.E., D.C. Leggett, T.F. Jenkins, R.P. Murrmann, and W.I.Jr. Rose. 1971. "Organic Compounds in Volcanic Gas from Santiaguito Volcano, Guatemala." *Geological Society of America Bulletin* 82 (8): 2299–2302.

- Strlič, Matija, Jana Kolar, Vid-Simon Šelih, Drago Kočar, and Boris Pihar. 2003. "A Comparative Study of Several Transition Metals in Fenton-like Reaction Systems at Circum-Neutral pH." *Acta Chimica Slovenica* 50: 633–44.
- Sutton, Rebecca, and Garrison Sposito. 2005. "Molecular Structure in Soil Humic Substances: The New View." *Environmental Science & Technology* 39 (23): 9009–15.
- Svensen, H., S. Planke, A. G. Polozov, N. Schmidbauer, F. Corfu, Y. Y. Podladchikov, and B. Jamtveit. 2009. "Siberian Gas Venting and the End-Permian Environmental Crisis." *Earth and Planetary Science Letters* 277 (3–4): 490–500.
- Tang, Q., M. Zhang, C. Li, M. Yu, and L. Li. 2013. "The Chemical Compositions and Abundances of Volatiles in the Siberian Large Igneous Province: Constraints on Magmatic CO₂ and SO₂ Emissions into the Atmosphere." *Chemical Geology* 339 (February): 84–91.
- Thomas, R., J. D. Webster, and W. Heinrich. 2000. "Melt Inclusions in Pegmatite Quartz: Complete Miscibility between Silicate Melts and Hydrous Fluids at Low Pressure." *Contributions to Mineralogy and Petrology* 139 (4): 394–401.
- Ubl, M. 2011. "Methodenentwicklung Zur Quantitiven Bestimmung Flüchtiger Organischer Verbindungen Aus Gestein." B.Sc. Thesis. Rupert-Karls Universität Heidelberg.
- Van den Kerkhof, A. M., and U. F. Hein. 2001. "Fluid Inclusion Petrography." *Lithos, Fluid Inclusions: Phase Relationships - Methods - Applications. A Special Issue in honour of Jacques Touret*, 55 (1–4): 27–47.
- Vanholme, Ruben, Brecht Demedts, Kris Morreel, John Ralph, and Wout Boerjan. 2010. "Lignin Biosynthesis and Structure." *Plant Physiology* 153 (3): 895–905.
- Veksler, Ilya V. 2004. "Liquid Immiscibility and Its Role at the Magmatic–hydrothermal Transition: A Summary of Experimental Studies." *Chemical Geology, The magmatic to hydrothermal transition and its bearing on ore-forming processes*, 210 (1–4): 7–31.
- Vignerresse, J. L. 2009. "Evaluation of the Chemical Reactivity of the Fluid Phase through Hard–soft Acid–base Concepts in Magmatic Intrusions with Applications to Ore Generation." *Chemical Geology, Halogens in Volcanic Systems and Their Environmental Impacts*, 263 (1–4): 69–81.
- Volk, H. D. Fuentes, A. Fuerbach, C. Miese, W. Koehler, N. Bärsch, S. Barcikowski. 2010. "First on-line analysis of petroleum from single inclusion using ultrafast laser ablation." *Organic Geochemistry*, 41 (2): 74–77.
- von Rohden, C., A. Kreuzer, Z. Chen, and W. Aeschbach-Hertig, W., 2010. „Accumulation of natural SF₆ in the sedimentary aquifers of the North China Plain as a restriction on groundwater dating." *Isotopes in Environmental and Health Studies*, 46(3): 279–290.
- Warneck, P. 2000. "Chemistry of the Natural Atmosphere." San Diego: Academic Press. pp. 927.
- Warneck, P. and J. Williams. 2012. "The Atmospheric Chemist's Companion: Numerical Data for Use in the Atmospheric Sciences." Heidelberg: Springer. pp. 436.
- Warren, J. K. 2006. "Evaporites: Sediments, Resources and Hydrocarbons: Sediments, Resources, and Hydrocarbons." Heidelberg: Springer. pp: 943.
- Watts, Simon F. 2000. "The Mass Budgets of Carbonyl Sulfide, Dimethyl Sulfide, Carbon Disulfide and Hydrogen Sulfide." *Atmospheric Environment* 34 (5): 761–79.

- Weaver, John D. 1984. "Preparation of Antimony Trifluorodichloride and Fluorination of Fluorinatable Hydrocarbons and Halocarbons Therewith." US Patent 4438088.
- Webster, J. D., J. R. Holloway, and R. L. Hervig. 1987. "Phase Equilibria of a Be, U and F-Enriched Vitrophyre from Spor Mountain, Utah." *Geochimica et Cosmochimica Acta* 51 (3): 389–402.
- Wedepohl, H. K. 1995. "The Composition of the Continental Crust." *Geochimica et Cosmochimica Acta* 59 (7): 1217–32.
- Weissflog, L., C. A. Lange, A. Pfennigsdorff, K. Kotte, N. Elansky, L. Lisitzyna, E. Putz, and G. Krueger. 2005. "Sediments of Salt Lakes as a New Source of Volatile Highly Chlorinated C1/C2 Hydrocarbons." *Geophysical Research Letters* 32 (1): L01401.
- Welhan, John A. 1988. "Origins of Methane in Hydrothermal Systems." *Chemical Geology, Origins of Methane in the Earth*, 71 (1–3): 183–98.
- Werdin-Pfisterer, Nancy R., Knut Kielland, and Richard D. Boone. 2009. "Soil Amino Acid Composition across a Boreal Forest Successional Sequence." *Soil Biology and Biochemistry* 41 (6): 1210–20.
- Wieser, M. 2010. "Imprints of Climatic and Environmental Change in a Regional Aquifer System in an Arid Part of India Using Noble Gases and Other Environmental Tracers." Dissertation. University of Heidelberg.
- Wignall, P. B. 2007. "The End-Permian Mass Extinction – How Bad Did It Get?" *Geobiology* 5 (4): 303–9.
- Wilcox, W. R. 1968. "Removing Inclusions from crystals by gradient techniques." *Industrial & Engineering Chemistry* 60 (3): 12–23.
- Wishkerman A and S. Gebhardt. 2008. "Abiotic Methyl Bromide Formation from Vegetation, and Its Strong Dependence on Temperature." *Environmental Science & Technology* 42 (18): 6837–42.
- Yanagi, T. 2011. "Chemical Composition of Continental Crust and the Primitive Mantle." In *Arc Volcano of Japan*, 9–17. Lecture Notes in Earth Sciences. Heidelberg: Springer. pp. 136.
- Yang, S F, and N E Hoffman. 1984. "Ethylene Biosynthesis and Its Regulation in Higher Plants." *Annual Review of Plant Physiology* 35 (1): 155–89.
- Yang, Z., L. Kong, J. Zhang, L. Wang, and S. Xi. 1998. "Emission of Biogenic Sulfur Gases from Chinese Rice Paddies." *Science of the total Environment* 224 (1–3): 1–8.
- Zhang, Z., P. Greenwood, Q. Zhang, D. Rao, and W. Shi. 2012. "Laser ablation GC-MS analysis of oil-bearing fluid inclusions in petroleum reservoir rocks." *Organic Geochemistry*, 43: 20-25.
- Zimm, B. H., and J. E. Mayer. 1944. "Vapor Pressures, Heats of Vaporization, and Entropies of Some Alkali Halides." *The Journal of Chemical Physics* 12 (9): 362–69.
- Zinder, S. H., and T. D. Brock. 1978. "Methane, Carbon Dioxide, and Hydrogen Sulfide Production from the Terminal Methyl Group of Methionine by Anaerobic Lake Sediments." *Applied and Environmental Microbiology* 35 (2): 344–52

6

Appendix

Table 6.1 –part 1/3: List of available samples.

sample #	other #	source	location	Lithological remarks	GPS-coordinates	
F1PS	-	1	unknown;	banded green-violet with altered granite	n/a	n/a
F2PS	-	1	Mine Hermine, Lissenthau, Germany	banded green-white, sawn specimen	N49°26'24.778"	E12°6'53.948"
F3PS	-	1	Mine Hermine, Lissenthau, Germany	banded green-white, untreated	N49°26'24.778"	E12°6'53.948"
F4PS	-	1	Wölsendorf, Marienschacht, Germany	banded cream, green, dark blue to violet color	N49°24'25.421"	E12°10'53.841"
Q1PS	-	1	Fichtelgebirge, Germany	bulky mass of small crystals	n/a	n/a
G01MW	R01	2	Cambay Basin, Eklara, India	granite, outcrop	N 23°44'55.74"	E 72°48'56.52"
G02MW	R02	2	Cambay Basin, Recharge, India	granite, outcrop	N 23°49'58.20"	E 72°58'40.98"
G03MW	R03*	2	Cambay Basin, Gozharla, India	schist from local debris	N 23°29'28.32"	E 72°34'5.09"
G04MW	R03	2	Cambay Basin, India	limestone from local debris	N 23°54'30.72"	E 73° 4'46.44"
H1Elt	Elton	3	Lake Elton	single crystals 2-3 mm in aggregates of up to 5 cm thickness	N49° 8' 59.28"	E46° 47' 18.12"
H2Elt	Elton II	3	Lake Elton	2-3mm single crystals skimmed under 10 cm of lake water	N49° 8' 59.28"	E46° 47' 18.12"
H3Elt	Elton III	3	Lake Elton	similar to H1Elt with visible dispersed organic matter	N49° 8' 59.28"	E46° 47' 18.12"
H4Elt	Elton III Kruste	3	Lake Elton	crust with thickness of of 1-4 cm on layer of organic matter	N49° 8' 59.28"	E46° 47' 18.12"
H5Elt	Elton III Kruste OM	3	Lake Elton	crust with thickness of of 1-4 cm	N49° 8' 59.28"	E46° 47' 18.12"
H6Kas	Kasin I	3	Lake Kasin	single crystals up to 3 mm and aggregates of up to 3 cm thickness	N47° 36' 9.66"	E47° 27' 7.14"
H7Kas	Kasin I Kruste (1-3cm)	3	Lake Kasin	crust with thickness of 1-3 cm	N47° 36' 9.66"	E47° 27' 7.14"
G1Bas	Gips Bas II-1 (Rosen)	3	Lake Bakuntschak	lense shaped	N48° 14' 25.86"	E48° 49' 30.9"
G2Bas	Gips Bas II-2 (Streifen)	3	Lake Bakuntschak	elongated bars	N48° 14' 25.92"	E48° 49' 30.96"
H26Bas	Bas III	3	Lake Bakuntschak	crust with dissolution patterns and single crystal shapes in aggregate up to 4mm	N48° 14' 37.98"	E46° 49' 51.78"
H8SND	Sebkah Te-n-Dghamcha	4	Sebkah N'Drancha XIV	cauliflour-shaped efflorescence	N 18°51'03.1"	W 15°39'01.8"
H9SND	Sebkah Te-n-Dghamcha	4	Sebkah N'Drancha VI	crust of fine grained salt crystals, undulated surface, brown organic matter on bottom side	N 18°53'23.6"	W 15°39'42.9"
H10SND	Sebkah Te-n-Dghamcha	4	Sebkah N'Drancha VIII	aggregates of 1 mm large crystals, slight rose-tint	N 18°51'14.7"	W 15°38'23.3"
H11SND	Sebkah Te-n-Dghamcha	4	Sebkah N'Drancha IX	crust of fine-grained halite crystals, thin organic matter at bottom, fine gypsum needles interspersed	N 18°51'10.2"	W 15°38'23.7"

Table 6.1 – part 2/3: List of available samples.

sample #	other #	source	location	Lithological remarks	GPS-coordinates	
H12SND	Sebkah Te-n-Dghamcha	4	Sebkah N'Drancha X	crust of fine-grained crstals	N 18°51'0.71''	W 15°38'29.0''
H13Doue	Douemina I	4	Douemina I	inhomogenous, with crustal aggregates of 4mm large crystals, some aggregated dark from organic matter, white, brown, rose and transparent	N 19°52'22.7''	W 16°14'03.2''
H14SP	Sua Pan I	4	Sua Pan I	pieces of thin crust (up to 0.5mm)	S20° 27' 12"	E25° 55' 36"
H15SP	Sua Pan 3 la	4	Sua Pan 3 la	pieces of thin crust (up to 0.5mm)	S20° 28' 57.18"	E26° 3' 41.4"
H16SP	Sua Pan 3 lb	4	Sua Pan 3 lb	crust thickness of 0,5-1 cm with ormatter at bottom side	S20° 28' 57.18"	E26° 3' 41.4"
H17WBSR	WBSR I	4	Walvis Bay salt refinery	refinery salt from evaporation pond	S23° 1' 52.38"	E14° 26' 38.52"
H18Boht	Bohtash	4	Bohtash, Botswana	spherical aggregates of 3 cm diameter, pink	n/a	n/a
H19Sib	"salt"	5	Siberia, Oblast Irkutsk, Russia	rock salt, unspecified borehole	n/a	n/a
H20Sib	"blue salt"	5	Siberia, Oblast Irkutsk, Russia	intensive blue color	n/a	n/a
H21Sib	194/7	5	Siberia, Oblast Irkutsk, Russia	rock salt, borehole 194	n/a	n/a
H22Sib	194/24	5	Siberia, Oblast Irkutsk, Russia	rock salt, borehole 194	n/a	n/a
H23Sib	194/3	5	Siberia, Oblast Irkutsk, Russia	rock salt, reported in Svensen et al. 2009, borehole 194	n/a	n/a
H24Sib	194/4	5	Siberia, Oblast Irkutsk, Russia	rock salt, reported in Svensen et al. 2009, borehole 194	n/a	n/a
H25Sib	215/4	5	Siberia, Oblast Irkutsk, Russia	rock salt, borehole 215	n/a	n/a
H27Gor	-	6	Schacht Gorleben	rock salt from around 600 m below surface, orange color	N53° 1' 35.292"	E11° 21' 1.364"
P01BB	R06-09	7	Bratsk, Siberia	dolerite, magnetic grain fraction	N56° 16' 57.698"	E101° 54' 59.393"
P02BB	R06-09	7	Bratsk, Siberia	dolerite, slightly magnetic grain fraction	N56° 16' 57.698"	E101° 54' 59.393"
P03BB	R06-09	7	Bratsk, Siberia	dolerite, coarse rock fragments	N56° 16' 57.698"	E101° 54' 59.393"
MORB	-	8	synthetic	Mid Ocean Ridge Basalt, synthesis according to appended protocol	-	-
H28Lht	Lht-2	9	Bochnia Mine, poland	rock salt	N49°58'13.0"	E20°25'54.7"
H29WG	WG-3	9	Wieliczka Mine, Poland	rock salt	N49° 59' 5.52"	E20° 3' 23.94"
H30WG	WG-5	9	Wieliczka Mine, Poland	rock salt	N49° 59' 5.52"	E20° 3' 23.94"
H31WG	WG-6	9	Wieliczka Mine, Poland	rock salt	N49° 59' 5.52"	E20° 3' 23.94"
H37LSF	LSF	10	Lake Springfield, Australia	salt crust	S32°27'42.41"	E119° 9'58.32"

Table 6.1 – part 3/3: List of available samples.

sample #	other #	source	location	Lithological remarks	GPS-coordinates
H38LW	LW	10	Lake Whurr, Australia	salt crust	S33° 2'35.23" E119° 0'31.75"
H40LM	LM	10	Lake Magic Australia	salt crust	S32°25'58.69" E118°54'19.30"
H41LK	Lk1a	10	Lake King Australia	salt crust	S33° 5'20.44" E119°37'7.72"
H42LD	LD3	10	Lake Dune Australia	salt crust	S33° 4'58.58" E119°38'18.13"
H43LO	LO2	10	Lake Orr, Australia	salt crust	S34°14'50.84" E118°10'7.76"
H44Bol	SLT Spec-Jira, 0-2cm Kruste, 18.05.2011	11	Jirira, Salar de Uyuni, Bolivia	salt crust	S19°52'6.20" W67°33'40.40"
H45Bol	CO/o1-ENT, 0-2cm Kruste, 19.05.2011	11	Salar de Coipasa,	salt crust	S19°32'35.05" W68° 3'50.81"
HTV114	HTU114	12,13	Michelbach, Taunus, Germany	quartz veins with Pb-Zn-Cu ores, ages postvariscic (270-130Ma), homogenisation temperature 90-180°C, reported in Kimbauer et al., 2012	N50°12'37.286316 E8°2'11.757624
HTV115	HTU115	12,13	Naurod, Taunus, Germany	giant quartz veins, ages postvariscic (270-130Ma), homogenisation temperature 110-170°C, reported in Kimbauer et al., 2012	N50°9'28.4004 E8°2'15.5436
HTV116	HTU116	12,13	Usingen, Taunus, Germany	giant quartz veins, ages postvariscic (270-130Ma), homogenisation temperature 110-170°C, reported in Kimbauer et al., 2012	N50°20'53.172564 E8°33'39.113532
SM5	SM5	12	Schoemaker Crater, Australia	hydrothermal quartz	S25°51'28.08" E120°57'26.834"
SM6	SM6	12	Schoemaker Crater, Australia	hydrothermal quartz	S25°51'17.582" E120°57'26.96"
SM7	SM7	12	Schoemaker Crater, Australia	hydrothermal quartz	S25° 51'16.697" E120°57'26.748"
MU2	MU2	12	Muchison, Australia	hydrothermal quartz	S26° 52'9.995" E115°56'51.173"
MU4	MU4	12	Muchison, Australia	hydrothermal quartz	N26° 52'14.79" E115°56'50.154"
MU7	MU7	12	Muchison, Australia	hydrothermal quartz	N26°50'20.454" E115°56'27.748"

1 = private collector Günther Schönlein, Bamberg

2 = sampling campaign, Martin Wieser, University of Heidelberg

3 = own sampling campaign, University of Heidelberg, DFG project 763

4 = sampling campaign Stefan Huber, University of Heidelberg, DFG project 763

5 = sampling campaign Henrik Svenson, University of Oslo, Norway

6 = own sample, private collection

7 = provided by Benjamin Black, Massachusetts Institute of Technology, Cambridge, USA

8 = provided by Stefan Dultz, University of Heidelberg

9 = provided by Marek Dulinski/Krzysztof Bukowski, AGH University of Science and Technology, Krakow

10 = sampling campaign Torsten Krause/HF Schöler, University of Heidelberg, DFG project 763

11 = sampling campaign, Kasten Kotte, University of Heidelberg, DFG project 763

12 = sampling campaigns by Ulrich Schreiber, Universität Duisburg-Essen

13 = sampling campaigns by Thomas Kirnbauer, Universität Bochum

Table 6.2: Volatile compounds from mixed mineral and rock samples 12/2009-08/2010.

	carbon tetrafluoride	sulfur hexafluoride	carbonylsulfide	methyl chloride	isobutene	1,3-butadiene	trans-2-butene	carbon disulfide	benzene	comment
	relative peak intensity (kCounts)									
MORB 300rpm 10 min	-	-	-	-	-	-	-	-	-	- decfluorbutane?
P01BB 8.49 g	-	-	454549	-	-	-	-	33439	62481	Xenon peak in control
P02BB	-	-	71621	565	-	-	-	-	28417	Xenon peak in control
P03BB	-	-	327982	4190	-	-	247750	170973	56309	Xenon peak in control
F1PS 10 min	1209	-	-	-	-	-	-	-	-	- decfluorbutane?
F4PS 15 g	20610	2568	-	5012	-	-	-	-	-	- arsine?
halite Kasin 15 g	-	-	-	31674	117605	9801	-	-	-	-

Table 6.3: Volatile compounds from halites and gypsum samples 04/2010, after grinding or heating to 150°C and in unground control (if detected). (Part of Bugla's BSc. thesis.)

	<i>carbonyl sulfide*</i>		<i>methyl chloride</i>		<i>isobutene[§]</i>		<i>chloroethene</i>	<i>methyl bromide</i>		<i>dichloroethane</i>		<i>bromoethane</i>	<i>chloroform</i>		<i>chlorobutane</i>	<i>tetrachloromethane</i>		<i>benzene</i>			
	ground	heated	ground	heated	ground	heated	heated	ground	heated	ground	heated	heated	ground	heated	heated	ground	heated	control	ground	heated	
	kcounts		ng [#]		kcounts		ng	kcounts		kcounts		kcounts		ng	kcounts		ng		ng		ng
H1EIt	0.5	-	12.9	-	-	15.0	-	-	0.9	-	-	-	-	-	-	-	-	-	3.9	-	5.8
H2EIt	-	-	2.6	195.7	-	6.0	-	-	6.9	-	-	13.1	-	-	2.6	-	-	-	4.6	4.4	5.7
H3EIt	0.2	1.1	22.1	4.8	-	29.0	4.5	-	-	-	-	-	6.3	-	-	-	-	-	4.6	-	8.2
H4EIt	-	0.6	5.2	320.5	0.3	4.6	-	-	0.3	-	-	-	-	2.2	-	-	-	-	4.3	-	7.5
H5EIt	-	4.0	3.5	0.4	-	15.5	-	-	0.4	-	-	0.3	-	9.1	4.9	-	0.2	-	-	-	11.7
H26Bas	2.8	-	33.6	17.3	9.3	11.5	-	-	-	-	-	-	-	-	8.3	-	-	-	4.3	6.7	4.7
H6Kas	1.9	0.3	20.3	137.4	4.7	3.9	-	-	0.4	-	0.3	-	5.4	-	-	-	-	-	-	8.8	5.5
H7Kas	0.3	0.1	3.5	-	1.4	0.0	-	-	-	-	-	-	-	-	-	-	-	-	4.1	5.1	4.5
H8SND	0.5	1.0	5.5	200.3	0.6	13.5	5.3	-	1.2	-	-	0.9	-	5.5	17.5	-	-	-	4.7	5.0	57.9
H9SND	-	-	3.2	16.2	-	0.0	-	-	-	-	-	-	-	5.3	1.4	-	-	-	4.4	4.4	4.8
H10SND	0.6	-	3.1	-	1.2	0.4	-	-	0.1	-	-	0.2	-	-	-	-	-	-	3.9	4.5	4.6
H11SND	0.6	-	3.0	-	3.1	3.4	-	-	-	-	-	-	-	-	-	-	-	-	5.6	4.8	4.7
H12SND	0.3	0.1	-	56.3	0.8	1.9	-	-	0.7	-	-	1.5	-	5.0	3.1	-	-	-	3.4	3.5	8.2
H13Doue	-	0.8	4.9	260.8	4.0	17.6	-	-	2.5	-	0.5	4.5	-	8.3	2.8	-	-	-	4.2	6.7	5.8
H14SP	-	0.4	-	8.1	0.0	15.4	4.8	-	-	-	-	-	-	-	-	-	-	-	4.0	4.5	6.6
H15SP	0.2	0.3	3.5	2.0	3.2	9.5	-	-	-	-	-	-	-	-	-	-	-	-	4.0	4.5	6.4
H16SP	-	-	-	6.4	0.0	25.0	5.6	-	-	-	-	-	-	-	-	-	-	-	-	3.9	7.2
H17WBSR	-	0.2	3.0	297.1	0.0	12.5	4.6	-	4.1	-	-	0.4	-	5.6	6.0	-	-	-	4.5	3.9	14.8
H18Boht	0.1	-	3.1	-	2.0	1.1	-	-	-	-	-	-	-	-	-	-	-	-	3.8	4.3	4.9
H19salt	-	-	-	65.8	0.0	1.0	-	-	3.0	-	-	0.5	-	5.4	-	-	-	-	-	-	4.7
H20Sib	0.9	-	14347.2	156.6	2.1	1.9	9.5	4.4	7.8	-	-	1.6	42.3	88.9	0.7	5.3	-	-	-	4.0	5.1
H21Sib	4.0	10.1	8.3	-	0.0	0.5	-	-	1.7	40.0	1.1	4.0	-	5.5	1.8	-	-	-	-	4.6	4.8
H22Sib	1.9	0.7	13.9	65.0	1.9	13.0	-	-	4.9	9.5	-	0.9	-	-	8.5	-	-	-	3.9	4.8	5.9
H23Sib	1.6	-	2.8	-	0.5	0.5	-	-	-	-	44.5	-	-	-	-	-	-	-	4.1	3.8	948.2
H24Sib	1.0	0.5	5.1	13.5	1.1	-	-	-	1.8	10.0	0.1	0.6	-	10.5	-	-	-	-	4.1	5.2	5.1
H25Sib	0.3	2.4	-	78.2	0.2	1.6	-	-	1.8	-	-	1.1	-	5.2	-	-	0.2	-	3.9	3.7	5.0
H27Gor	0.1	0.6	3.8	103.5	1.3	3.0	-	-	3.1	-	-	0.5	-	5.7	1.0	-	-	-	4.2	4.5	5.3
G1Bas	0.2	0.2	4.7	30.7	2.0	23.5	-	-	-	-	-	-	-	-	0.6	-	-	-	-	4.3	5.5
G2Bas	-	0.1	-	73.2	-	36.3	8.2	-	-	-	-	-	-	-	-	-	-	-	-	-	5.9

* small amounts partly found in unground sample

values above 50 ng outside of calibration

§ originally 2-butene assumed but later data with calibration standard suggest that isobutene is more likely

Table 6.4a: Volatile compounds from granites, fluorites and quartz 08/2011 (Marcus Ubl, BSc. thesis).

	sulfur hexafluoride	carbon tetrafluoride	xenon	carbonylsulfide	norfluorane	comments
	ng	ng	kcounts			
F1PS	-	64.27	-	✓	-	hydrocarbons
F2PS	0.17	2.89	16365	✓	-	benzene
F3PS	0.29	4.01	6958	-	-	
F4PS	1.31	9.62	7511	✓	-	hydrocarbons?
G01MS	-	1.69	7547	✓	-	
G02-ungewaschen	-	-	27591	-	✓	
G03MS	-	-	6803	-	✓	
G04MS	-	-	12623	-	✓	
Q01PS*	0.17	-	14298	✓	-	
H22	-	-	3519	-	✓	

Table 6.4b: Volatile compounds from fluorite and halite 11/2011.

	carbon tetrafluoride	sulfur hexafluoride	carbonylsulfide	methyl chloride	isobutene	1,3-butadiene	comments
	ng	ng	kcounts	ng	kcounts	kcounts	
F4PS	190.5	19.8	5817	61.7	-	-	recorded only till 22.5 min
H7Kas	-	-	6589	62.9	289466	61855	recorded only till 22.5 min, various hydrocarbons

Table 6.5: Results from halites 01/2012.

	carbonyl sulfide	methyl chloride	vinyl chloride	isobutene	1,3-butadiene	1-butene-3-yne	methyl bromide	trans-2-pentene	cis-2-pentene	cyclopentene	dimethyl sulfide	carbon disulfide	thiirane	ethynyl cyclopropane	1-chlorbutane	benzene	comment
	kcounts	ng	ng	ng	ng	kcounts	ng	kcounts	kcounts	kcounts	ng	kcounts	kcounts	kcounts	kcounts	kcounts	
	1167	0.13	-	0.81	0.98	30334	2.31	17103	55338	-	0.28	3734	105030	144023	2675	90751	
H2EIt		0.75	-	0.26	0.35	11702	-	13843	22946	1254	-	4045	-	170118	-	39265	
8SND	647	0.18	-	0.45	0.48	3855	-	8935	14921	-	-	-	187312	95131	-	20532	carbon tetrachloride
H16SP	1066	0.06	-	0.22	-	4141	-	18561	3989	-	-	-	28803	-	-	14302	dichloromethane
H26Bas	12282	2.59	0.03	0.06	1.24	-	-	-	-	28454	-	35327	-	-	11980	67688	bromobutane, 1-chloropentene thiophene?
H28Lkt	1793	0.03	-	0.60	0.39	5291	-	3036	3630	-	3.26	-	-	25382	6026	45871	methyl cyclohexane
H29WG	2202	0.24	-	1.16	0.60	9790	-	17881	19556	-	5.37	-	-	13	-	102014	strong dichloromethane
H37LSF	1420	0.02	-	1.70	2.21	-	-	37675	28408	-	-	-	58487	374973	-	88434	carbon tetrachloride
H38lw	8912	0.10	-	0.91	0.81	24440	-	36174	72014	-	-	-	84793	274631	-	29516	carbon tetrachloride
H40LM	0	0.01	-	0.59	1.30	26116	-	33116	8347	-	-	-	91209	100857	-	37155	carbon tetrachloride
H41LK	374	0.01	-	0.69	0.50	3	-	1	-	-	-	-	11039	145882	-	50530	
H42LD	817	0.04	-	1.51	1.53	12415	-	16477	25819	11620	-	-	-	223966	-	17235	2,3-pentadiene
H43LO	0	0.03	-	0.41	0.25	36418	-	19451	8658	-	-	-	12071	221734	-	65398	2,4-hexadiene
H44Bol	323	0.02	-	-	-	25410	-	19068	17783	-	-	-	3202	-	-	1155	
H45Bol	0	0.03	-	-	-	19518	-	22823	34336	-	-	-	1789	-	-	20031	

Table 6.6: Results from mixed samples 05-08/2012.

	carbon tetrachloride	sulfur hexafluoride	carbonylsulfide	methyl chloride	isobutene	1,3-butadiene	trans/cis-2-butene	1-butene-3-yne	methyl bromide	trans-2-pentene	carbon disulfide	ethynyl cyclopropane	n-hexane	2-chlorbutane	benzene	comment
	ng	ng	kcounts	ng	ng	ng	ng	kcounts	ng	kcounts	kcounts	kcounts	kcounts	kcounts	kcounts	
F4PS	3.17	21.12	13445	0.60	-	-	-	-	-	-	24305	-	-	-	-	13500 chromatographic quality low
quartz gravel	-	-	7776	0.04	1.588666	0.72	6.08	44865	2.46	-	-	17499	38668	1000	107970	thiophene?42min
G1Bas	-	-	2055	0.04	1.116419	0.12	4.26	2063	-	3883	-	-	-	-	-	17968 2,3-pentadiene, methyl cyclohexane, methylated alkane/alkene?

Table 6.7: Results from quartz 05-08/2012.

	carbonylsulfide	norfluorane	methyl chloride	vinylchloride	isobutene	1,3-butadiene	trans-2-butene	cis-2-butene	methyl bromide	carbon disulfide	trans-1,2-dichlorethene	1,1-dichlorethane	2-chlorbutane	chloroform	benzene	comment
	kcounts	kcounts	ng	ng	ng	ng	ng	ng	ng	kcounts	kcounts	ng	kcounts	ng	kcounts	
HTV114	-	-	0.05	-	-	-	-	-	-	58379	-	-	-	-	17437	dichlormethane 1-chlorobutene, bromoethane,
HTV 115	123473	93541	15.08	5.11	0.24	0.62	0.68	1.14	74.51	213033	66896	-	46497	-	304426	bromochlormethane
HTV116	1711	462	-	-	-	-	0.09	-	-	32471	-	-	-	-	-	
SM5	481	-	0.31	-	-	-	-	-	-	26223	-	-	-	-	165915	
SM6	17809	-	0.19	-	-	-	-	-	-	56302	-	-	-	-	119484	1-brombutane in control
SM7	-	-	-	-	-	-	-	-	-	35287	-	-	-	-	226515	1-brombutane in control
MU2	5440	-	-	-	-	-	-	-	-	-	-	-	-	-	461445	1- brombutane in control
MU4	-	10619	26.80	-	-	-	-	-	99.62	305561	6085	8.44	-	0.03	4647314	1-bromobutane, toluene
MU7	-	-	-	-	-	-	-	-	-	-	-	-	-	-	283132	

Table 6.8: Anion concentrations of halite samples.

		Cl ⁻	Br ⁻	SO ₄ ²⁻
		g / g	ng / g	mg / g
South Russia	H1EIt	0.54 ± 0.01	290.8 ± 51.1	19.41 ± 0.06
	H2EIt	0.55 ± 0.01	220.2 ± 5.9	18.05 ± 0.54
	H3EIt	0.48 ± 0.01	317.8 ± 11.5	47.05 ± 0.73
	H4EIt	0.48 ± 0.00	150.2 ± 37.5	77.44 ± 0.60
	H5EIt	0.55 ± 0.00	131.2 ± 30.9	17.29 ± 0.17
	H6Kas	0.57 ± 0.04	0.0 ± 0.0	3.06 ± 0.16
	H7Kas	0.60 ± 0.01	0.0 ± 0.0	2.34 ± 0.02
	H26Bas	0.59 ± 0.00	0.0 ± 0.0	10.89 ± 0.15
Mauretania	H8SND	0.53 ± 0.00	30.7 ± 43.4	8.51 ± 0.40
	H9SND	0.59 ± 0.00	0.0 ± 0.0	15.34 ± 0.42
	H10SND	0.61 ± 0.00	0.0 ± 0.0	3.01 ± 0.07
	H11SND	0.60 ± 0.00	0.0 ± 0.0	9.24 ± 0.13
	H12SND	0.60 ± 0.01	0.0 ± 0.0	9.64 ± 0.24
	H13Doue	0.59 ± 0.00	148.0 ± 59.4	3.61 ± 0.02
Bostuana / Namibia	H14SP	0.58 ± 0.00	83.3 ± 0.5	3.51 ± 0.02
	H15SP	0.61 ± 0.01	46.5 ± 65.8	0.28 ± 0.01
	H16SP	0.61 ± 0.01	0.0 ± 0.0	0.14 ± 0.02
	H17WBSR	0.60 ± 0.00	202.7 ± 30.6	3.12 ± 0.04
	H18Boht	0.56 ± 0.01	40.3 ± 57.0	1.21 ± 0.02
Mine or drill core samples / Siberia, Gorleben, Poland	H19Sib	0.59 ± 0.00	965.0 ± 25.9	1.48 ± 0.00
	H20Sib	0.56 ± 0.00	1197.3 ± 33.5	0.39 ± 0.06
	H21Sib	0.57 ± 0.01	335.0 ± 20.3	0.34 ± 0.02
	H22Sib	0.59 ± 0.00	743.5 ± 16.3	9.70 ± 0.13
	H23Sib	0.60 ± 0.00	237.8 ± 28.5	1.86 ± 0.00
	H24Sib	0.61 ± 0.00	261.0 ± 16.0	1.60 ± 0.08
	H25Sib	0.60 ± 0.00	415.0 ± 33.0	1.96 ± 0.02
	H27Gor	0.61 ± 0.00	193.5 ± 3.5	4.49 ± 0.00
	H28LKT	0.51 ± 0.01	0.0 ± 0.0	3.56 ± 0.00
	H29WG	0.61 ± 0.01	0.0 ± 0.0	2.92 ± 0.04
	H30WG	0.58 ± 0.00	0.0 ± 0.0	6.28 ± 0.26
	H31WG	0.57 ± 0.00	0.0 ± 0.0	1.85 ± 0.10
	H32WG	0.59 ± 0.01	0.0 ± 0.0	0.94 ± 0.03
	H33BZ	0.44 ± 0.01	0.0 ± 0.0	4.91 ± 0.04
	H34BZ	0.53 ± 0.00	0.0 ± 0.0	1.23 ± 0.01
H35BZ	0.59 ± 0.01	0.0 ± 0.0	0.24 ± 0.03	
H36BZ	0.28 ± 0.01	0.0 ± 0.0	9.94 ± 0.16	
Bolivia	H44Bol	0.60 ± 0.01	0.0 ± 0.0	3.44 ± 0.08
	H45Bol	0.59 ± 0.00	0.0 ± 0.0	10.15 ± 0.30
	H46Bol	0.60 ± 0.01	0.0 ± 0.0	1.28 ± 0.04
Southwest Australia	H37LSF	0.52 ± 0.01	202.8 ± 17.2	16.68 ± 0.17
	H38LW	0.51 ± 0.01	267.2 ± 10.1	24.29 ± 0.47
	H39LSB	0.58 ± 0.00	192.8 ± 29.9	4.71 ± 0.00
	H40LM	0.54 ± 0.01	134.7 ± 11.8	9.75 ± 0.08
	H41LK	0.56 ± 0.01	139.5 ± 16.7	9.17 ± 0.25
	H42LD	0.58 ± 0.01	97.7 ± 4.2	4.47 ± 0.06
	H43LO	0.59 ± 0.01	119.7 ± 4.7	7.39 ± 0.12
	H47LST	0.58 ± 0.01	135.3 ± 27.1	5.13 ± 0.14
	H48LHH	0.59 ± 0.01	98.6 ± 12.8	12.08 ± 1.01
	H49LD	0.58 ± 0.01	29.2 ± 25.3	4.65 ± 0.44
H50LO	0.59 ± 0.01	57.8 ± 50.1	10.38 ± 0.16	


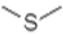
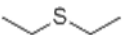
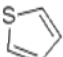
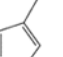
Table 6.9: Organic carbon concentrations of halite samples.

sample ID	organic carbon mg/g
H1Elt x	0.46 ± 0.12
H2Elt	0.38 ± 0.22
H3Elt x	0.56 ± 0.04
H4Elt	0.36 ± 0.12
H5Elt	0.46 ± 0.02
H6Kas untreated	0.36 ± 0.17
H7Kas	0.24 ± 0.05
H8SND x	0.19 ± 0.01
H9SND x	0.46 ± 0.07
H10SND	0.11 ± 0.03
H11SND x	0.16 ± 0.11
H12SND x	0.09 ± 0.06
H13Doue	0.14 ± 0.02
H14SP	5.26 ± 0.27
H15SP x	0.80 ± 0.09
H16SP	1.27 ± 0.57
H17WBSR	0.74 ± 0.20
H18Boht	9.00 ± 0.08
H19Sib	0.42 ± 0.09
H20Sib	0.22 ± 0.09
H21Sib	5.57 ± 0.04
H22Sib	0.27 ± 0.13
H23Sib	2.47 ± 3.34
H24Sib	0.20 ± 0.08
H25Sib	0.24 ± 0.05
H27Gor	0.21 ± 0.02
G1Bas	0.09 ± 0.00
G2Bas	0.25 ± 0.08

Table 6.10: Examples of aliphatic and aromatic hydrocarbons from FIs. ‘Grinding’ as a treatment implies that these measurements were performed with the system as presented in Chapter 2.

compound name	formula	structure	matrix	treatment	reference
methane	CH ₄		halite	grinding	e.g. Goldstein, 2001; see section 1.4
ethane	C ₂ H ₆		halite	grinding	Krieger, 2014
ethene	C ₂ H ₄		halite	grinding	Krieger, 2014
propane	C ₃ H ₈		halite	grinding	Krieger, 2014
propene	C ₃ H ₆		halite	grinding	Krieger, 2014
butane	C ₄ H ₁₀		halite	crushing, heating	Sevensen et al., 2009
isobutane	C ₄ H ₁₀		halite	grinding	Krieger, 2014
1-butene	C ₄ H ₈		halite	grinding	Krieger, 2014
cis-2-butene	C ₄ H ₈		halite	grinding	Krieger, 2014
trans-2-butene	C ₄ H ₈		halite	grinding	Krieger, 2014
2-butyne	C ₄ H ₆		halite	grinding	Krieger, 2014
1-butene-3-yne	C ₄ H ₄		halite	grinding	Krieger, 2014
1,3-butadiene	C ₄ H ₆		halite	grinding	Krieger, 2014
2-methylbuta-1,3-diene	C ₅ H ₈		halite	grinding	Krieger, 2014
2,2-dimethylbutane	C ₆ H ₁₄		halite	grinding	Krieger, 2014
3-methyl-1,4-pentadiene	C ₆ H ₁₀		halite	grinding	Krieger, 2014
3-methyl-1-pentene	C ₆ H ₁₂		halite	grinding	Krieger, 2014
methylcyclopentane	C ₆ H ₁₂		halite, dolerite sill	grinding	Dutkiewicz et al., 2004; Krieger 2014
3-methylpentane	C ₆ H ₁₄		halite	grinding	Krieger, 2014
2,2-dimethylpentane	C ₇ H ₁₆		halite	grinding	Krieger, 2014
cyclohexane	C ₆ H ₁₂		halite	grinding	Krieger, 2014
methylcyclohexane	C ₇ H ₁₄		halite	grinding	Krieger, 2014
3-methylhexane	C ₇ H ₁₆		halite	grinding	Krieger, 2014
3,5-dimethylheptane	C ₉ H ₂₀		halite	grinding	Krieger, 2014
benzene	C ₆ H ₆		halite, dolerite sill	crushing, heating	Sevensen et al., 2009; Dutkiewicz et al., 2004

Table 6.11: VOSC from minerals. The term ‘grinding’ under treatment implies that these compounds were detected with the system presented in Chapter 2.

compound name	formula	structure	matrix	treatment	reference
sulfur dioxide	SO ₂	O=S=O	halite	crushing, heating	Sevensen et al., 2009
methyl tioethane	C ₃ H ₈ S		halite	crushing, heating	Sevensen et al., 2009
dimethyl sulfide	C ₂ H ₆ S		halite	crushing, heating	Sevensen et al., 2009
diethyl sulfide	C ₄ H ₁₀ S		halite	crushing, heating	Sevensen et al., 2009
carbonyl sulfide	COS	O=C=S	halite, fluorit, quartz, granite	grinding	Bugla, 2010; Ubl, 2011; Krieger, 2014
thiophene	C ₄ H ₄ S		halite	grinding	Krieger, 2014
carbon disulfide	CS ₂	S=C=S	halite	grinding	Krieger, 2014
2-/3-methylthiophene	C ₅ H ₆ S		halite	grinding	Krieger, 2014
methanethiol	CH ₄ S	HS—	halite	grinding	Krieger, 2014

Synthesis of MORB glass

A basaltic glass was synthesized representing a chemical composition of average primitive MOR basalt. Pure analyzed oxides (MgO, MnO, FeO, Al₂O₃, TiO₂ and SiO₂) and carbonates (Na₂CO₃, K₂CO₃, CaCO₃) were molten in a Pt crucible at 1500°C, cooled on air, ground and molten again. The chemical composition was determined by electron microprobe analysis on a polished surface using a Cameca microprobe (SX100) with 15 kV accelerating voltage, 5 nA beam current and a defocused beam with 10-30 μm in diameter. The normalized composition of the starting material is 49.67 % SiO₂, 0.87 % TiO₂, 16.08 % Al₂O₃, 8.64 % FeO, 0.15 % MnO, 9.78 % MgO, 12.45 % CaO, 2.28 % Na₂O and 0.08 % K₂O.

(source: Stefan Dultz – personal communication)

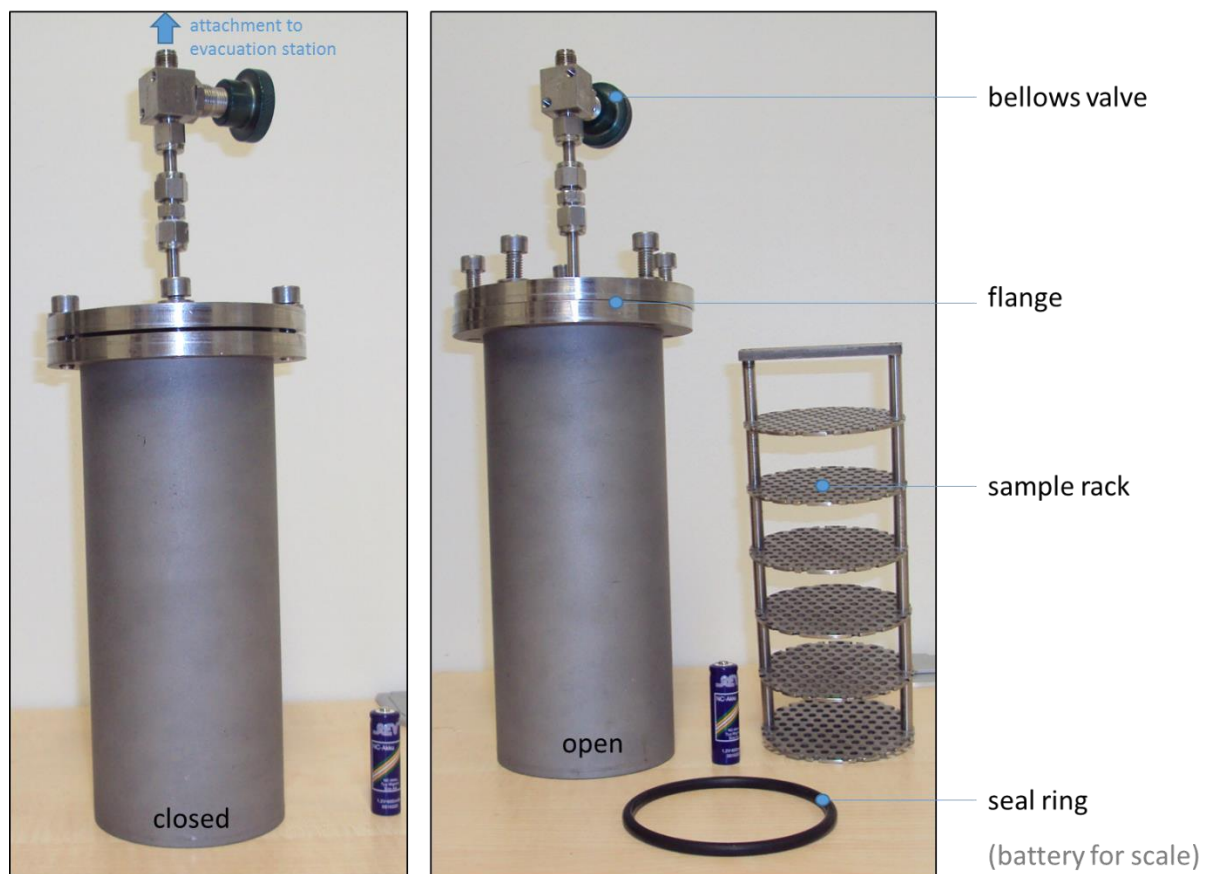


Figure 6.1: Stainless steel cylinder used to evacuate cleaned mineral samples before GC-MS analysis.

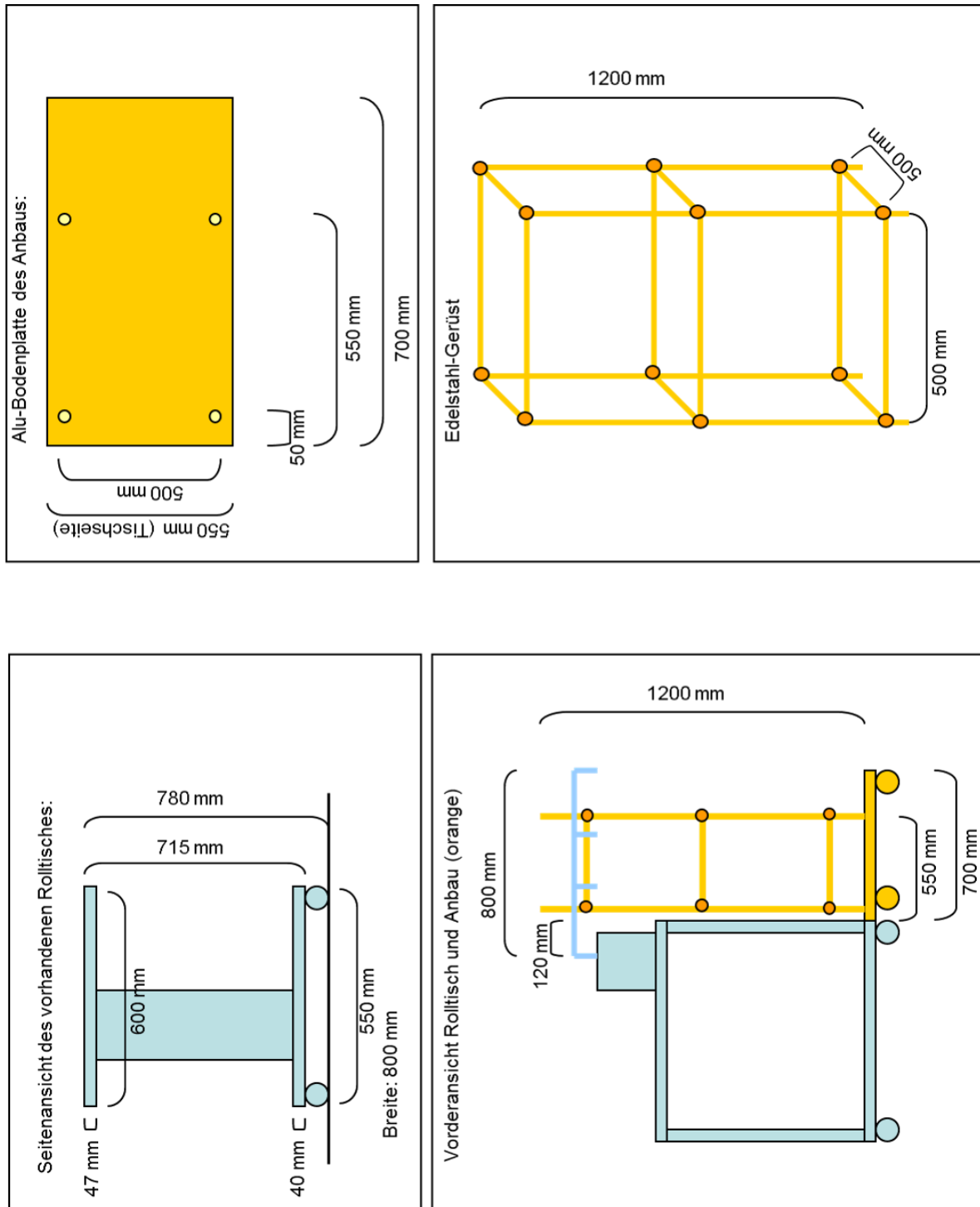


Figure 6.2: Construction drawing of moveable rack for gas mixing station/sample evacuation station.

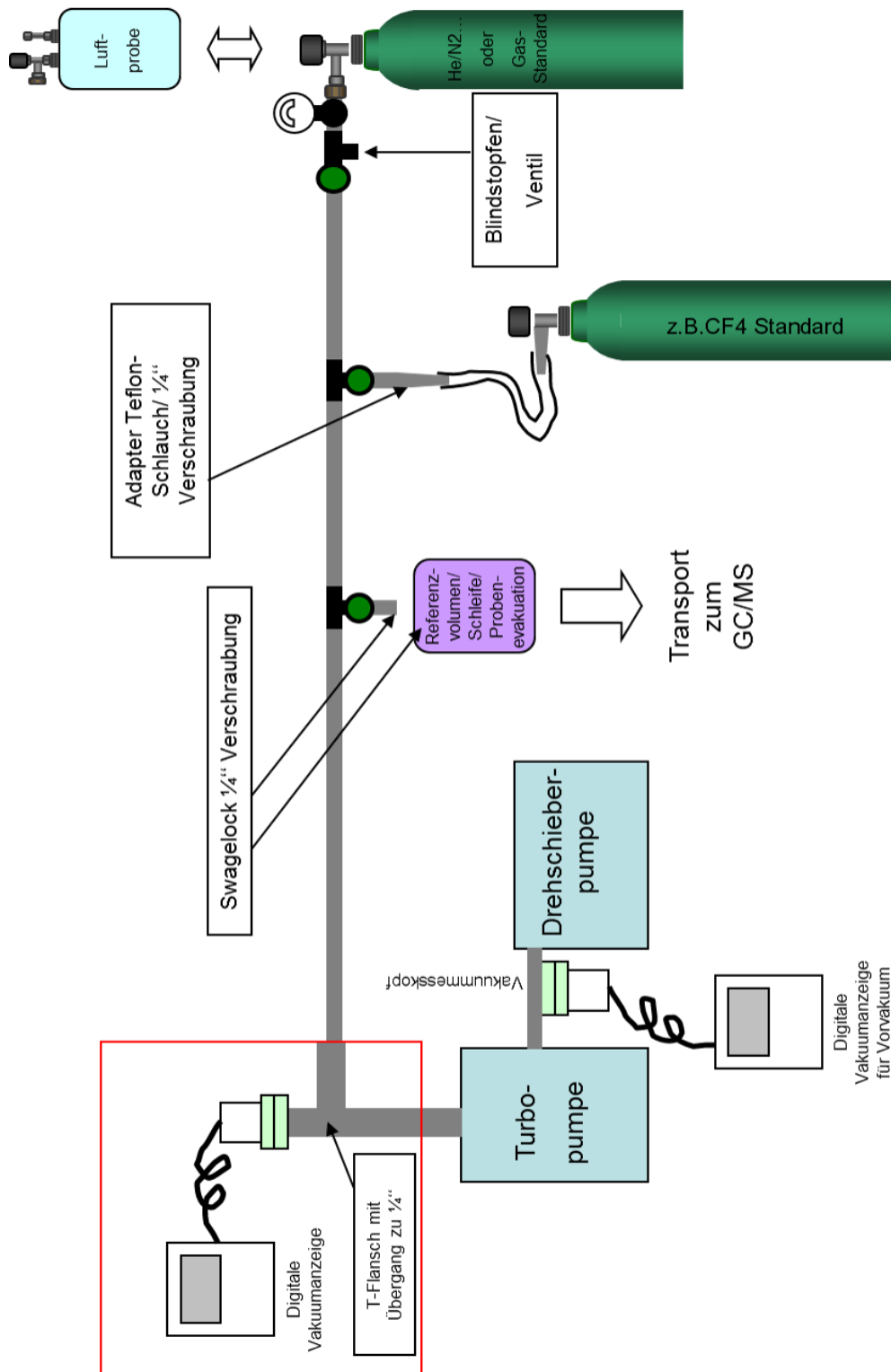


Figure 6.3: Construction scheme of sample evacuation/gas mixing station.

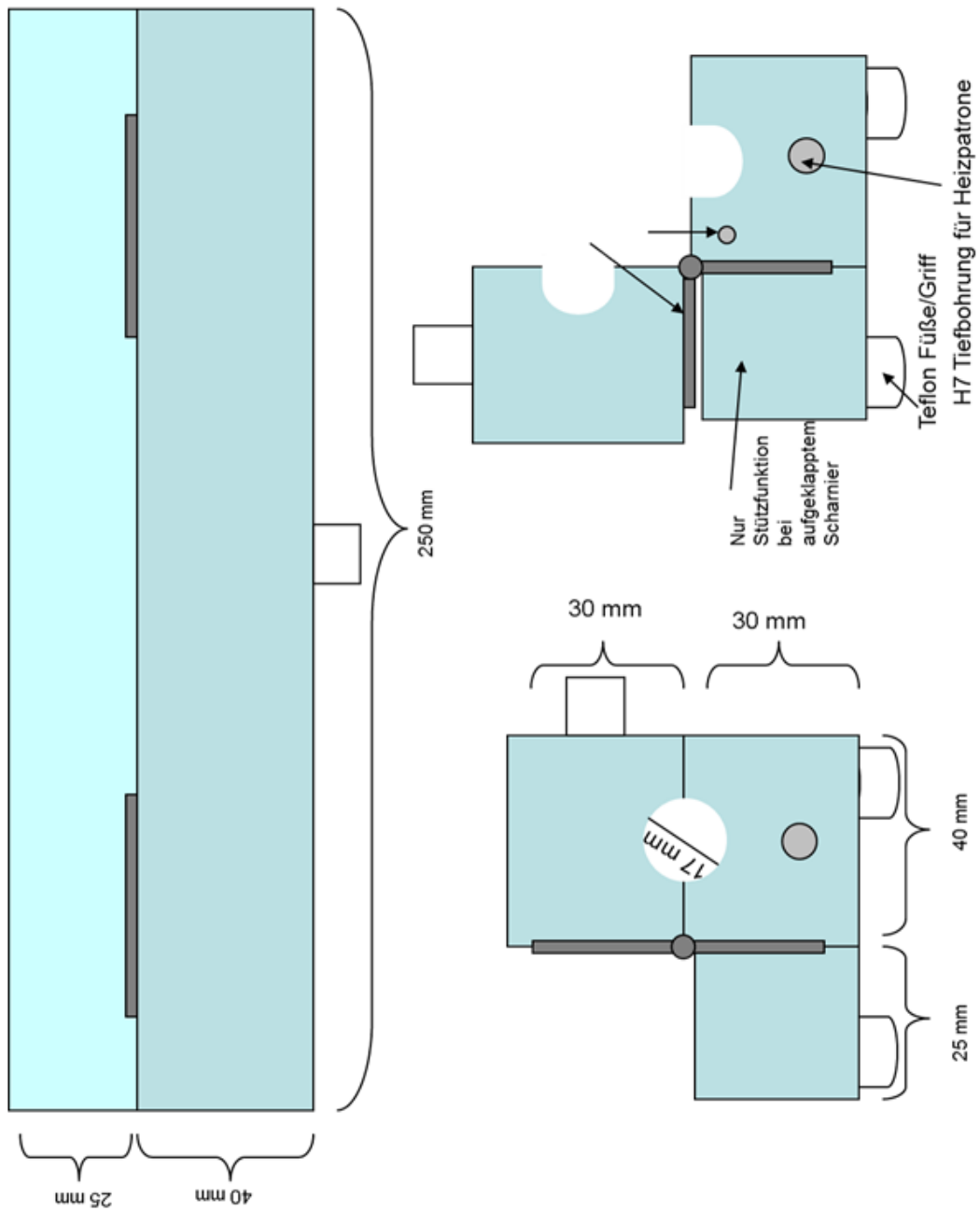


Figure 6.4: Construction drawings of aluminum heating block for water trap.

DECLARATION

The following publication was embedded in my thesis:

Mulder, Ines, Stefan G. Huber, Torsten Krause, Cornelius Zetsch, Karsten Kotte, Stefan Dultz, and Heinz F. Schöler. 2013. "A New Purge and Trap Headspace Technique to Analyze Low Volatile Compounds from Fluid Inclusions of Rocks and Minerals." *Chemical Geology* 358 (November): 148–55.
doi:10.1016/j.chemgeo.2013.09.003.

The major part of this work was performed by Ines Mulder and can be attested by the following co-authors:



Heinz F. Schöler



Torsten Krause

DECLARATION

The following submitted manuscript was embedded in my thesis:

Ines Mulder, Torsten Krause, Tobias Sattler, Christoph Tubbesing, Sabine Studenroth, Krzysztof Bukowski, Elliot Atlas and Heinz F. Schöler. 2014. "Thermolytic degradation of methyl methionine and implications for its role in DMS and MeCl formation in hypersaline environments." *Environmental Chemistry (under review)*

The major part of this work was performed by Ines Mulder and can be attested by the following co-authors:



Heinz F. Schöler



Tobias Sattler

**Eidesstattliche Versicherung gemäß § 8 der Promotionsordnung der
Naturwissenschaftlich-Mathematischen Gesamtfakultät
der Universität Heidelberg**

1. Bei der eingereichten Dissertation zu dem Thema

Volatile Organohalogens from Fluid Inclusions of Rocks and Minerals

handelt es sich um meine eigenständig erbrachte Leistung.

2. Ich habe nur die angegebenen Quellen und Hilfsmittel benutzt und mich keiner unzulässigen Hilfe Dritter bedient. Insbesondere habe ich wörtlich oder sinngemäß aus anderen Werken übernommene Inhalte als solche kenntlich gemacht.
3. Die Arbeit oder Teile davon habe ich wie bislang nicht an einer Hochschule des In- oder Auslands als Bestandteil einer Prüfungs- oder Qualifikationsleistung vorgelegt.
4. Die Richtigkeit der vorstehenden Erklärungen bestätige ich.
5. Die Bedeutung der eidesstattlichen Versicherung und die strafrechtlichen Folgen einer unrichtigen oder unvollständigen eidesstattlichen Versicherung sind mir bekannt.

Ich versichere an Eides statt, dass ich nach bestem Wissen die reine Wahrheit erkläre und nichts verschwiegen habe.

Ort und Datum

Unterschrift